Catalytic Hydrogenation of Nitrile Rubber in High Concentration Solution

by

Ting Li

A thesis
presented to the University of Waterloo
in fulfillment of the
thesis requirement for the degree of
Master of Applied Science
in
Chemical Engineering

Waterloo, Ontario, Canada, 2011

Author's Declaration

I hereby declare that I am the sole author of this thesis. This is a true copy of the thesis, including any required final revisions, as accepted by my examiners.

I understand that my thesis may be made electronically available to the public.

Abstract

Chemical modification is an important way to improve the properties of existing polymers, and one of the important examples is the hydrogenation of nitrile butadiene rubber (NBR) in organic solvent by homogeneous catalysis in order to extend its application. This process has been industrialized for many years to provide high performance elastomers (HNBR) for the automotive industry, especially those used to produce components in engine compartments.

In the current commercial process, a batch reactor is employed for the hydrogenation step, which is labor intensive and not suitable for large volume of production. Thus, novel hydrogenation devices such as a continuous process are being developed in our research group to overcome these drawbacks. In order to make the process more practical for industrial application, high concentration polymer solutions should be targeted for the continuous hydrogenation. However, many problems are encountered due to the viscosity of the high concentration polymer solution, which increases tremendously as the reaction goes on, resulting in severe mass transfer and heat transfer problems. So, hydrogenation kinetics in high concentration NBR solution, as well as the rheological properties of this viscous solution are very essential and fundamental for the design of novel hydrogenation processes and reactor scale up.

In the present work, hydrogenation of NBR in high concentration solution was carried out in a batch reactor. A commercial rhodium catalyst, Wilkinson's catalyst, was used with triphenylphosphine as the co-catalyst and chlorobenzene as the solvent. The reactor was modified and a PID controller was tuned to fit this strong exothermic reaction. It was observed that when NBR solution is in a high concentration the kinetic behavior

was greatly affected by mass transfer processes, especially the gas-liquid mass transfer. Reactor internals were designed and various agitators were investigated to improve the mechanical mixing. Experimental results show that the turbine-anchor combined agitator could provide superior mixing for this viscous reaction system.

The kinetic behavior of NBR hydrogenation under low catalyst concentration was also studied. It was observed that the hydrogenation degree of the polymer could not reach 95% if less than 0.1%wt catalyst (based on polymer mass) was used, deviating from the behavior under a normal catalyst concentration.

The viscosity of the NBR-MCB solutions was measured in a rotational rheometer that has a cylinder sensor under both room conditions and reaction conditions. Parameters that might affect the viscosity of the solutions were studied, especially the hydrogenation degree of polymer. Rheological properties of NBR-MEK solutions, as well as NBR melts were also studied for relevant information.

It is concluded that the hydrogenation kinetics deviates from that reported by Parent et al. [6] when polymer is in high concentration and/or catalyst is in low concentration; and that the reaction solution (HNBR/NBR-MCB solution) deviates from Newtonian behavior when polymer concentration and hydrogenation degree are high.

Acknowledgements

At the time I am finishing my Master's program, I would like to gratefully acknowledge the following individuals:

Professor Garry L. Rempel for his excellent guidance and supervision throughout the whole master's program.

Professor Qinmin Pan for her academic guidance in my research work.

My friends in the laboratory: Yin Liu, Minghui Liu, Hui Wang, Lijuan Yang, Ray Zou, Yan Liu and Robert. You are my friends that I work with everyday. It's so nice to share the time with you.

Thai students: Sue, Anong, Nikom, Benz and Boong for their help when it was needed.

A special thank goes to Dr Jialong Wu for his kind help with many issues in the lab.

Financial assistance from Lanxess Inc. and Natural Sciences and Engineering Research Council (NSERC) is gratefully acknowledged.

Table of Contents

List of Figures

List of Tables

Chapter 1 Introduction

1.1 Background

Chemical modification of polymer materials through catalysis is an efficient way to improve properties of existing polymers and extend their application. One of the examples is the chemical modification of nitrile rubber (NBR) to produce hydrogenated NBR (HNBR) via catalytic hydrogenation.

Nitrile rubber is widely used to make oil seals, O-rings, gaskets, as well as transmission belts and V belts, due to its remarkable oil-resistant property and good mechanical property. However, the residual unsaturated carbon-carbon double bonds in the polymer structure are sites of degradation, which greatly restrict the application especially when exposed to heat, acids, oxygen and aggressive solvents. By catalytic hydrogenation, these unsaturated bonds could be removed to get desirable properties. Figure 1-1 [1][2] shows the structure and property changes through the hydrogenation process.

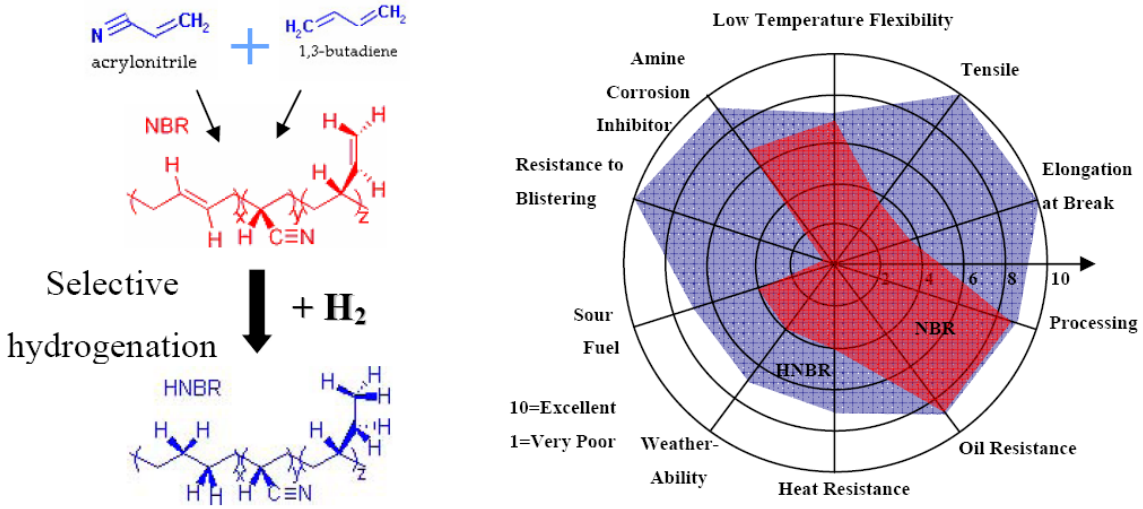

Figure 1-1 Changes in Structure and Property from NBR to HNBR [1]

Due to its excellent integrated performance, HNBR is now widely used in the automotive industry, particularly for components in engine compartments. Nippon Zeon Corp. and Lanxess Inc. are the two major manufacturers of HNBR in the worldwide market. Nippon Zeon produces HNBR through heterogeneous hydrogenation, while Lanxess uses homogeneous hydrogenation. The schematic process for the production of HNBR is shown in Figure 1-2 [3], starting from emulsion polymerization of acrylonitrile and butadiene monomers.

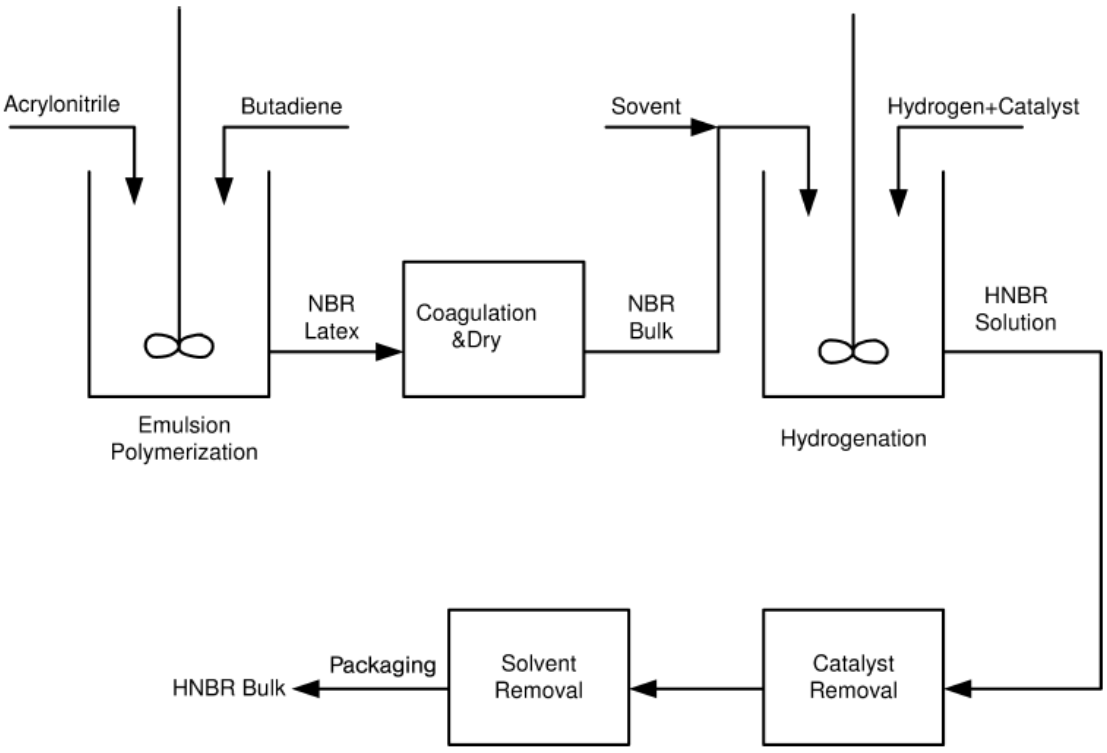

Figure 1-2 Schematic Process for the Production of HNBR [3]

The NBR bulk prepared from the latex is dissolved by mono-chlorobenzene and later on hydrogenated in the presence of a rhodium catalyst at certain temperature and pressure (Lanxess Inc.). The catalyst and solvent are recovered. The HNBR is ready for commercial use after vulcanization [3].

1.2 Motivation of the Work

Currently, a batch reactor is employed for the hydrogenation step of HNBR production (Figure 1-2), which is labor intensive and not suitable for large production. Also, there are disadvantages for energy and material integration in a batch process. Thus, continuous devices are being developed in our research group using a commercial rhodium catalyst, based on previous work [4][5]. The experimental results for continuous hydrogenation of NBR in low concentration solution are promising. In order to make the continuous process more practical for industrial application, NBR solution used is extended to high concentration. However, some difficulties are encountered during this process, due to the high viscosity of the concentrated NBR solution which affects the mass transfer and heat transfer.

Although the reaction kinetics of NBR hydrogenation with a low polymer concentration and the commercial rhodium catalyst has been established [6] and a numerical study for the coupling behavior of reaction kinetics and mass transfer in batch reactor [7] has also been carried out, it still lacks the first-hand experimental data for hydrogenation of NBR in concentrated solution. Also, it is observed that the viscosity of the solution increased significantly as the conversion increases during the continuous hydrogenation process, while the viscosity is an essential parameter for reactor design. Thus, how viscosity of the solution changes as reaction goes on is an important issue. To our knowledge, there is still no report on this aspect until now, although there are some reports [8][9] concerning the viscosity of the NBR/chlorobenzene system under various concentrations and temperatures.

1.3 Scope of the Research

Catalytic hydrogenation of NBR was carried in a batch reactor with the commercial rhodium catalyst (Wilkinson's catalyst). High concentration NBR solutions were used in order to observe the mass transfer affected kinetic behavior. Different agitators were employed to study the mechanical mixing for the viscous system. The reactor was modified and a PID controller was tuned to fit the severe exothermic process. The kinetic behavior of the hydrogenation reaction when low catalyst concentration was used was also researched, comparing with that under normal catalyst concentration.

On the other hand, rheological properties of NBR-chlorobenzene solutions were studied in a rheometer with a cylinder sensor. The measurement was carried out under both reaction conditions and room conditions, in order to provide rheological data for reactor design and equipment selection (e.g. pump selection), respectively. Emphasis was put on the effect of hydrogenation degree on the viscosity of solution, that is to say, how viscosity changes as the reaction goes on.

The rheological properties of NBR-methyl ethyl ketone (MEK) solutions and NBR melts were also studied to provide relevant information.

1.4 Outline of the Thesis

After general introduction in Chapter 1, literature will be reviewed in Chapter 2 with respect to the overview of NBR hydrogenation, mass transfer and mechanical mixing, as well as some basic information of rheology & rheometry especially for polymer systems. Then, the research methodology and approaches will be introduced in Chapter 3, where both the hydrogenation and rheological experiments will be described.

Chapter 4 presents the rheological properties of NBR melts, NBR-MEK solutions, as well as NBR-MCB solutions. Detail operation procedures of the rheological experiments will be described, both for measurement with the cylinder sensor (solutions) and measurement with the cone-plate sensor (melts). Viscosities of the NBR-MCB solutions will be emphasized; and the relation between viscosity and hydrogenation degree will be investigated. Other parameters which may also affect the viscosity of NBR-MCB solutions will be reported as well.

Then, in Chapter 5 the hydrogenation of NBR in high concentration solution using Wilkinson's catalyst is presented. After describing the modification of the reactor, the operation procedure will be introduced in detail. Then, the internal structures and agitators used will be presented. Operation techniques aimed for better experiment reproducibility, such as the temperature control method, will also be mentioned. In the results and discussion section, parameters that affect hydrogenation rate are analyzed, including agitator shapes, stirring speeds, hydrogen pressures, polymer concentrations and catalyst concentrations.

Chapter 6 reports on the kinetic behavior when low catalyst concentration is applied in the hydrogenation experiments. Concentrations of every species in the solution will be calculated according to the accepted catalytic mechanism in order to analyze the observed phenomena. Hydrogenation experiments of styrene butadiene rubber (SBR) will also be carried out, comparing with the phenomena observed in NBR hydrogenation.

Finally, in Chapter 7 conclusions are listed and recommendations for future research will be given based on the current work.

Chapter 2 Literature Review

2.1 Catalytic Hydrogenation of Nitrile Rubber

In this part, the catalytic technologies for nitrile rubber hydrogenation will be reviewed briefly. Then, the reaction kinetics for hydrogenation of NBR in organic solvent with Wilkinson's catalysts will be introduced. The solution hydrogenation of NBR in continuously operated reactors, i.e. the continuous hydrogenation process, is also included here.

2.1.1 Hydrogenation Technologies

Solution hydrogenation of NBR is the main commercial process for HNBR production, during which the carbon-carbon double bonds of NBR are hydrogenated in organic solvent in the presence of a transition metal catalyst. The commonly used solvents include mono-chlorobenzene (MCB), o-dichlorobenzene, toluene, xylol, cyclohexane, methyl ethyl ketone (MEK), and acetone. The solution hydrogenation could be a heterogeneous catalytic process [10][11], where catalyst is dispersed on a solid support while the polymer is dissolved in the liquid phase. This heterogeneous hydrogenation technology was commercialized by Nippon Zeon Corp. Another successful case commercialized by Lanxess Inc. is a homogeneous catalytic process [12][13]. In the homogeneous catalytic hydrogenation, both catalyst and polymer can be dissolved in the organic solvent, thus in the same phase, enabling high activity of the catalyst. The catalysts used are usually complexes of transition metals. The reported transition metals used for NBR hydrogenation in this process include rhodium [12][13], palladium[14][15], ruthenium[16][17], and osmium[18]. Catalyst consisting of bimetallic complexes [19] has also been reported.

In addition to the solution hydrogenation, nitrile rubber can also be hydrogenated in the latex form (emulsion) [20][21][22], which means that nitrile rubber could be directly hydrogenated after its synthesis through emulsion polymerization from butadiene & acrylonitrile. Researchers in Rempel's group also reported hydrogenation of nitrile rubber in bulk form [23][24], i.e. in complete absence of solvent. However, emulsion hydrogenation and bulk hydrogenation technologies are still at the laboratory scale.

2.1.2 Hydrogenation Kinetics

Wilkinson's catalyst $RhCl(PPh_3)_3$ is applied commercially for the selective hydrogenation of nitrile rubber with mono-chlorobenzene as the solvent. The reaction kinetics of this catalytic process has been well studied. Mohammadi and Rempel [25] designed an automated gas-consumption measuring system which could be used to keep constant or time-variable pressure and record continuously the consumption or production of gases in a batch-type microreactor. Based on this gas consumption system, the kinetics for the hydrogenation of NBR using Wilkinson's catalyst was studied at 65 ℃ and ambient pressures [13]. A catalytic mechanism was presented based on the study as shown in Figure 2-1.

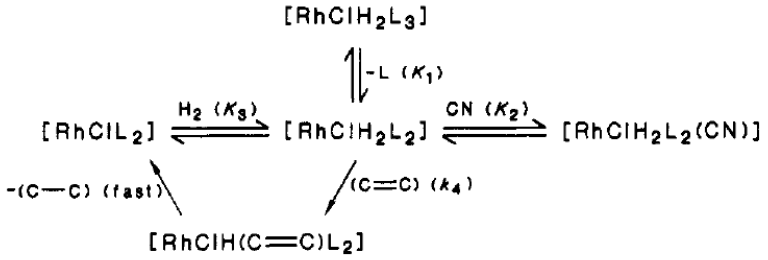

L = $P(C_6H_5)_3$; CN = nitrile group in the copolymer; (C=C) = carbon–carbon unsaturation in the copolymer; (C—C) = saturated polymer product.

Figure 2-1 Mechanism of NBR Hydrogenation Reported by Mohammadi and Rempel [13]

In Figure 2-1, $RhClH_2(PPh_3)_3$ is generated by the oxidative addition of molecular hydrogen onto $RhCl(PPh_3)_3$ and this process is well established [26].

Bhattacharjee et al. [27] also carried out a study on this system, extending the reaction conditions to 100℃ and 56bar.

Parent et al. [6] detailed the study of catalytic behavior at reaction conditions approaching those found in industrial settings. The reactive species $RhCl(CN)(PPh_3)_2$ was found to affect the kinetic route and a revised mechanism for the hydrogenation of NBR was proposed as shown in Figure 2-2.

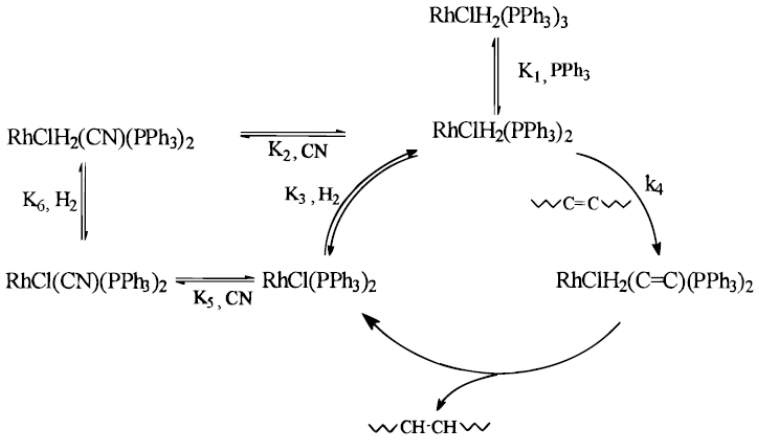

Figure 2-2 Mechanism of NBR Hydrogenation Reported by Parent et al. [6]

According to the work of Parent [28], the reaction rate is first-order with respect to the concentration of the carbon-carbon double bond (Equation 2-1).

$$-\frac{d[C=C]}{dt} = k'[C=C] \tag{2-1}$$

The apparent first-order rate constant could be estimated by regression of conversion profiles. The relation between this constant and those parameters shown in Figure 2-2 can be expressed by the Equation 2-2.

$$k' = \frac{k_4 K_1 K_3 [Rh]_T [H_2]}{K_1 + K_1 K_3 [H_2] + K_3 [H_2][PPh_3] + K_1 K_5 [C \equiv N] + K_1 K_2 K_3 [H_2][C \equiv N]} \quad (2\text{-}2)$$

The values of the parameters in the kinetic model are listed in Table 2-1.

Table 2-1 Model Parameters Estimates [28]

([NBR] < 4%wt; 100 ℃-170 ℃)

Parameter	Estimate	A.S.E.	Lower <95% > Upper	
k_4,(mMs)$^{-1}$	1.19	0.17	0.85	1.53
K_1, mM	1.44	0.38	0.67	2.21
K_2, mM^{-1}	3.98E-02	5.94E-03	2.76E-02	5.19E-02
K_3, mM^{-1}	3.41E-03	2.06E-04	2.99E-03	3.83E-03
K_5, mM^{-1}	2.71E-02	3.20E-03	8.12E-03	4.61E-02
K_6, mM^{-1}	6.28E-03	3.78E-04	5.51E-03	7.05E-03

In this kinetic study, the NBR concentration in the reaction solution was very low (<4%wt) and mass transfer processes have a marginal influence on the hydrogenation rates [28].

2.1.3 Continuous Hydrogenation

In the current production of Lanxess, a batch process is employed, which is labour intensive and not suitable for a large scale of production. Thus, a great of effort has been put into the development of a continuous hydrogenation process. Parent [28] set up a column reactor packed with non-porous ceramic saddles to study the feasibility of continuous hydrogenation of NBR. Then, the hydrodynamic performance of this packed bed reactor was further investigated [29][30]. Later on, Pan et al. [31] studied the continuous process numerically and proposed that the optimum design of the continuous system was a large plug flow reactor (PFR) with a small continuous stirred tank reactor (CSTR) at the inlet of it.

Madhuranthakam et al.[4][32]-[34] developed a continuous process for the hydrogenation of NBR hydrogenation using a static mixer (SM) reactor. The

hydrodynamic performance of this reactor in air/water system and hydrogen/polymer solution system was studied with respect to residence time distribution and liquid hold-up. The reactor was investigated numerically and the hydrogenation performance was predicted by modeling. Hydrogenation experiments with 2.5%wt & 5.0%wt NBR solutions were also carried out using an osmium catalyst and 97% hydrogenation degree was achieved.

Another novel continuous process was developed by Zhang et al. [5] [35]-[38], in which a multistage agitated contactor (MAC) was employed. A cascade of stirred tanks with back flow (CTB) model could be used to describe this reactor. The hydrodynamics in air/water system and air/viscous fluids system was studied with respect to residence time distribution and gas hold up. The hydrogenation process was modeled and simulated. Hydrogenation experiments with 2%wt to 5%wt NBR solutions were also carried out using an osmium catalyst and the hydrogenation degree achieved was over 95%.

2.2 Mass Transfer and Mechanical Mixing

Solution hydrogenation of nitrile rubber will be affected by transfer problems when scaled up or higher concentration solution is used. In this part, the hydrogenation kinetics which is affected by mass transfer, the mechanical mixing, as well as the design of agitated vessels will be introduced briefly.

2.2.1 Mass Transfer Affected Kinetics

The kinetic mechanism of NBR hydrogenation that was established by Parent et al. [6] is based on laboratory experiments with dilute polymer solutions. If a larger reactor is used or NBR solution is extended to high concentration, the mass transfer problem needs to be taken into account.

Pan and Rempel [7] carried out numerical investigation of semi-batch processes for hydrogenation of diene-based polymers and studied the coupling behavior between the catalytic hydrogenation and mass transfer. The solution hydrogenation of nitrile rubber is a gas-liquid system and the rate of dissolution of hydrogen into the liquid phase could be expressed by the Equation 2-3 [7].

$$\frac{d[H_2]}{dt} = k_L a([H_2]_e - [H_2]) - R_{C=C} \tag{2-3}$$

where $R_{C=C}$ is the rate of $[C=C]$ disappearance, given by Equation 2-1; $k_L a$ is the volumetric mass transfer coefficient between gas and liquid phases; $[H_2]_e$ is the saturated hydrogen concentration, which is in equilibrium with the hydrogen pressure in the gas phase; $[H_2]$ is the actual hydrogen concentration in the liquid phase.

In Parent's work [28], low concentration NBR solution was used and it was found that $[H_2]/[H_2]_e = 91.5\%$. Thus, it was regarded that $[H_2] = [H_2]_e$ and $\frac{d[H_2]}{dt} = -R_{C=C}$. The mass transfer process has a marginal influence on the hydrogenation rates acquired in the study [28]. The reaction is chemical controlled. However, when the hydrogenation system is extended to high concentration, the solution becomes very viscous. In this case, it becomes difficult for the agitator to provide bubbles into the solution, i.e. less gas-liquid interfacial area. $[H_2]$ might differ much from $[H_2]_e$. Then, the effect of gas-liquid mass transfer could not be neglected. The reaction is both chemical and mass transfer controlled. If the concentration of polymer in the solution becomes even higher, besides the gas-liquid mass transfer, the mass transfer inside the liquid phase might also become a problem. The reaction might be dominantly controlled by mass transfer.

2.2.2 Mixing and Agitators

In a high concentration NBR hydrogenation system, besides mass transfer, heat transfer also becomes a problem due to the relatively high viscosity of the reaction media. Thus, agitators should be properly designed to provide sufficient mixing.

Generally, an agitator is described in the following aspects: the power number N_P, the pumping number N_Q, as well as the characteristics of flow it creates including the shear level and the flow pattern. For traditional and turbulent flow application, i.e. low and medium viscosity, agitators could be divided into four types: axial flow agitators, radial flow agitators, hydrofoil agitators and high-shear agitators, according to the flow patterns and level of shear they create; Or more generally, divided into two types, according to the predominant flow pattern created: radial flow agitators and axial flow agitators. The pitched blade turbine (PBT) has a good balance of pumping and shear capabilities and therefore is considered to be a general-purpose impeller. More than one impeller are needed for the agitator in "tall and thin" reactors (high aspect ratio $Z/T > 1.5$) [39].

The viscosity of the liquid where agitators were applied is also a key parameter during design. Various agitators are illustrated in Figure 2-3 according to the predominant flow patterns they produce, as well as the range of viscosities over which they can be effectively used [40][41].

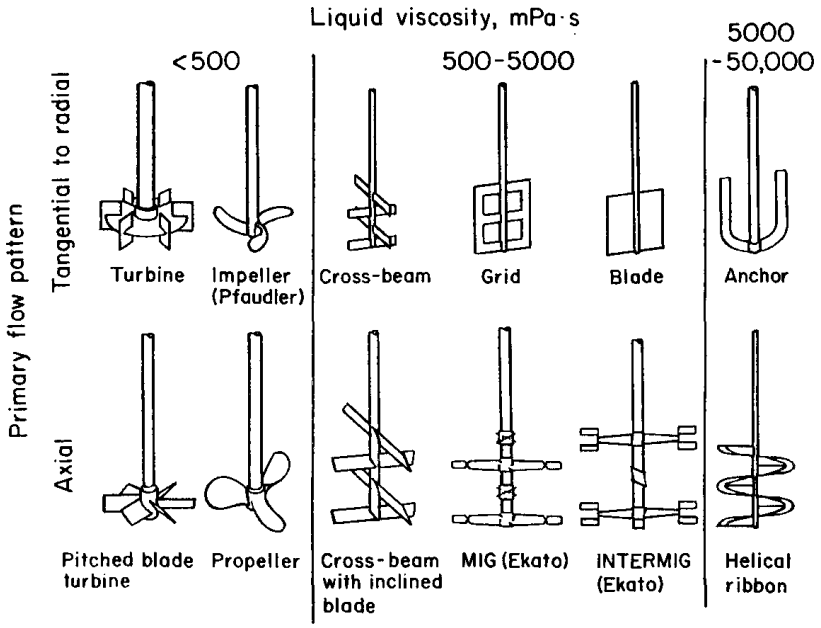

Figure 2-3 Various Agitators (Shah [40]; Zlokarnik and Judat[41])

For viscous mixing, i.e. medium to high viscosity, sometimes combined agitators are employed, as they could meet the needs in many characteristics compared with the single impeller. Gu et al. [42][43] reported a couple of combined agitators, including an anchor-turbine combined agitator, which can provide well circulation (pumping) and high shear simultaneously. Similar design was also reported by Todd [44], where an anchor and/or a helical were combined with turbines. Figure 2-4 shows these combined agitators.

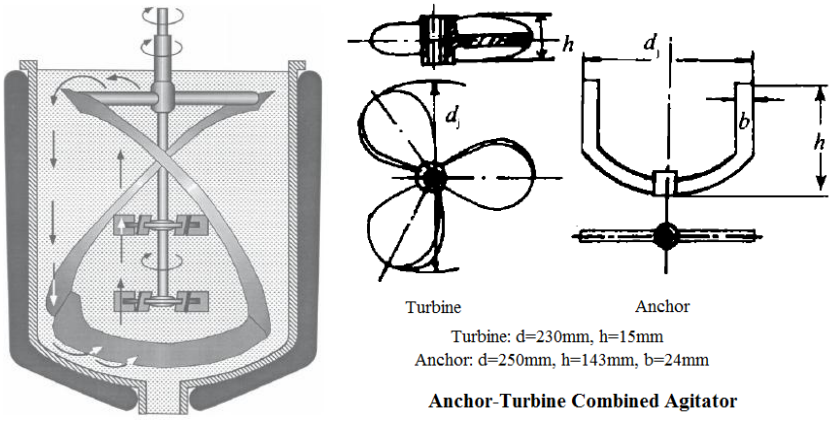

Figure 2-4 Combined Agitators (Gu et al. [42][43]; Todd[44])

2.2.3 Design of Reactor Internals

For a stirred reactor, the internals in the vessel may include heat transfer coils, wall baffles, feed pipes, dip tubes, thermocouples, pressure sensors and so on. Internals of the mechanically agitated vessel should be properly designed in order to improve the reactor performance.

Here are some design parameters. The installation of baffles is usually adopted in cylindrical vessels to prevent the bulk rotation generated by the agitator. Baffles are usually attached to the vessel wall by means of welded brackets, or made in the form of a basket with pressure-fitted rings [39][40]. The internal coil is used to achieve heat transfer (cooling/heating) inside the reactor. Sometimes, the internal coil also play a role similar as the baffles and it shall meet the flow pattern generated by the agitator. For an axial flow agitator, a spiral coil is effective because it provides good liquid circulation between the coil and the reactor wall. For radial flow agitators, the meander coil is more suitable since this arrangement does not deflect the radial flow pattern, but prevents bulk rotation of the liquid; while the spiral coils deflect the liquid circulation, resulting in insufficient flow between the coil and the reactor wall [40].

2.3 Rheological Properties

In this part, rheology for polymer and the experiment technology, i.e. rheometry, will be introduced first. Then, the research on rheological properties of NBR melts, as well as NBR solutions will be reviewed.

2.3.1 Rheology and Rheometry for Polymer System

The polymer fluid is a viscoeleatic fluid, that is to say, presents both viscous and elastic properties. The mathematical models for viscoelastic fluids are rather complicated

involving both viscous and elastic parameters; and the simplest model is the Maxwell model [47]. Although polymer melts and solutions present elastic property, in many situations this property is not important compared with the viscous property or even negligible, such as in low concentration polymer solution and some polymer melts depending on the processing ways. In this case, the polymer fluid could be regarded as a pure-viscous fluid [45].

The mathematical models for pure-viscous fluids are much simpler compared with those for viscoelastic fluids, containing only viscous parameters. The generalized Newtonian fluid, the Bingham fluid and the plastic fluid are examples of pure-viscous fluids, while the generalized Newtonian fluid can be described by Equation 2-4:

$$\tau = \eta\dot{\gamma} \tag{2-4}$$

where τ is shear stress (Pa); $\dot{\gamma}$ is shear rate (s^{-1}); and η is viscosity ($Pa \cdot s$).

For Newtonian fluids, η in Equation 2-4 is a constant, i.e. viscosity does not change with shear rate. In other cases, η is a function of $\dot{\gamma}$ and common models include the power law [49], the Carreau model, the Cross-Williamson model and the Carreau-Yasuda model. The power law, given by Equation 2-5 or Equation 2-6 is widely used especially in high shear rate circumstance[45][46].

$$\eta = k\dot{\gamma}^{n-1} \tag{2-5}$$

$$\ln\eta = (n-1)\ln\dot{\gamma} + \ln k \tag{2-6}$$

The relation between viscosity and temperature for a Newtonian fluid or for a fluid at a given shear rate could be expressed by Arrhenius equation (Equation 2-7 or Equation 2-8) when $T > (T_g + 100K)$ [45] [48].

$$\eta = Ae^{\frac{E_a}{RT}} \tag{2-7}$$

$$\ln \eta = \frac{E_a}{RT} + \ln A \tag{2-8}$$

The equipment that can be used to test rheological properties of fluids include rheometers such as capillary rheometers, rotational rheometers, torque rheometers and extensional rheometers, as well as instruments like melt flow index tester and Ubbelohde viscometer. Those equipments are designed to measure different rheological properties in different ranges and circumstances. The rotational rheometer is very commonly used in the research laboratory and will be introduced here. The sensors used for testing in rotational rheometer could be rotor-cylinder, cone-plate and parallel plate; and the measuring modes could be static modes and dynamic modes [45]. In static mode, the shear rate usually increases linearly as time goes; and the viscous parameter (η) can be tested in this mode. In the dynamic mode, shear stress varies according to an oscillatory function as time goes; both the viscous parameters (η^*) and elastic parameters (G^*) can be tested in this mode. The equations listed below are the relations of parameters measured in the dynamic mode [45].

$$G^* = G' + \mathrm{iG}",\ |G^*| = \sqrt{G'^2 + \mathrm{G}"^2},\ G' = |G^*|cos\delta,\ \mathrm{G}" = |G^*|sin\delta$$

$$\eta^* = \eta' + \mathrm{i}\eta",\ |\eta^*| = \sqrt{\eta'^2 + \eta"^2},\ \eta' = |\eta^*|sin\delta,\ \eta"=|\eta^*|cos\delta$$

$$G^* = i\omega\eta^*,\ \eta' = \mathrm{G}"/\omega,\ \eta" = G'/\omega,\ \omega = 2\pi f,\ tan\delta = \mathrm{G}"/G' = \eta'/\eta"$$

where G^* is the complex modulus; G' is the storage modulus;$G"$ is the loss modulus; i is the imaginary unit; $|G^*|$ is the value of G^*; η^* is the complex viscosity; η' is the in-phase elastic component; $\eta"$ is the out-of-phase viscous component; $|\eta^*|$ is the value of η^*; δ is

phase lag between stress and strain; ω is the frequency of oscillation, rad/s; f is frequency of oscillation, Hz.

The parameters measured from static modes and dynamic modes can be related with each other by the Cox-Merz rule[45][46], given by:

$$|\eta^*| = \eta \text{ when } \omega = \dot{\gamma} \tag{2-9}$$

Just as in the static mode, there are also power law and Arrhenius equation for $|\eta^*|$ in the dynamic mode [50][51], as shown below.

The power law:

$$|\eta^*| = k\omega^{n-1} \tag{2-10}$$

$$\ln|\eta^*| = (n-1)\ln\omega + \ln k \tag{2-11}$$

The Arrhenius equation:

$$|\eta^*| = Ae^{\frac{E_a}{RT}} \tag{2-12}$$

$$\ln|\eta^*| = \frac{E_a}{RT} + \ln A \tag{2-13}$$

So, the dynamic mode can be adopted to extend the measurement range for viscous parameters, as the two modes have different measurement ranges for the same sample.

2.3.2 Rheological Properties of NBR Melts and Solutions

Anandhan et al. [50][51] reported the rheological properties of blends containing NBR. The measurement was carried out in a rotational rheometer with the parallel plate sensor under dynamic modes. Results show that $n = 0.62 - 0.80$, $k = 1.1\times10^3 - 8.9\times10^3$ $Pa\cdot s^n$ in the power law when $T = 190 - 230°C$ for the NBR melts; $E_a = 110\ kJ/mol$ at $\omega = 10 rad/s$, while $E_a = 15 kJ/mol$ at $\omega = 100 rad/s$ in Arrhenius equation for a sample containing 80%wt NBR. Nayak et al. [52] used the Monsanto Processibility

Tester (capillary rheometer) to study the rheological behavior of nitrile rubber/high styrene resin composites. Parameters for NBR melts reported are: $n = 0.59 - 0.62$, $k = 1.54 \times 10^4 - 2.81 \times 10^4 \ \ Pa \cdot s^n$ in the power law when $T = 100 - 140℃$; and $E_a = 3.34 - 5.07 \ \ kJ/mol$ in Arrhenius equation when $\dot{\gamma} = 316 - 1532 s^{-1}$. Kumar et al. [53] also studied the rheological properties of NBR blends with a capillary rheometer, reporting $n = 0.43$ at $T = 185℃$.

Rheological property of NBR-chlorobenzene solution was reported by Lei et al [8]. In their work, the solution shows Newtonian behavior in the shear level of $\dot{\gamma} : 10^1 - 10^2 s^{-1}$ and a correlation equation (Equation 2-14) was developed in the range of $T : 40 - 120℃ \ \& C\% : 2\% wt - 15\% wt$.

$$\eta = \exp(-8.109 + 0.03535C + \frac{807.9}{T} + \frac{140.658C}{T}) \tag{2-14}$$

where $C(0-100)$ is the weight percentage of NBR; T is in K; η is in $Pa \cdot s$.

Pan and Rempel [9] also studied the rheological properties of NBR-chlorobenzene solution, which was reported to behave approximately like Newtonian fluids in the shear level of $\dot{\gamma} : 10^1 - 10^2 s^{-1}$. Correlations were also developed (Equation 2-15 & 2-16).

$$\eta = c_1 \eta_{100} \exp(\frac{c_2 \eta_{100}^{c_3}}{T}) \tag{2-15}$$

where $c_1 = 0.0006439 Pa \cdot s$, $c_2 = 2736$, $c_3 = 0.01291$, and η_{100} is the viscosity at 100 ℃.

or:

$$\eta = 0.0001115 \exp\left[\frac{1704}{T} + C\left(13.41 + \frac{5315}{T}\right)\right] \tag{2-16}$$

where $C(0-1)$ is the weight percentage of NBR; T is in K; η is in $Pa \cdot s$.

Chapter 3 Research Methodology and Approaches

As mentioned in Chapter 1, there are mainly two topics for the current project: 1) the hydrogenation of NBR in high concentration solution; and 2) the rheological study of NBR melts and NBR solutions. In this chapter, some general information of experiments will be presented, both for the hydrogenation experiments and the rheological measurement. Detail information, such as modification of equipment and the detail operation procedure for a certain experiment, can be found in the corresponding chapter. The approach strategies for this research are also introduced here.

3.1 Experimental

3.1.1 Materials

All the chemicals were used as received. Nitrogen and hydrogen, both of 99.999% purity, were purchased from Praxair Inc. Chlorobenzene (laboratory grade) and methyl ethyl ketone (technical grade) were obtained from Fisher Scientific. Triphenylphosphine purchased from Acros Organics had a purity of 99%. Nitrile rubber (Perbunan T3429) containing 34%wt acrylonitrile unit was obtained from Lanxess Inc. Wilkinson's catalyst $RhCl(PPh_3)_3$ was also from Lanxess with 11.10%wt metal content.

3.1.2 Equipment

The main equipments used in this work include: (1) Parr 4560 Mini Bench Top Reactor (300mL) with Parr 4842 Temperature Controller; (2) Bio-Rad Excalibur 300MXPC System (FTIR) operated with Merlin software; (3) Thermo HAAKE MARS Rheometer operated with RheoWin 3 Software: for NBR melts the C20/1^o cone-plate sensor and Controlled Test Chamber (CTC) were used, while for solution samples

Pressure Sensor D400/300 (with PZ38b Rotor) and Temperature Controlled Cup Holder (heat jacket) were employed; (5) Vicotek GPCmax VE 2001 GPC Solvent/Sample Module with TDA 305 Triple Detector Array; (6) HE493 Dri-Train (Glovebox) from Vacuum Atmosphere Company; (7) Ohaus Analytical Plus Balance AP250D with a resolution of 0.01mg for catalyst weight and Sartorius Laboratory LC3200D for general purpose use.

3.1.3 FTIR Characterization

The hydrogenation degree, i.e. the conversion of hydrogenation reaction, is defined by Equation 3-1.

$$HD = \frac{[C=C]_0 - [C=C]}{[C=C]_0},\ HD = X \tag{3-1}$$

where $[C=C]_0$ is the $C=C$ concentration at the beginning and $[C=C]$ is the $C=C$ concentration at a certain time.

The rubber solution sampled during the reaction was spread on *NaCl* disc, which was tested in FTIR after it was dried. There are four main characteristic peaks in the FTIR spectrum of rubber solution, as shown in Table 3-1.

Table 3-1 Characteristic Peaks of FTIR Spectrum for NBR and HNBR

(modified from the original table in Wei's work [2])

Peak	Wave Number	Structure	Note
A	2236 cm^{-1}	$-CN$	internal standard
B	970 cm^{-1}	$-CH=CH-$, backbone	Decreases and disappears
C	920 cm^{-1}	$-CH=CH_2$, vinyl	Decreases and disappears
D	723 cm^{-1}	$-(CH_2)_n-$, $(n>4)$	appears and increases

Before hydrogenation reaction, there are peak A, B and C in NBR spectrum. As the hydrogenation reaction goes on, peak A keeps constant, peak B & C decrease, while

peak D appears and increases. Finally, in HNBR there are peak A and D, while peak B & C disappears or have very low values (Figure 3-1).

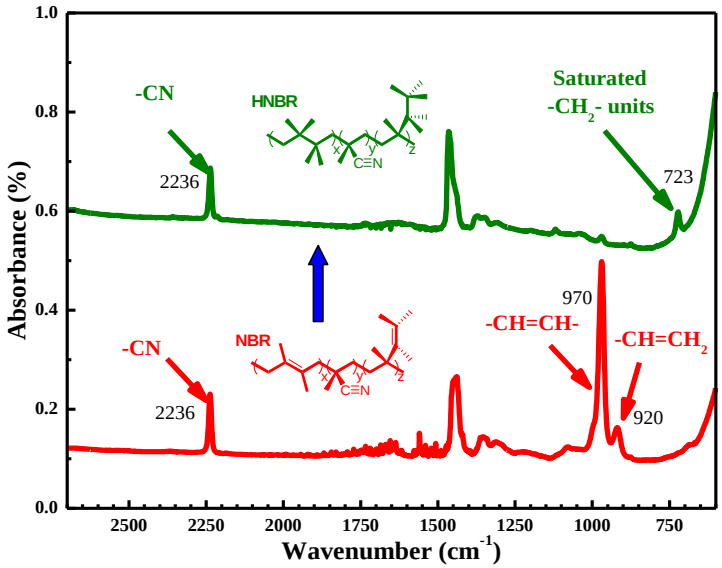

Figure 3-1 FTIR Spectrum: from NBR to HNBR (Modified from Wei's Work [2])

The hydrogenation degree is calculated based on corresponding absorbance of the important peaks shown in Figure 3-1. Peak A is taken as internal standard, as $-CN$ group is not hydrogenated during the reaction. As for $C=C$, only peak B is counted because less than 5% of the $C=C$ in NBR present in the vinyl form ($-CH=CH_2$). Let A_{2236}, A_{970} and A_{723} represent the absorbance at peak A, B and D respectively, as follows [2]:

$$A(970)=\frac{A_{970}}{A_{2236}},\ A(723)=\frac{A_{723}}{A_{2236}}$$

Also,

$K(970)=2.3$, a constant specific to peak B;

$K(723)=0.255$, a constant specific to peak D;

$$F=1+\frac{A(970)}{K(970)}+\frac{A(723)}{K(723)}$$

Then, the relative amount of residual $-CH=CH-$(peak B) and the relative amount of forming methylene groups $-(CH_2)_n-$ (peak D) could be expressed as follows:

$$C_{-CH=CH-}=\frac{A(970)}{K(970)\times F},\ C_{-(CH_2)-}=\frac{A(723)}{K(723)\times F}$$

So, the hydrogenation degree could be expressed by Equation 3-2 [2].

$$HD=\left[1-\frac{C_{-CH=CH-}}{C_{-CH=CH-}+C_{-(CH_2)-}}\right]\times 100\% \qquad (3\text{-}2)$$

The calculation process can be finished in Microsoft Excel, as long as the values of A_{2236}, A_{970} and A_{723} are provided.

During the experiment, it is found that the absorbance peak for the co-catalyst (TPP) is around 720cm^{-1}, which will affect the reading of peak D. Thus, TPP is removed before FTIR test, especially when relatively high amount of catalyst is used. By adding ethanol into the reaction solution, polymer is precipitated, while TPP is still dissolved in the solvent. Then, rubber is re-dissolved in MCB for the FTIR analyses.

3.2 Approach Strategies

First, the batch reactor was modified and the controller was tuned to fit the hydrogenation in high concentration solution which is a severe exothermic reaction. In this process, the recipe of reactants was the same. Temperature-time curves were recorded and reproducibility under different conditions was compared.

Then, hydrogenation of NBR in high concentration solution was carried out systemically, focusing on parameters that might affect the reaction rate, such as the agitator shape, the stirring speed, catalyst concentration and so on. During this process, an interesting phenomenon was observed when low catalyst concentration was applied.

Thus, several more experiments were designed to investigate this aspect; and experiments for SBR hydrogenation were also carried out for comparison.

Meanwhile, rheological measurements were carried out. The NBR-MCB samples with different hydrogenation degree were prepared in the hydrogenation experiments. The viscosity data measured was used for agitator design, which in turn provided useful information for the hydrogenation reactions. NBR melts, as well as the NBR-MEK solutions were also tested in rheometer, in order to get a better overview of the rheological properties of this rubber.

Chapter 4 Rheological Properties of NBR Melts and NBR Solutions

Rheological properties, such as viscosity and modulus, are fundamental physical properties for polymer materials. These parameters are essential during the reactor design process, e.g., the selection of reactor type, the design of agitator and reactor internals. Although there are some reports on the rheological properties of nitrile rubber, detail information for the current research system is still insufficient. In the current work, NBR melts and NBR solutions were tested in the HAAKE MARS rheometer, to get the rheological properties. The information collected from these experiments is useful for reactor design and scale up for bulk hydrogenation, hydrogenation in high concentration solution and continuous solution hydrogenation.

4.1 Viscosity of NBR Melts

Rheological parameters include viscous parameters such as viscosity η, and elastic parameters such as storage modulus G' and loss modulus G". The NBR melts is a viscoelastic fluid, instead of a pure-viscous fluid or pure elastic substance. Thus, both the viscous and elastic properties of the NBR melts should be considered during rheological studies. In the current study, the static mode was adopted to investigate the viscous parameters, i.e. the shear rate increases linearly as time goes. To get elastic parameters, the dynamic mode, i.e. shear rate varies according to sine function as time goes, was also performed.

4.1.1 Experimental

Materials and equipment were described in Chapter 3. The detail operation procedure was shown below.

Step 1: Sample Preparation

The NBR crumb was wrapped with weighting paper and then left under a heavy lead brick. A thin layer of NBR around 1 mm thick was formed after a few hours, which was further cut into rubber discs with a diameter of 2 cm.

Step 2: Loading & Preheat

The rheometer system was set up with the C20/1 ° cone-plate sensor. The gap between the cone and the plate (C20/1 °) was zeroed by pressing "Automatic Zero". Then, the rubber disc was loaded onto the plate. The chamber was closed and the heater was activated. During the heating process, nitrogen was used as a protection gas to prevent oxidation, burning or crosslinking of the rubber sample. (CAUTION: the "go to gap" button was used to lower the cone to the plate to reach the measurement gap which was very narrow. Do NOT press "go to gap" in this step, otherwise the rheometer could be damaged, as the rubber was still very hard.)

Step 3: Remove the Overloaded Sample

After the temperature reached 120 ℃, the cone was lowered to reach the measurement gap by pressing "go to gap", which might take a few seconds as the rubber showed strong elastic properties. Then, the chamber was opened and the edge of the cone was shaved by a spatula to remove overloaded rubber, after which the chamber was closed. During this process the temperature in the chamber would be interrupted.

Step 4: Measurement

When the temperature reached the set point and became steady, measurement was started. Detail instruction of the software operation could be found in the manual.

Step 5: After Measurement

After measurement was finished, the heater was stopped. Then, the chamber was opened and the cone was raised up. After the system cooled down, the sensor was cleaned using soft materials. (Hard materials or sharp tools could destroy the surface of the cone/plate.)

4.1.2 Results and Discusstion

4.1.2.1 Static Mode

NBR melts was tested in rheometer with C20/1 °cone-plate sensor under the static mode, i.e. the shear rate/ shear stress increases linearly as time goes, in order to find out the effect of temperature on viscosity.

The temperature studied ranged from 138 ℃ to 155 ℃ and the shear rate varies from $0s^{-1}$ to $1s^{-1}$. Figure 4-1 is the $\eta - \dot{\gamma}$ curves, showing how viscosities vary with shear rate at different testing temperatures.

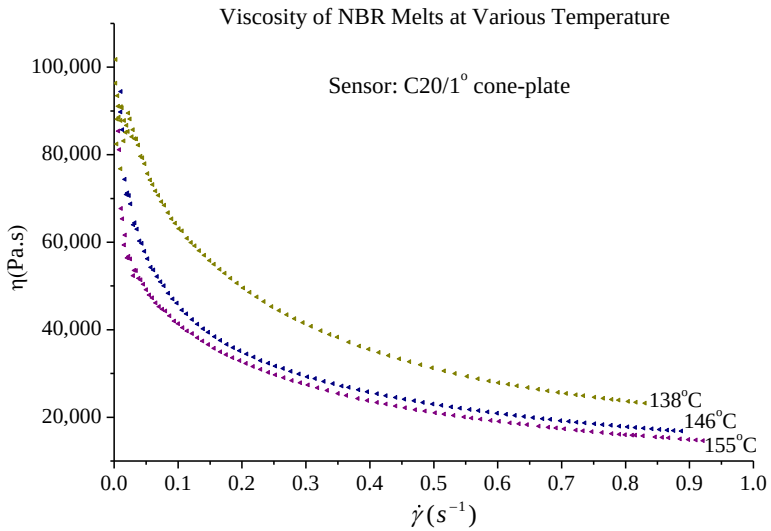

Figure 4-1 $\eta - \dot{\gamma}$ Curves for NBR Melts under 138 ℃, 146 ℃ and 155 ℃

As can be seen in Figure 4-1 that as the shear rate increases the viscosity of NBR melts decreases; while, at the same shear rate, as the temperature increases, the viscosity of NBR melts decreases.

(1) The Power Law

Natural logarithm of the values for both viscosity and shear rate (Figure 4-1) were taken and then the $\ln\eta - \ln\dot{\gamma}$ curve was plotted (Figure 4-2).

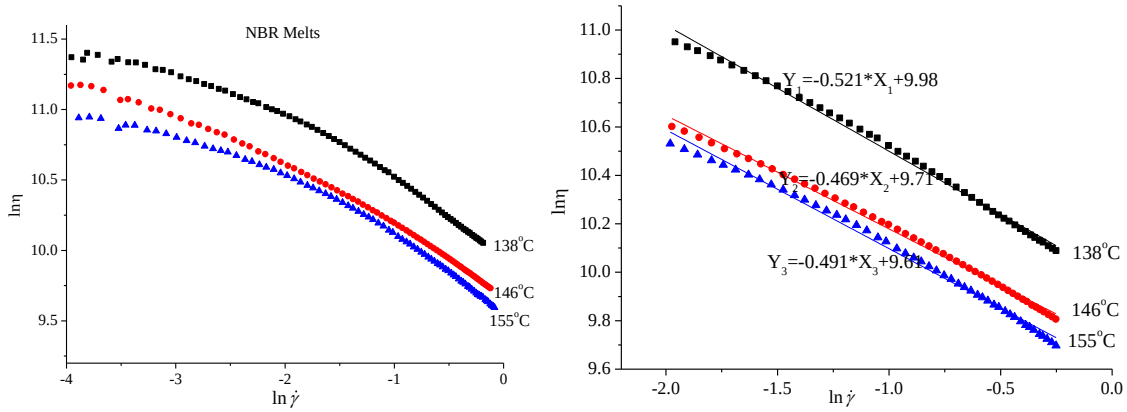

(a) (b)

Figure 4-2 $\ln\eta - \ln\dot{\gamma}$ Plot for NBR Melts under 138 ℃, 146 ℃ and 155 ℃

It is shown in Figure 4-2 that the dots in $\ln\eta - \ln\dot{\gamma}$ diagram approximately fall on a line, especially dots in late stage. This means that the sample shows some Newton properties at relatively high shear rate. The power law for static modes is given by Equation 2-5 or Equation 2-6. After linear regression of the dots in late stage as shown in Figure 4-2(b), parameters in the power law could be calculated as listed in Table 4-1.

Table 4-1 Parameters in Power Law for NBR Melts (Static Mode)

T(℃)	n	$k(Pa\cdot s^n)$
138	0.479	21,590
146	0.531	16,481
155	0.509	14,913

The value of k decreases as the temperature increases, corresponding to the experimental results that the viscosity decreases as temperature increases at a certain shear rate.

(2) The Arrhenius Equation

The relation between viscosity η and temperature T could be presented by the Arrhenius equation (Equation 2-7 and Equation 2-8). The viscosity of NBR melts under different temperatures at the same shear rate ($0.7s^{-1}$) was listed in Table 4-2.

Table 4-2 Viscosities of NBR Melts at $\dot{\gamma} = 0.7s^{-1}$

T(°C)	$\eta(Pa \cdot s)$ at $\dot{\gamma} = 0.7s^{-1}$
138	25,500
146	19,200
155	17,400

Natural logarithm of the data (Table 4-2) was taken and then $\ln\eta - \frac{1}{T}$ curve was plotted as shown in Figure 4-3.

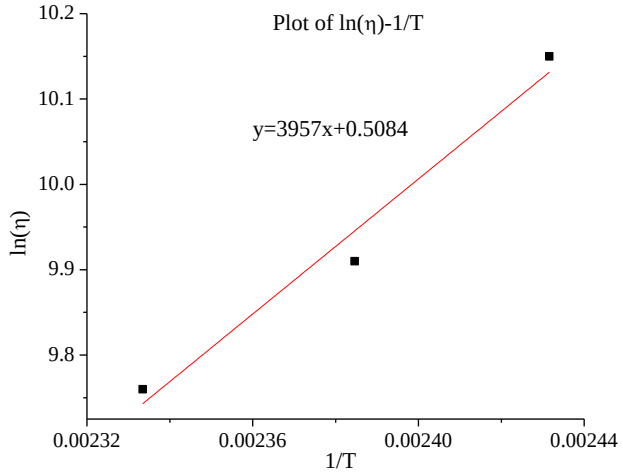

Figure 4-3 $\ln\eta - \frac{1}{T}$ Plot for NBR Melts

Linear regression was carried out as shown in Figure 4-3 and the activity energy was calculated to be 33kJ/mol (at $\dot{\gamma} = 0.7s^{-1}$).

4.1.2.2 Dynamic Mode

(1) Strain Sweep

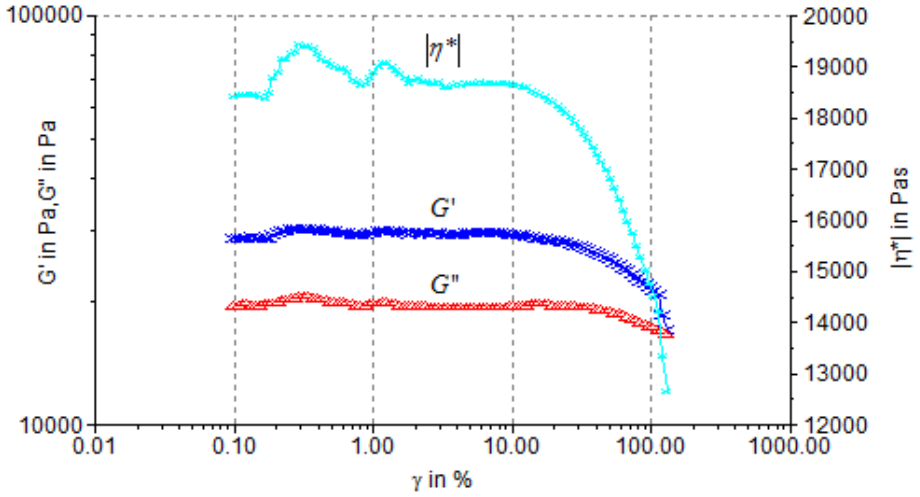

Figure 4-4 Strain Sweep of NBR Melts

($\gamma = 0.100\% - 129\%$; $T = 168°C$; $f = 0.3Hz$)

Figure 4-4 the strain sweep of NBR melts shows that the linear elastic range of NBR under 168 ℃ is within the strain of 10%.

(2) Stress Sweep

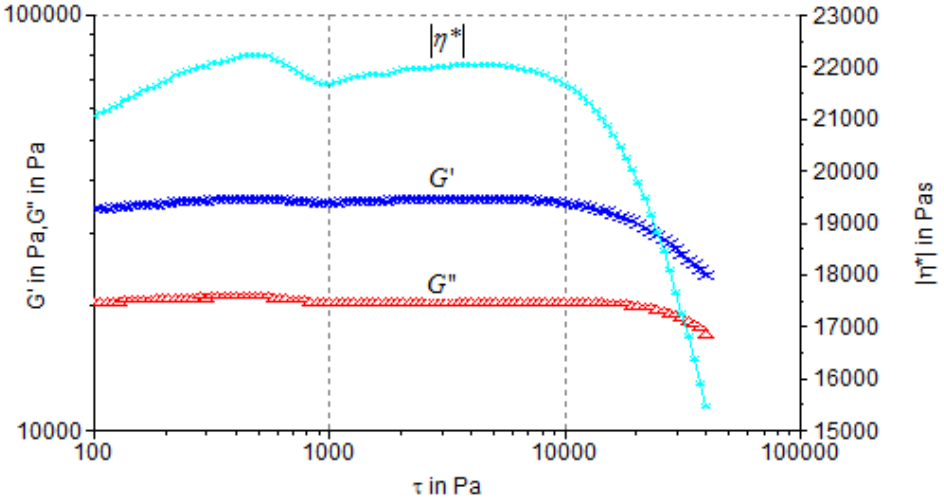

Figure 4-5 Stress Sweep of NBR Melts

($\tau = 100.0Pa - 40000Pa$; $T = 168°C$; $f = 0.3Hz$)

Figure 4-5 the stress sweep of NBR melts shows that the linear elastic range of NBR under 168 ℃ is within the stress of 10000Pa.

(3) Time Sweep

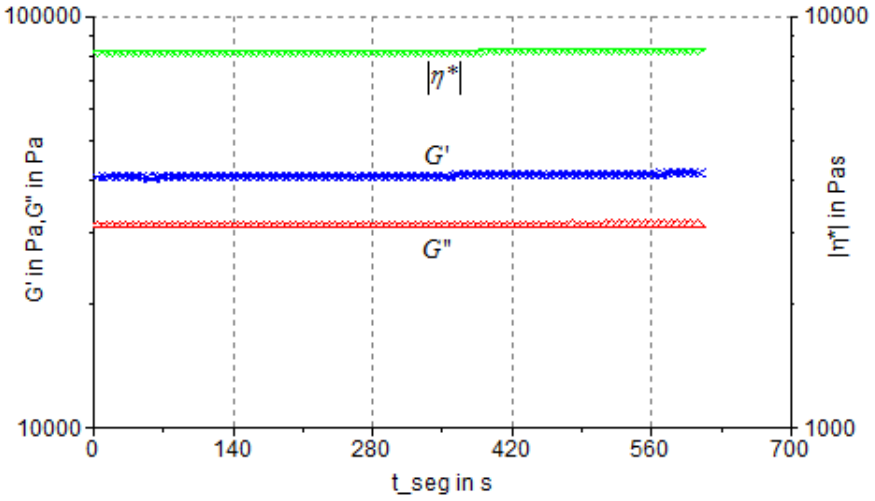

Figure 4-6 Time Sweep of NBR Melts

($t = 0 - 600s$; $T = 168℃$; $f = 1.000Hz$; $\gamma = 30\%$)

Figure 4-6 the time sweep of NBR melts shows that the sample is thermal steady under the test temperature 168 ℃, during the test time 10min.

(4) Temperature Sweep

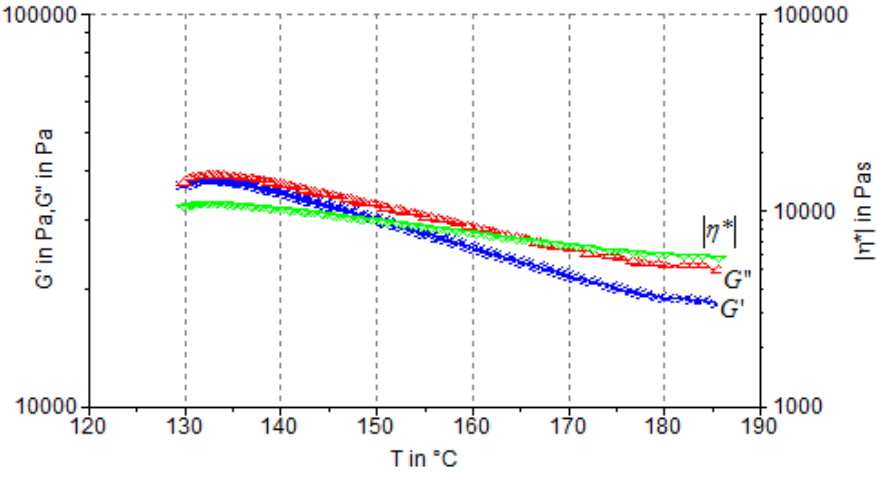

Figure 4-7 Temperature Sweep of NBR Melts

($T = 130 - 185℃$; $\tau = 6000Pa$; $f = 0.8000Hz$)

Figure 4-7 the temperature sweep of NBR melts shows that the storage modulus G' and the loss modulus $G"$, as well as the value of the complex viscosity $|\eta^*|$, decrease linearly as temperature T increases.

For dynamic modes, the relation between viscosity η and temperature T can also be presented by the Arrhenius equation (Equation 2-12 and Equation 2-13). Natural logarithm of the $|\eta^*| / Pa \cdot s - T / K$ data (Figure 4-7) was taken and then the $\ln|\eta^*| - \frac{1}{T}$ curve was plotted, as shown in Figure 4-8.

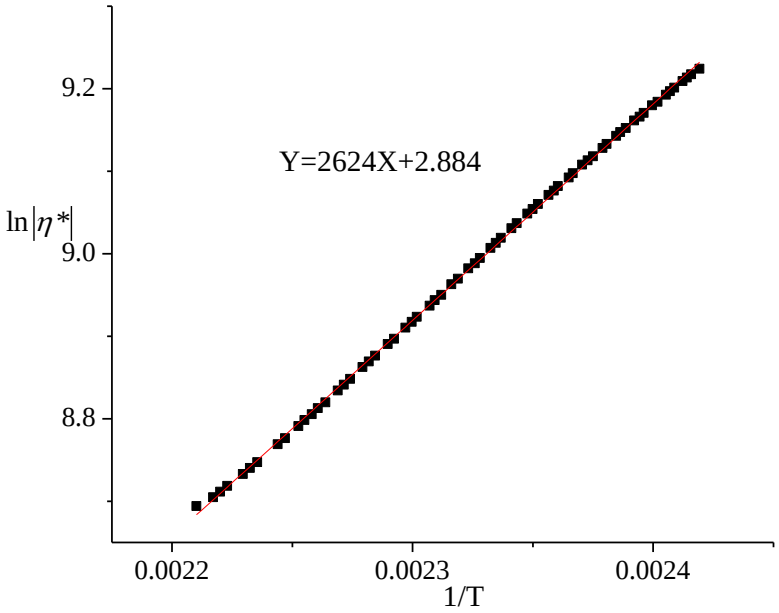

Figure 4-8 $\ln|\eta^*| - \frac{1}{T}$ Plot for NBR Melts

Linear regression was carried out (Figure 4-8) and the activity energy was calculated to be 21.8kJ/mol (at $f = 0.80Hz$).

(5) Frequency Sweep

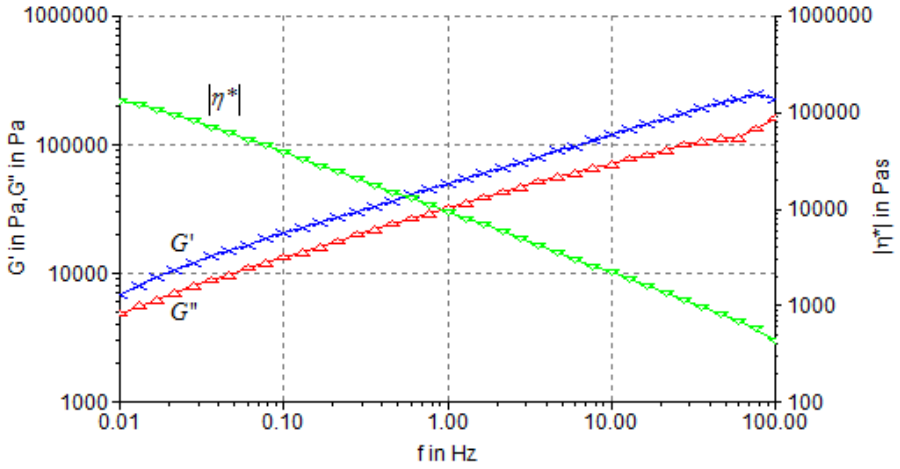

Figure 4-9 Frequency Sweep of NBR Melts

($f = 0.010Hz - 100Hz$; $T = 168℃$; $\tau = 3000Pa$)

As frequency f increases, the storage modulus G' and the loss modulus $G"$ increase while the value of the complex viscosity $|\eta^*|$ decreases. The power law for dynamic modes is given by Equation 2-10 or Equation 2-11. The data shown in Figure 4-9 was converted from $f(Hz)$ to $\omega(rad/s)$. Then, Natural logarithm was taken and the $\ln|\eta^*| - \ln\omega$ curve was plotted as shown in Figure 4-10.

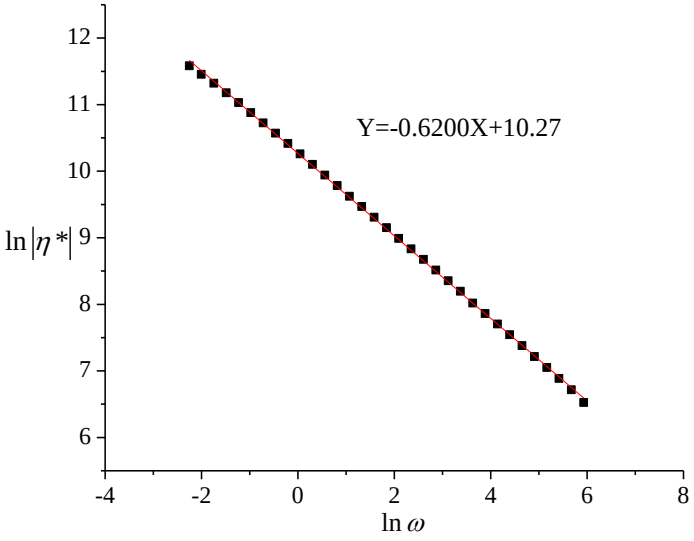

Figure 4-10 $\ln|\eta^*| - \ln\omega$ Plot for NBR Melts

Linear regression was carried out (Figure 4-10) and the parameters in power law was calculated to be $n = 0.38$ and $k = 28,854 Pa \cdot s^n$

4.1.3 Summary

Experimental results measured under static modes and dynamic modes could be related by the Cox-Merz rule (Equation 2-9). Thus, the dynamic mode could be adopted to extend the measurement range, where the static mode is not suitable.

Table 4-3 & 4-4 shows the comparison of parameters calculated from the two different measurement modes.

Table 4-3 Parameters for the Power Law, Static vs. Dynamic

Mode	T(°C)	$\dot{\gamma}(s^{-1})$ or $\omega(rad/s)$	n	$k(Pa \cdot s^n)$
Static Mode	138	0.135 – 0.779	0.479	21,590
	146	0.135 – 0.779	0.531	16,481
	155	0.135 – 0.779	0.509	14,913
Dynamic Mode	168	0.135 – 403	0.380	28,854

Table 4-4 Parameters for the Arrhenius Equation, Static vs. Dynamic

Mode	T(°C)	$\dot{\gamma}(s^{-1})$ or $\omega(rad/s)$	$E_a(kJ/mol)$
Static Mode	138 – 155	0.7	33
Dynamic Mode	140 – 180	5.02	21.8

As seen in Table 4-3 and Table 4-4, parameters calculated from the two modes are at the same level, although not exactly the same.

The experimental values measured in the current work are also compared with those reported in literature as listed in Chapter 2. Parameters in the power law have similar values with those reported, while the activity energy is apparently lower than the reported values.

4.2 Viscosity of NBR in MEK

Methyl ethyl ketone(MEK) solution of nitrile rubber was tested in Thermo HAAKE MARS rheometer with the cylinder sensor to measure the viscosity.

4.2.1 Experimental

Materials and equipments were described in Chapter 3. The detail operation procedure was shown below.

Step 1: Sample Preparation

Nitrile rubber (10g) was dissolved in methyl ethyl ketone (90g, 111.8ml), left on the shaker for several hours to ensure complete dissolution.

Step 2: Samples Loading & Sensor Assembly

The rheometer system was set up for the D400/300 Pressure Sensor with the cup holder. The polymer solution (20mL) was loaded into the measuring cup of the sensor using a syringe or a graduated cylinder. Then, the PZ38b rotor was put into the measuring cup slowly. After making sure the rotor had touched the bottom of measuring cup, the cover flange was fixed to seal the cylinder. Then, the outer magnet was attached to rheometer head.

Step 3: Measurement

The gap between the outer magnet and the cover flange was zeroed by pressing "Automatic Zero" and then set to the measurement gap by pressing "Go to Gap". After this, the measurement was started. Detail instruction of software operation could be found in the manual of the rheometer.

Step 4: After Measurement

After measurement was finished, the rheometer head was raised up and the outer magnet was detached. Before unloading the measuring cup from the rheometer, the cover flange should be opened with the rotor pulled out. When cleaning the sensor, soft materials should be used instead of hard materials or sharp tools which could destroy the surface of rotor/measuring cup.

4.2.2 Results and Discussions

NBR-MEK solutions were tested at room temperature (25 ℃), using a cylinder sensor. The shear rate increases linearly from 0 to 1000s^{-1} in 120s. The experimental result was shown in Figure 4-11.

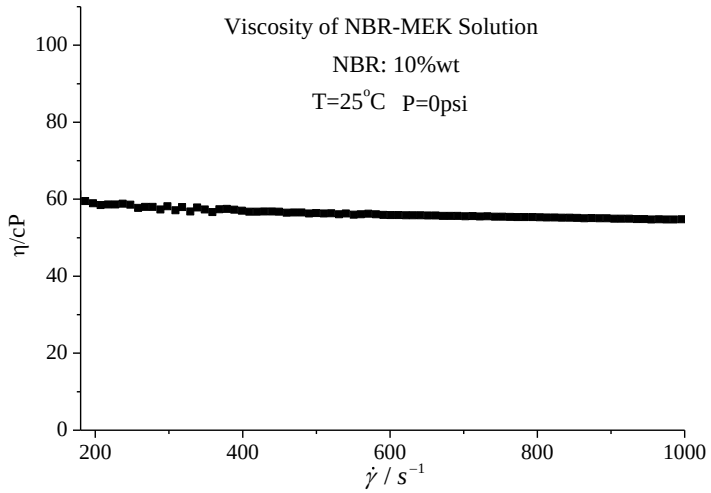

Figure 4-11 $\eta - \dot{\gamma}$ Curve for 10% NBR-MEK Solution under 25 ℃

As can be seen in Figure 4-11 that the 10% NBR-MEK solution could be regarded a Newtonian fluid and the viscosity is around 55 cP at room temperature.

4.3 Viscosity of NBR solutions in MCB

Rheological properties of NBR-MCB solutions with different hydrogenation degree were studied in the MARS rheometer with the cylinder sensor. Measurement was carried out under both the static and dynamic mode to study the viscous and elastic properties, respectively.

4.3.1 Experimental

Materials and equipment were generally described in Chapter 3. Accurate temperature control of the cylinder sensor was achieved by using the following two equipments together: 1) HAAKE DC30-B5 Heating Circulator; and 2) Thermo NESLAB RTE-10 Digital One Refrigerated Bath.

4.3.1.1 Operation Procedure

Step 1: Sample Preparation

The NBR-MCB solutions were prepared in Parr reactor, with differences in polymer concentration, hydrogenation degree and catalyst concentration. The detail process could be found in Chapter 5.

Step 2: Sample Loading & Sensor Assembly

The rheometer system was set up for the D400/300 Pressure Sensor with the cup holder. The polymer solution (20mL) was loaded into the measuring cup by a syringe. Then, the PZ38b rotor was put into the measuring cup slowly. After making sure that the rotor had touched the bottom of measuring cup, the cover flange was fixed to seal the cylinder. Then, the outer magnet was attached to the rheometer head.

Notes: 1) it was not suitable to use graduated cylinders for loading samples, as the solutions were very viscous and a large portion of the sample would stick on the cylinder

wall; 2) due to the high viscosity, it was difficult for the rotor to sink down into the measuring cup, so it was suggested to rotate the rotor and push it down slowly with hands. Do NOT put on the cover flange until the rotor touch the bottom; otherwise, the sapphire bearing might be damaged.

Step 3 Cooling & Degassing

The gap between the outer magnet and the cover flange was zeroed by pressing "Automatic Zero" and then set to the measurement gap by pressing "Go to Gap". The 3-way valve TV2 was turned to RTE-10 Refrigerated Bath. The RTE-10 was started with the setpoint of 2.2℃. Then, the DC30-B5 Heating Circulator was started with the setpoint of 4.1 ℃. At this time, DC30-B5, which was connected to the cup holder, was used to cool down the cylinder sensor; while RTE-10 was used to cool down DC 30-B5 through the internal cooling coil in DC30-B5, as shown in Figure 4-12. After about 30min, the temperature inside the measuring cup settled around 8-9℃. At this temperature, the volatilization of chlorobenzene during degassing should be effectively suppressed. The nitrogen cylinder and the purge tubing were connected to the 3-way valve TV1. Then, the needle valve V1 was opened and degassing was started.

Step 3-1:

The TV1 was switched to nitrogen and the cylinder was pressurized to 500psi. Then, the TV1 was switched to purge tubing to release the pressure (down to 50psi). This step (Step 3-1) should be repeated for 3-5 times.

Step 3-2:

The cylinder was pressurized up to 500psi. Then, the outer magnet was started with a very low rotation speed, e.g. $\dot{\gamma} = 0.1s^{-1}$. After 20 minutes, the rotation of outer magnet

was stopped, and then the pressure was released to 100psi. This step (Step 3-2) should be repeated for 3 times.

Note: it was suggested to stop the rotation of the outer magnet when increasing or decreasing the pressure inside the cylinder sensor, in order to protect the sapphire bearing.

Step 4 Heating

The RTE-10 was turned off and the TV2 was switched to air supply. The needle valve V2 was opened to introduce air from utility. After the residual water in the cooling coil was blown out, the valve V2 was turned off. The DC30-B5 was set to 150.3℃, starting to heat. The initial pressure inside the cylinder sensor was around 100 psi. After a few minutes, the outer magnet was started with a low rotation speed, e.g. $\dot{\gamma} = 5s^{-1}$, to improve the heat transfer inside the cylinder sensor. After around 50min, the temperature was steady at 145℃ and the pressure inside cylinder sensor was around 300psi. The rotation of outer magnet was stopped, and then TV1 was switched to nitrogen to pressure the cylinder sensor up to 500psi. Then, both TV1 and V1 were turned off.

Step 5 Measurement

Measurement was carried out under the static mode or the dynamic mode. Detail instruction of software operation could be found in the manual.

Step 6: After Measurement

After measurement was finished, the rheometer head was raised up. The DC30-B5 was set to 4.1℃. The TV2 was turned to RTE-10. The RTE-10 was started with the setpoint of 2.2℃ to cool down the system to room temperature. After 30min, the rheometer, DC30-B5 and RTE-10 were all turned off. Then, the outer magnet was detached from the rheometer head. Before unloading the measuring cup from the

rheometer, the cover flange should be opened with the rotor pulled out. Methyl ethyl ketone was used to clean the rotor and the measuring cup. When cleaning the sensor, soft materials should be used instead of hard materials or sharp tools which could destroy the surface of rotor/measuring cup.

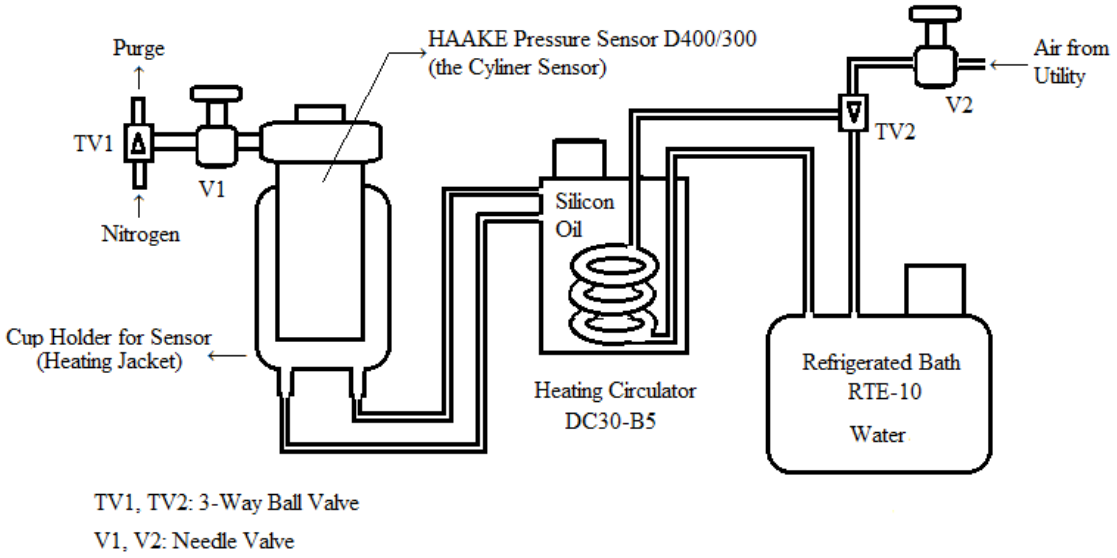

Figure 4-12 Flowsheet of the Rheometer System

4.3.1.2 Temperature Control

Bath Liquid:

For optimum temperature accuracy, it is important that the heat transfer liquid be of low viscosity. Especially for our measurement system, lots of heat is produced when the rotor rotates in the high viscosity samples. If the heat transfer liquid (bath liquid) cannot flow fast enough to take away the heat produced, heat will accumulate inside the cylinder sensor and raise the temperature. According to the manual of DC30-B5, the viscosity of the bath liquid should be below 30cP for proper working. If accurate temperature control should be achieved, the viscosity of bath liquid should be kept under 10cP at working temperature. So, the silicon oil "Sil 180" was ordered from Thermo

HAAKE (Ord-No. 999-0204), with the following properties: 1) working temperature range: 95℃ to 200 ℃; 2) operating temperature range: -40 ℃ to 95 ℃; 3) viscosity under room temperature: 11cP.

Hoses selection:

The length of a hose and its diameter combined with the circulating capacity have a large effect on the temperature control effectiveness. So, choose a hose that is wider in diameter and place the circulator to the rheometer as close as possible. In the current case, the hose should also be compatible with high temperature (over 160 ℃) silicon oil. Insulation wraps for the hose, made from material which can bear high temperature, is needed as well. According to this, suitable hoses (Con Bore Ins wrap 3/8") were ordered from Swagelok (Ord-No. SS-NC6TA6TA6-36), with the following features: 1) internal diameter 3/8"; 2) length 36 inch/ 3 feet; 3) Teflon core; 4) with insulation; 5) as flexible as PVC hoses.

Others:

Some silicon oil was spread on the surface of the measuring cup, to improve the heat transfer between the measuring cup and the cup holder (heating jacket). The jacket was wrapped with cloth, to reduce heat loss.

After improvement, the temperature inside the cylinder sensor (inside the measuring cup) can be controlled at 145 ℃ with ±0.1 ℃ difference.

4.3.1.3 Protection Gas

At a certain temperature, the viscosity of the solution is related with the pressure applied, as well as the type of gas that is used to pressure the system. Figure 4-13 shows that, at constant shear rate $100s^{-1}$, the viscosity of 15% NBR solution decreases as

temperature increases. At the time 4930 s, the system was pressurized from 0psi up to 500psi suddenly by N_2. The viscosity jumped up as the pressure was applied.

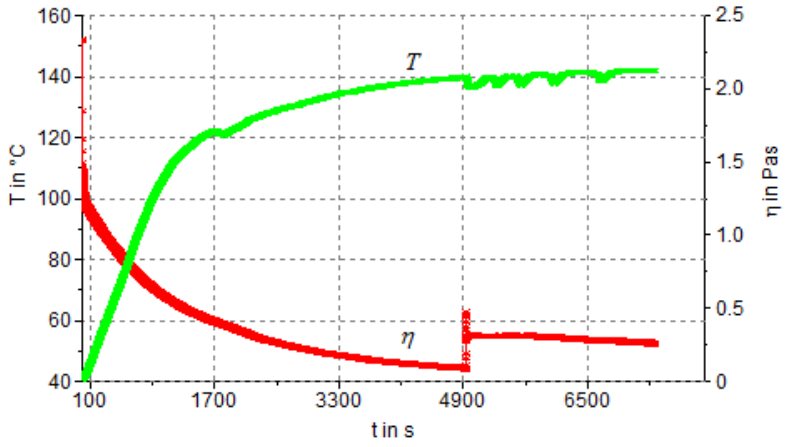

Figure 4-13 Viscosity of 15% NBR-MCB Solution at $\dot{\gamma} = 100 s^{-1}$

Both hydrogen and nitrogen were used to study the effect on the viscosity measurement. Figure 4-14 shows how the viscosity of 7% NBR solution changes when the pressure was applied, using nitrogen or hydrogen, at the constant temperature 25 ℃.

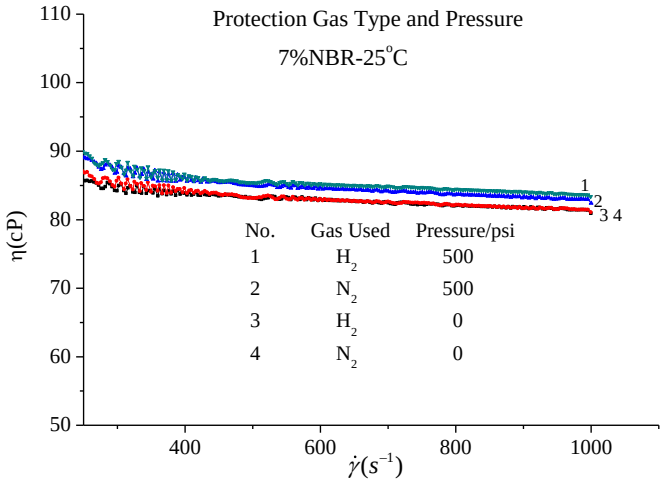

Figure 4-14 Viscosity of 7% NBR-MCB Solution: Protective Gas & Pressure

As shown in Figure 4-14, at low pressure the viscosity is not sensitive with the types of gas applied; while at high pressure there is small difference whether hydrogen or nitrogen was applied. In order to prevent the possible hydrogenation/crosslinking reactions during

measurement for samples containing catalyst, nitrogen will be used as the protection gas in the following research.

4.3.2 Results and Discussion

There are many parameters that may affect the viscosity of NBR solutions, such as hydrogenation degree, polymer concentration, catalyst concentration, crosslinking and mixing. Some of these parameters will be discussed in the following parts, and others are still left for future research.

4.3.2.1 The Effect of HD on Viscosity (7% solution)

Viscosities of the 7% NBR solutions with different hydrogenation degree were measured in rheometer under room conditions (25 ℃ & 0psi) and reaction conditions (145 ℃ & 500psi), using the cylinder sensor. Figure 4-15 & 4-16 show the viscosity-shear rate curves for experiment under room conditions and reaction conditions, respectively.

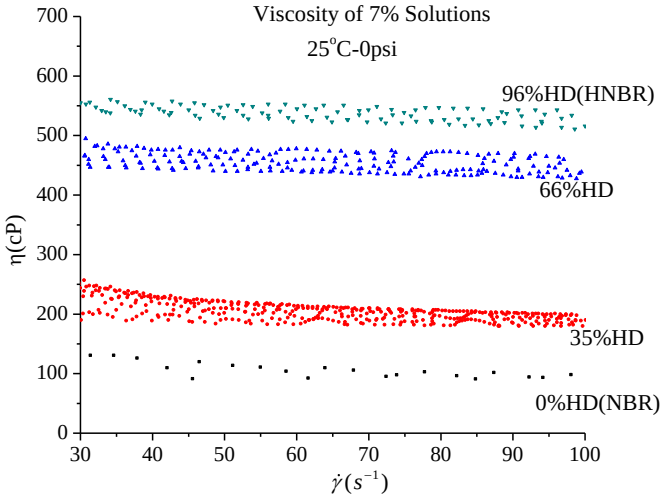

Figure 4-15 $\eta - \dot{\gamma}$ Curves for 7% NBR-MCB Solutions under Room Condition

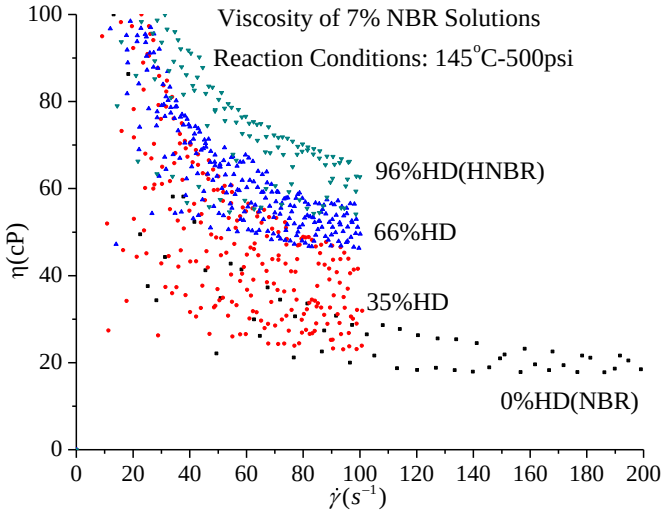

Figure 4-16 $\eta - \dot{\gamma}$ Curves for 7% NBR-MCB Solutions under Reaction Condition

As can see in Figure 4-15 & 4-16, the 7% NBR-MCB solutions could be regarded as a Newtonian fluid, if neglecting the first few data at low shear rate.

Table 4-5 is a summary of the viscosities of the 7% NBR-MCB solutions with different hydrogenation degree measured in rheometer under room conditions (25 ℃ & 0psi) and reaction conditions (145 ℃ & 500psi).

Table 4-5 Summary of the Viscosities of the 7% Solutions

Hydrogenation Degree	Viscosity/cP	
	25 ℃, 0psi	145 ℃, 500psi
0% (NBR)	81	17
35%	210	35
66%	440	50
96%(HNBR)	520	60

By plotting viscosity against hydrogenation degree for the viscosity under reaction conditions, i.e. 145 ℃, 500psi, Figure 4-17 was obtained.

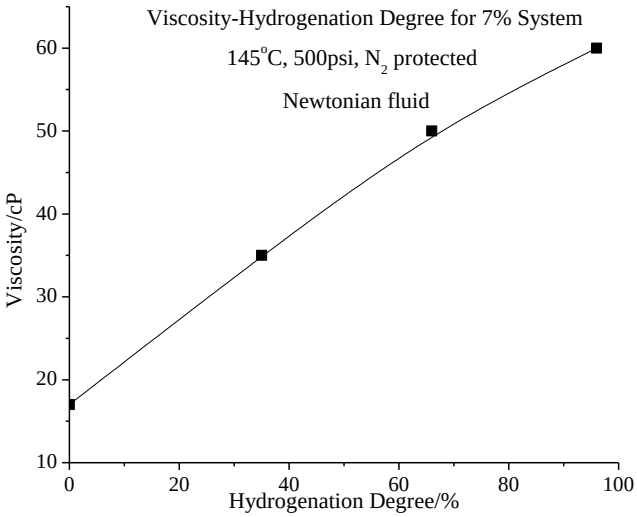

Figure 4-17 $\eta - HD$ Curve for 7% System under Reaction Condition

The curve in Figure 4-17 reflects how the viscosity of reaction solutions changes as the conversion of the reaction increases.

4.3.2.2 The Effect of HD on Viscosity (15% solution)

Viscosities of the 15% NBR solutions with different hydrogenation degree were measured in rheometer under room conditions (25 ℃ & 0psi). Figure 4-18 shows the viscosity-shear rate curves for experiment.

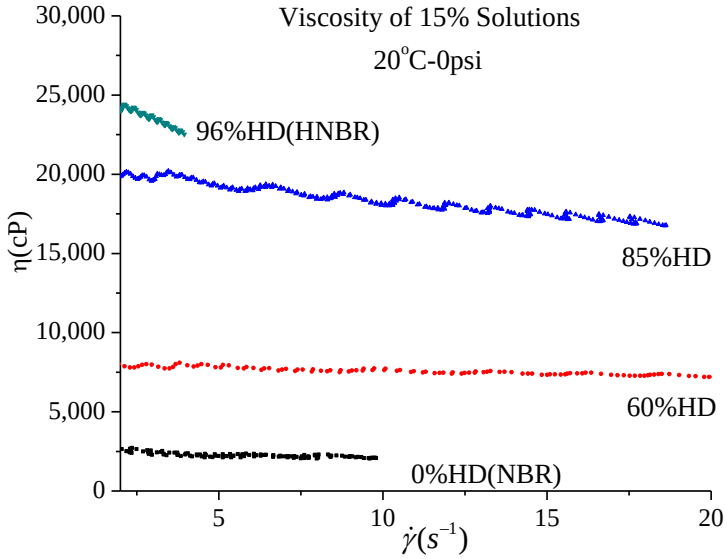

Figure 4-18 $\eta - \dot{\gamma}$ Curves for 15% NBR-MCB Solutions under Room Condition

As can be seen in Figure 4-18, the 15% NBR-MCB solutions with low hydrogenation degree (i.e. 0%HD & 60%HD) could be regarded as Newtonian fluids.

However, the samples with high hydrogenation degree (i.e. 85% HD& 96%HD) deviate from Newtonian behavior. Assuming the solution with a high hydrogenation degree is a generalized Newtonian fluid following the Equation 2-4 and the viscosity could be expressed by the power law (Equation 2-5 or Equation 2-6). Natural logarithm of the data (85%HD & 96%HD) in Figure 4-18 was taken and then $\ln\eta - \ln\dot{\gamma}$ curves were plotted as shown in Figure 4-19.

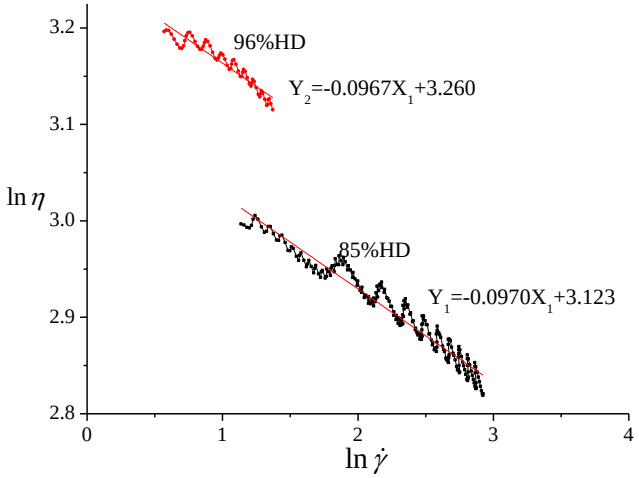

Figure 4-19 $\ln\eta - \ln\dot{\gamma}$ Plots for 85%HD and 96%HD Samples*

Linear regression was carried out (Figure 4-19) and the parameters in power law were calculated, as shown below.

For 85%HD sample,

$$n = 0.903, k = 22.7 Pa \cdot s^n, \eta = 22.7\dot{\gamma}^{0.903-1}$$

For 96%HD sample,

$$n = 0.9033, k = 26 Pa \cdot s^n, \eta = 26\dot{\gamma}^{0.9033-1}$$

*Note: the R^2 of Figure 4-19b is not very high. n value of 96%HD sample is very likely to be smaller than that of 85%HD sample; as shown in Figure 4-19, the curve for 96%HD sample is steeper than that of 85%HD sample.

Table 4-6 is a summary of the viscosities of the 15% NBR-MCB solutions with different hydrogenation degree measured under room conditions (25 ℃ & 0psi).

Table 4-6 Viscosities of the 15% Solutions under Room Condition

Hydrogenation Degree	Viscosity/cP (25 ℃, 0psi)
0%HD(NBR)	2,000cP, Newtonian, $n=1$
60%HD	6,600cP, Newtonian, $n=1$
85%HD	17,000cP ($\dot{\gamma}=20s^{-1}$), $\eta=22.7\dot{\gamma}^{0.903-1}$
96%HD(HNBR)	22,000cP ($\dot{\gamma}=4s^{-1}$), $\eta=26\dot{\gamma}^{0.9033-1}$

Viscosities of the 15% NBR solutions with different hydrogenation degree were also measured in rheometer under reaction conditions (145 ℃ & 500psi). The experimental results were shown in Figure 4-20.

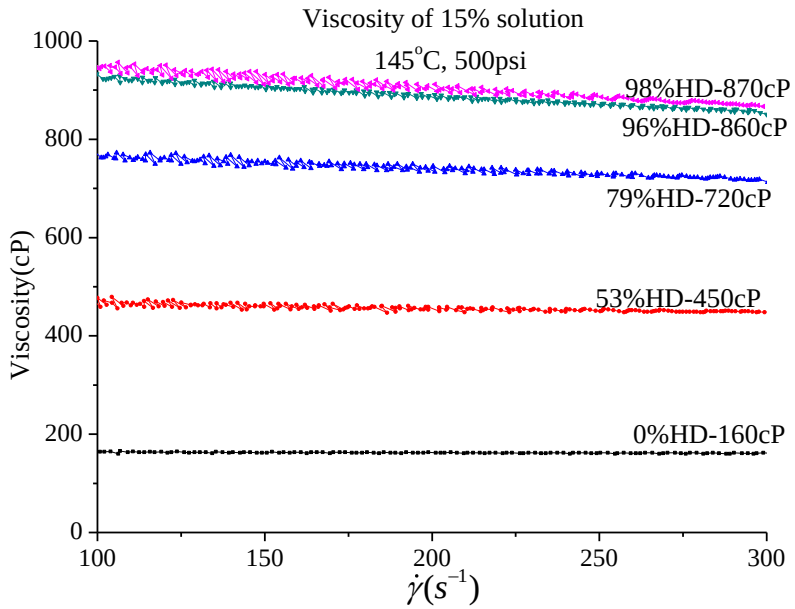

Figure 4-20 $\eta-\dot{\gamma}$ Curves for 15% NBR-MCB Solutions under Reaction Condition

As shown in Figure 4-20, the 15% NBR-MCB solutions with low hydrogenation degree (i.e. 0%HD & 53%HD) could be regarded as Newtonian fluids.

However, the samples with high hydrogenation degree (i.e. 79%HD, 96%HD & 98%HD) deviate from Newtonian behavior. Assuming the solution with a high hydrogenation degree is a generalized Newtonian fluid and the viscosity could be expressed by the power law (Equation 2-5 and Equation 2-6). Natural logarithm of the data (79%HD, 96%HD & 98%HD) in Figure 4-20 was taken and then $\ln\eta - \ln\dot{\gamma}$ curves were plotted as shown in Figure 4-21.

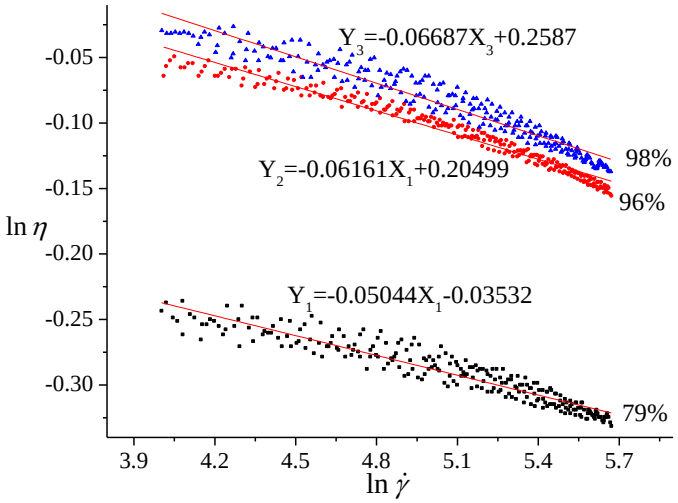

Figure 4-21 $\ln\eta - \ln\dot{\gamma}$ Plots for 79%HD, 96%HD and 98%HD Samples

Linear regression was carried out (Figure 4-21) and parameters in power law were calculated as shown below.

For 79%HD sample,

$$n = 0.9496,\ k = 0.9653 Pa\cdot s^n,\ \eta = 0.9653\dot{\gamma}^{0.9496-1}$$

For 96%HD sample,

$$n = 0.9384,\ k = 1.2275 Pa\cdot s^n,\ \eta = 1.2275\dot{\gamma}^{0.9384-1}$$

For 98%HD sample,

$$n = 0.93313,\ k = 1.2952 Pa\cdot s^n,\ \eta = 1.2952\dot{\gamma}^{0.93313-1}$$

Table 4-7 is a summary of the viscosities of the 15% NBR-MCB solutions with different hydrogenation degree measured under reaction conditions (145 ℃ & 500psi).

Table 4-7 Viscosities of the 15% Solutions under Reaction Condition

Hydrogenation Degree	Viscosity/cP (145 ℃, 500psi)
0%(NBR)	160, Newtonian, $n=1$
53%	450, Newtonian, $n=1$
79%	720 ($\dot{\gamma}=300s^{-1}$), $\eta=0.9653\dot{\gamma}^{0.9496-1}$
96%	860 ($\dot{\gamma}=300s^{-1}$), $\eta=1.2275\dot{\gamma}^{0.9384-1}$
98%	870 ($\dot{\gamma}=300s^{-1}$), $\eta=1.2952\dot{\gamma}^{0.93313-1}$

The viscosity under reaction conditions ($\dot{\gamma}=300s^{-1}$) was plotted against hydrogenation degree as shown in Figure 4-22.

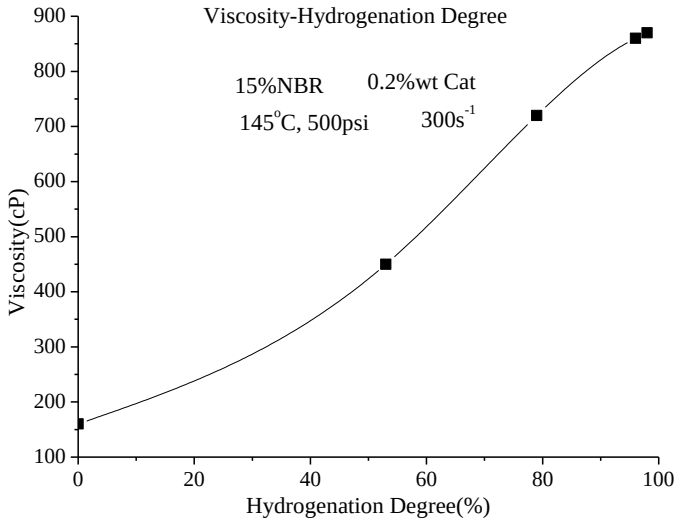

Figure 4-22 $\eta - HD$ Curve for 15% System under Reaction Condition

Figure 4-22 shows how the viscosity of reaction solutions changes as the conversion of the reaction increases in the 15% NBR hydrogenation system.

4.3.2.3 The Effect of Catalyst Concentration on Viscosity

Catalyst concentration used during sample preparation in Parr reactor may also affect the viscosity of the samples. The relation of hydrogenation degree and viscosity at various catalyst concentrations was studied. These samples were prepared in batch reactor. The experimental results were shown in Figure 4-23, during which catalyst concentration used was varied from 0.05%wt to 0.2%wt based on polymer mass in the 15% NBR solution. For the line labeled as 1, the catalyst used was 0.2%wt and hydrogenation degree reached 95% after 25min; for the three round dots labeled as 2, the catalyst used was 0.1%wt and the final hydrogenation degree was 92%; for the triangle dot labeled as 3, the catalyst used was 0.05%wt and the final hydrogenation degree was 67%.

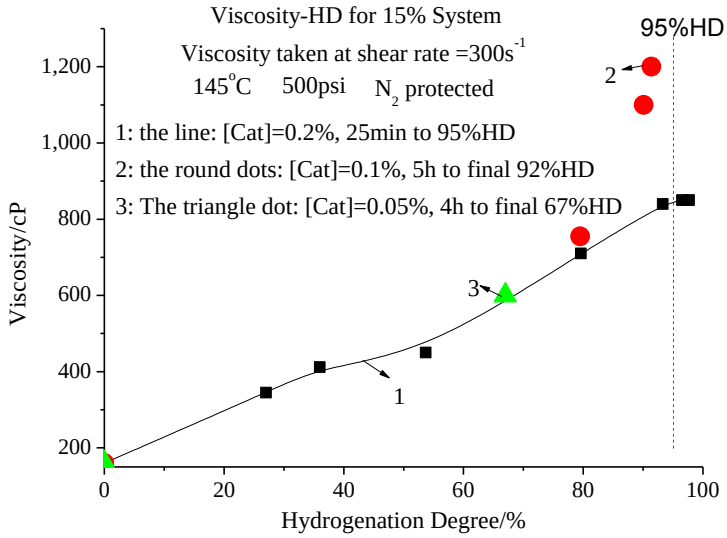

Figure 4-23 Viscosity-HD Relations at Various [Cat] for 15% Solutions

It is shown in figure 4-23 that viscosity increases as hydrogenation degree increases; at low catalyst concentration, hydrogenation reaction stops after a certain time, but the viscosity keeps increasing. As a result, if low catalyst concentration was applied, NBR solutions might have a higher viscosity than usual, due to longer reaction time, during which some invisible micro-gel may be generated by slight crosslinking.

4.3.2.4 The Effect of Molecular Weight on Viscosity

The 7%wt NBR-MCB solutions with different hydrogenation degree were analyzed in GPC and rheometer to get molecular weight and viscosity, respectively. Viscosity was tested under reaction conditions, i.e. 145℃ & 500psi. When carrying out GPC analysis, samples were vacuumed under room temperature overnight and the polymer was analyzed in its THF solutions. The results are shown in Table 4-8.

Table 4-8 HD-Molecular Weight-Viscosity for NBR Samples

(Viscosity measured at 145℃ & 500psi)

HD	Mw/ dalton	Mn/ dalton	Viscosity/cP
0%	204,000	98,000	17
35%	218,000	108,000	35
66%	237,000	127,000	50
96%	273,000	161,000	60

Figure 4-24 was obtained by plotting the number average molecular weight against hydrogenation degree, which shows how the molecular weight changes as the conversion of the reaction increases in the 7% NBR hydrogenation system.

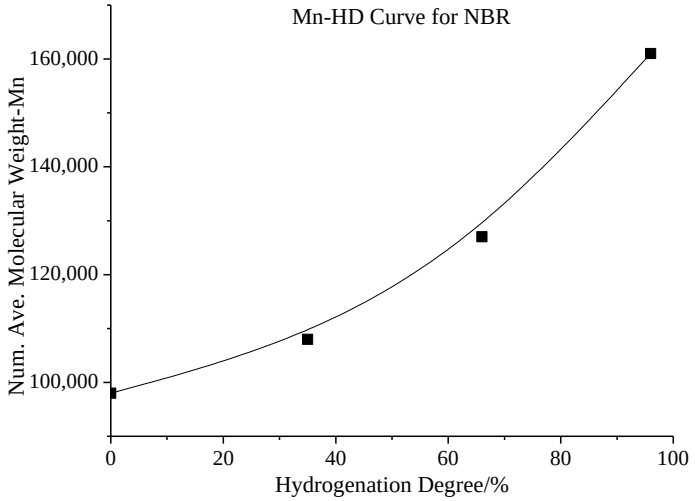

Figure 4-24 $M_n - HD$ Curve for Nitrile Rubber

The relation between the viscosity of the solution and the number average molecular weight of the polymer is shown in Figure 4-25. The increase of molecular weight during reaction might be responsible for the increase of viscosity.

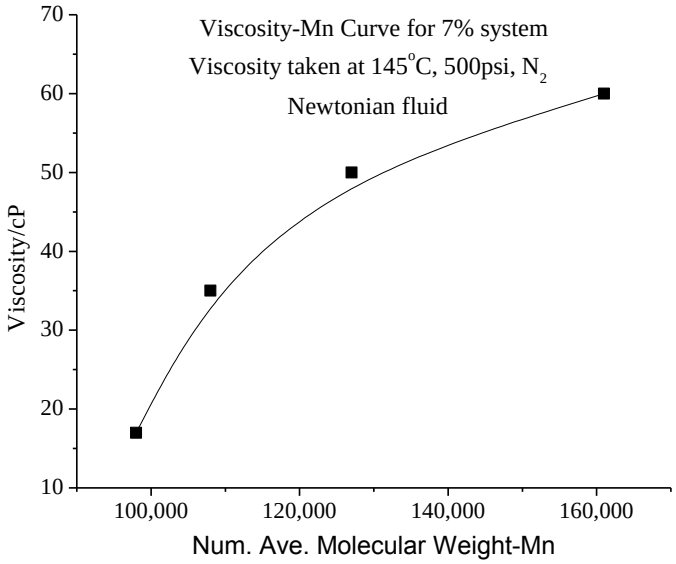

Figure 4-25 $\eta - M_n$ Curve for 7% NBR-MCB Solution under Reaction Condition

The addition of hydrogen onto $C = C$ bonds, i.e. hydrogenation reaction, and the possible micro-gel formation, i.e. slight crosslinking, may be reasons for the increase in polymer molecular weight.

4.3.2.5 Results of Dynamic Mode Test

The dynamic mode was also adopted to study the elastic aspect of the polymer solution, with the results shown in Figure 4-26 & Figure 4-27.

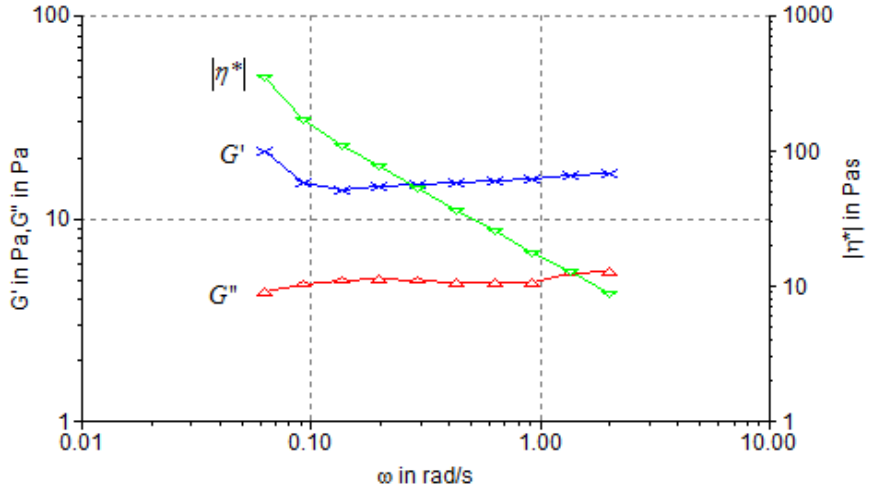

Figure 4-26 Frequency Sweep of 15% NBR-MCB Solution

$(\omega = 0.1-2.0 rad/s; T = 145°C;\ P = 500 psi;\ \gamma = 1.0\%)$

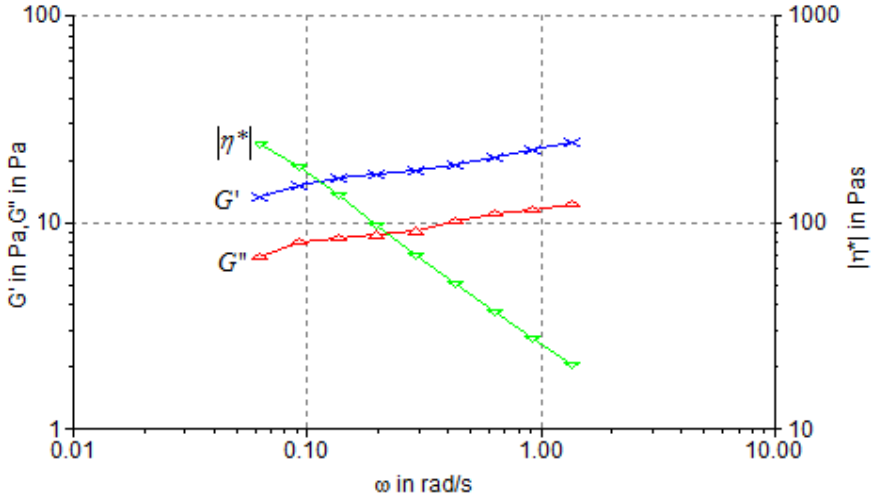

Figure 4-27 Frequency Sweep of 15% HNBR-MCB Solution

$(\omega = 0.1-1.5 rad/s;\ T = 145°C;\ P = 500 psi;\ \gamma = 1.0\%)$

As shown in Figure 4-26 & Figure 4-27, the storage modulus G' and the loss modulus $G"$ increase linearly as frequency ω increases; while the value of the complex viscosity $|\eta^*|$ decreases linearly as frequency ω increases. For dynamic modes the power law could be

expressed by Equation 2-10 and Equation 2-11. Natural logarithm of the $|\eta^*| - \omega$ data (Figure 4-26 & 4-27) was taken and then $\ln|\eta^*| - \ln\omega$ curves were plotted (Figure 4-28).

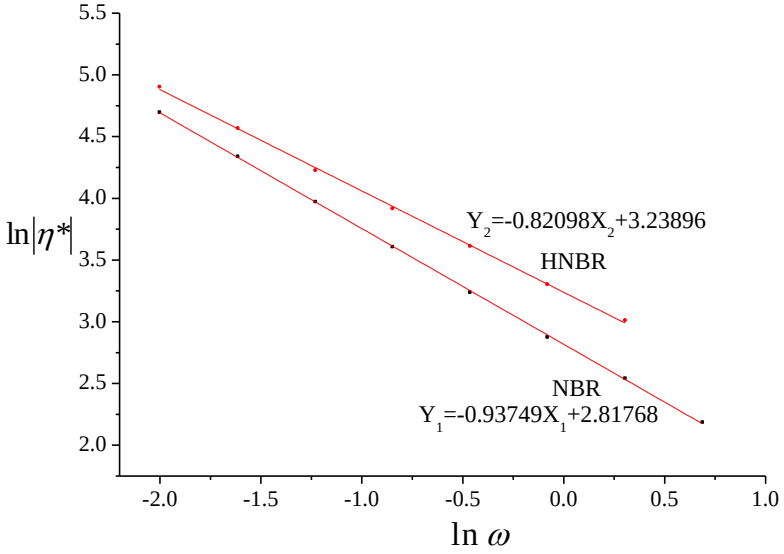

Figure 4-28 $\ln|\eta^*| - \ln\omega$ Plots for 15% NBR/HNBR-MCB Solutions

By linear regression of the curve shown in Figure 4-28, the parameters in power law could be calculated.

For the 15% NBR-MCB solution:

$n = 0.06251$, $k = 16.74 Pa \cdot s^n$, $|\eta^*| = 16.74\omega^{0.06251-1}$, wherein $\omega = 0.1 - 2.0 rad/s$

So, when $\omega = 0.1 rad/s$, $|\eta^*| = 145 Pa \cdot s$; when $\omega = 1.0 rad/s$, $|\eta^*| = 16.74 Pa \cdot s$.

For the 15% HNBR-MCB solution:

$n = 0.17902$, $k = 25.51 Pa \cdot s^n$, $|\eta^*| = 25.51\omega^{0.17902-1}$,wherein $\omega = 0.1 - 1.5 rad/s$

So, when $\omega = 0.1 rad/s$, $|\eta^*| = 169 Pa \cdot s$; when $\omega = 1.0 rad/s$, $|\eta^*| = 25.51 Pa \cdot s$.

Figure 4-29 was obtained by plotting G' or G'' against ω for the data shown in Figure 4-26 and Figure 4-27.

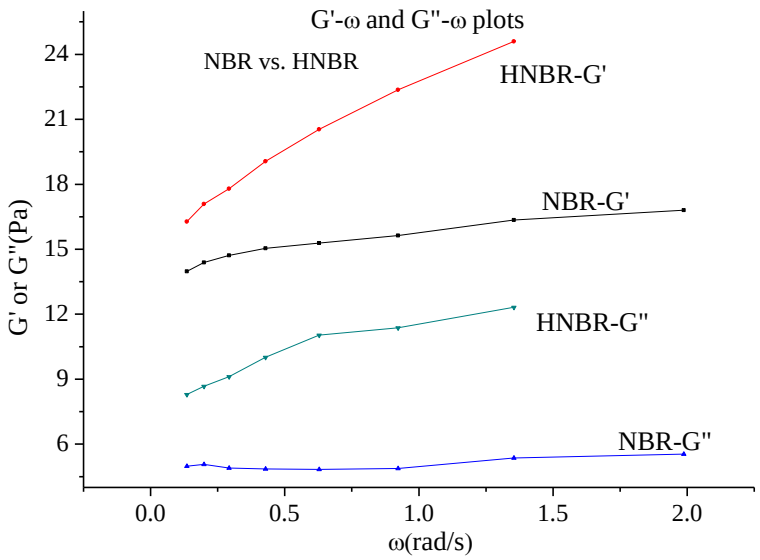

Figure 4-29 $G'-\omega$ and $G''-\omega$ Plots for 15% NBR/HNBR-MCB Solutions

It can be concluded from Figure 4-29 that the 15% HNBR-MCB solution presents stronger elastic property than the 15% NBR-MCB solution.

4.3.3 Summary

The 7% NBR-MCB solutions could be regarded as Newtonian fluids, in the shear range of $\dot{\gamma}:10^1-10^2 s^{-1}$. The 15% NBR-MCB solutions with low hydrogenation degree (< 60%HD) could be regarded as Newtonian fluids ($n=1$), in the shear range of $\dot{\gamma}:10^1-10^2 s^{-1}$. However, the samples with high hydrogenation degree (> 70%HD) deviate from Newtonian behavior ($n=0.9-1$), in the shear range of $\dot{\gamma}:10^1-10^2 s^{-1}$. Generally, n in the power law decreases as hydrogenation degree increases. At very low shear rate where the static mode is not suitable, the dynamic mode is adopted to test the sample. Both NBR and HNBR solutions deviate from Newtonian behavior, with a very low n. Appendix II provides a summary of the experimental results, compared with the corresponding values reported in the literature (Chapter 2).

4.4 Summary

The rheological properties of NBR melts, as well as NBR solutions were studied in a rotational rheometer with a cone-plate sensor and a cylinder sensor, respectively. The NBR melts shows both elastic and viscous properties, i.e. presents viscoelastic property. The viscous property has been studied in detail, both under dynamic and static modes, with parameters in power law and Arrhenius equation calculated respectively. Then, the experimental values of the viscous properties were compared with those reported.

The NBR-MCB solution mainly shows viscous properties, although it still exhibits some elastic property at very high concentration. Parameters that will affect the viscosity of the solution were studied in detail, especially the hydrogenation degree. Low concentration solutions are Newtonian fluids; while high concentration solutions deviate from Newtonian behavior when the hydrogenation degree is also high. At very low shear rate, the NBR-MCB solution also deviates from Newtonian behavior. Power laws were developed when the solution behaved as a non-Newtonian fluid. Viscosity values calculated with correlations from literature were compared with the experimental results.

The NBR-MEK solution was also measured. Generally, the NBR-MEK solution presents lower viscosity than the NBR-MCB solution at the same polymer concentration if other parameters are kept constant. As shown in the experiment results, the viscosity of 10%wt NBR-MEK solution is even lower than that of 7%wt NBR-MCB solution.

Chapter 5 Hydrogenation of NBR in High Concentration Solution

5.1 Introduction

The reaction mechanism of NBR hydrogenation in MCB using Wilkinson's catalyst has been well established. However, when polymer solutions were extended to high concentration, the kinetic behavior might be affected by mass transfer and firsthand experimental data under these conditions is still lacking. In this part, hydrogenation of NBR will be carried out in a batch reactor using Wilkinson's catalyst and the polymer concentration in the solution will be in high concentration.

5.2 Experimental

Materials and equipments were generally introduced in Chapter 3.

5.2.1 Modification of Reactor

The reactor was modified to fit the current system. The detail structure of reactor is shown in Appendix III. Among the 6 ports on the reactor head, 2 ports were used for internal cooling coil and another 2 ports were taken by thermocouple and safety rupture disc, respectively. So, only 2 ports were available during operation (port A & port B).

5.2.2 Operation Procedure

A typical recipe used when doing batch reaction was 1) NBR: 15%wt (weight of polymer/total weight of solution); 2) Wilkinson's Catalyst: 0.15%-0.2%wt (based on polymer, weight of Cat/ weight of NBR); and 3) triphenylphosphine (the co-catalyst): 10 times (weight of TPP/weight of Wilkinson's catalyst). Generally, there are 5 steps in the operation procedure of the hydrogenation experiments.

Step 1: Catalyst bomb charging

0.04g Wilkinson's Catalyst and 0.4g TPP were dissolved in 19.56g MCB which had been degassed with nitrogen before experiments. The catalyst solution was then filled into catalyst bomb. This filling process was carried out in glove box. Then, the catalyst bomb was pressurized up to 480psi by hydrogen.

Step 2: Polymer solution degassing

113g of 18% NBR solution was transferred to Parr reactor vessel. The catalyst bomb was connected to V1 through its lower 3-way valve. After connecting hydrogen cylinder to V2, degassing was started, with ice water bath to depress evaporation of MCB. The solution was stirred at around 300rpm. During degassing process, hydrogen was introduced from V2 through port A into vessel, and vented from V3 through port B. The lower 3-way valve of catalyst bomb was totally closed while V1 was open, so that the residual air in the pipes and valves can also be discharged. At the beginning, the vessel was pressurized to about 700psi and then released to about 100psi. Re-do this for 5-6 times, so that the air in the dead corner could be diluted. After this operation, the solution was degassed continuously at low pressure (around 150psi). The gas flow rate of continuous degassing should not be too high, otherwise great amount of MCB would be brought out. After about 1 hour, polymer solution was thoroughly degassed. The V3 should be closed before closing V2. Then, the hydrogen cylinder was disconnected to V2. The pressure inside the vessel was around 150psi after degassing.

Step 3: Polymer solution preheat

Two lines of hydrogen were used here, both of which were 500psi. One line was connected to the upper 3-way valve of catalyst bomb, and the other line was connected to

V3. The air in the tubing (both of the two lines) should be purged before heating. The polymer solution was preheated to 143 ℃. The preheat temperature was a bit lower than the reaction temperature (145 ℃), in order to get proper temperature control for the reaction, especially at the early stage. According to the properties of 1st order reaction in batch reactors, 90% of total reaction heat was released in the first half reaction time, if 100% conversion was reached. The pressure in the reactor after preheat was around 250psi. The hot water tap was opened for the cooling water pipeline, getting ready to take away the heat released in the next step.

Step 4: Catalyst solution loading

The catalyst solution was introduced into the polymer solution, by switching the lower 3-way valve on the catalyst bomb. Right at this time, timing should be started. Immediately after this, the upper 3-way valve of catalyst bomb was switched to raise hydrogen pressure up to 500psi. In this process, hydrogen flowed from the upper 3-way valve through the catalyst bomb, then through the lower 3-way valve and V1, and finally into the vessel. Any possible residual catalyst solution in the catalyst bomb was blown out by the gas flow. Right after the pressure was raised to 500psi, V1 was closed. Then, V3 was opened and the hydrogen line connected to V3 was in use. At this time, the catalyst bomb and the hydrogen line connected to the catalyst bomb were no more in use.

Step 5: Sampling

Samples were taken at regular intervals. Suitable amount of the solution was purged before sampling in order to vent residual solution in the dip tube.

Step 6 Analysis

Samples were analyzed in FTIR, GPC and rheometer to get hydrogenation degree, molecular weight & its distribution and rheological properties, respectively. Detail information of FTIR analysis could be found in Chapter 3.

5.3 Mechanical Mixing and Agitators

5.3.1 Internal Structure

The head of reactor and its internal structure were shown in Figure 5-1.

Figure 5-1 Reactor Head and Internals

All the parts used to modify reactor internals were standard accessories from Parr Company without modifications, and the detail information was listed below.

Table 5-1 Vessel Parts Used for Reactor Modification

Name	Part No.	Description
Cooling Loop	831HC	Cooling Loop for 300mL, Stainless Steel T316
Dip Tube	832HC	Dip Tube for 300mL, Stainless Steel T316
Thermocouple	A472E	Thermocouple, Grounded, 300mL, Type J
Stirrer Shafts	822HC15	Shaft, Magnetic Drive, 300mL, Removable Vessel
Impellers	A837HC	Impeller with Screw, for 822HC Series Shafts
Anchor	/	U-shaped, Flat Bar Anchor, 300mL, Stainless Steel

5.3.2 Agitators

For the current reaction system, the viscosity is very high. The turbine impeller could not provide sufficient mixing for the reaction, and it's essential to modify the agitator to improve the mass transfer and heat transfer. In hydrogenation of 15% NBR solution, the viscosity of the liquid increases from 200cP to 1000cP. Turbine impeller is suitable for liquid under 500cP, and is a high-speed agitator. Anchor is suitable for liquid above 5,000cP, and is a very-low-speed agitator. Between 500cP and 5,000cP, some cross-beam or grid agitators are more suitable. Based on this information, a new agitator was designed [Figure 5-2(B)], which is a combination of the turbine impeller and the anchor stirrer. Also, in our system, it's not just the stickiness of the liquid that causes the mass transfer problem, while the more important fact may be the difficulty of gas transfer into the liquid. One turbine is not enough, as it's far under the liquid-gas boundary, and near to the bottom of the reactor, which means that it cannot produce enough vortexes to bring the gas into the liquid. So, another new agitator was designed [Figure 5-2 (C)], which is a combination of two turbines. Detail information was shown in Appendix III.

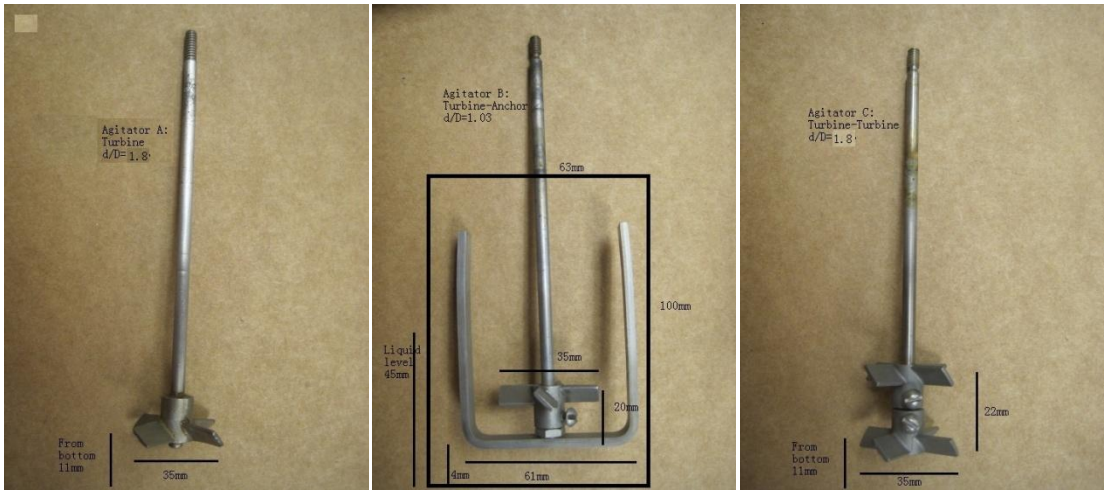

(A) Turbine (B) Turbine-Anchor (C) Turbine-Turbine

Figure 5-2 Agitators Used for Mechanical Mixing

5.4 Operation Techniques

For hydrogenation reaction carried out in the high concentration solution, proper operation techniques should be adopted to get better reproducibility and reliable results. Here, the temperature control method and the purge & sampling process will be described. Figure 5-3 is the hydrogenation degree-time curves for the catalytic hydrogenation in the same reaction condition. During the experiments, the temperature was not controlled properly and the liquid level was decreased gradually because of sampling and the purge procedure before it. As we can see, the reproducibility was not good, so the results were not reliable.

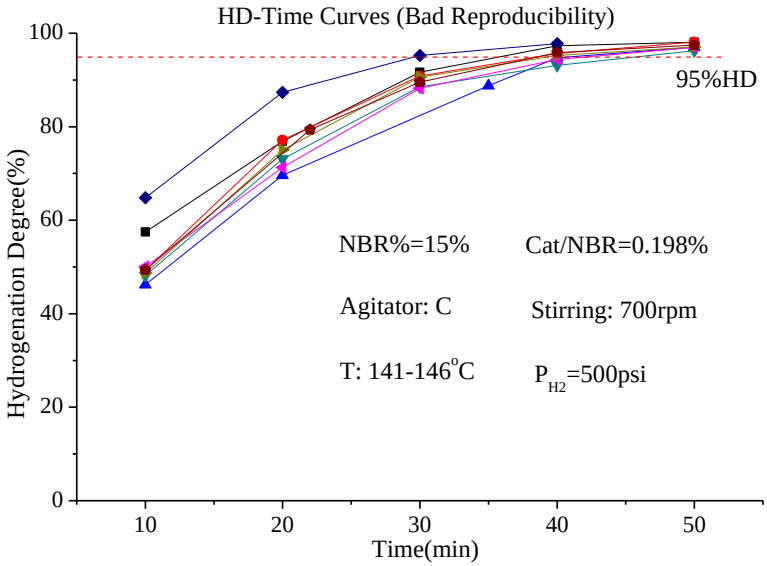

Figure 5-3 HD-Time Curves before Improvement

5.4.1 Temperature Control Method

Large amount of heat is released during the hydrogenation process in the high concentration solution, especially at the early stage of reaction. This will result in temperature fluctuation during reaction, sometimes even runaway. Figure 5-4 is a typical temperature-time curve before improvement.

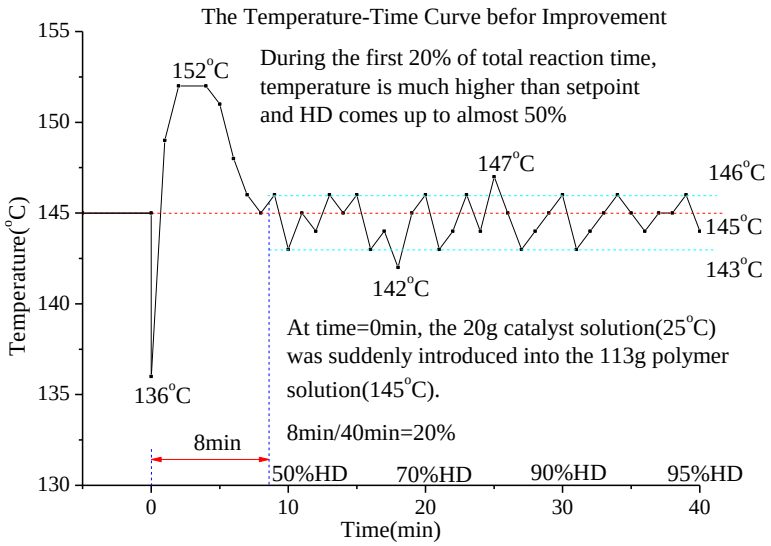

Figure 5-4 Temperature-Time Curve before Improvement

In Figure 5-4, the 25 ℃ catalyst solution was introduced into the 145 ℃ polymer solution at time=0min. The temperature dropped from 145 ℃ to 136 ℃ suddenly, and then went up to 152 ℃ in about 1min, due to large amount of reaction heat released. Although cooling system was adopted, the temperature still could not be controlled under 145 ℃. After 8min, the cooling water finally brought the temperature down to 145 ℃. Then, it fluctuated around 145 ℃, with an error of about ±2 ℃. In this case, the 8min for temperature to become steady was too long, which was 20% of the total reaction time (40min), corresponding to 50% conversion. So, a proper temperature control method was very essential for this very exothermic process, and the temperature control system was improved in the following aspects.

(1)PID controller tuning

The reaction temperature was controlled by a PID controller. In order to tune Parr reactor controller, some experiments were repeated many times, with their temperature-time curves recorded. Finally, a set of more suitable PID parameters were found for this

system. Compared with Figure 5-6, a better temperature control was reached. However, just setting PID parameters is not enough to solve the temperature control problem.

(2) Preheat Temperature

Although internal cooling coil was used, the temperature still ran over set point in the first few minutes of the reaction, even though cold water was used as coolant, because too much heat was released. In the improved temperature control method, the preheat temperature was set to be a bit lower than the reaction temperature. After catalyst was introduced and temperature arrived highest, the temperature was re-set to be the reaction temperature. So, it was important to choose a proper preheat temperature, so that the peak temperature could be equal to the reaction temperature. In the current system, this preheat temperature was 142-143 ℃, for the 145 ℃ reaction temperature.

(3) Cooling water temperature

The laboratory utilities provided both cold water (~ 10 ℃) and hot water (~80 ℃). The temperature of cooling water could affect the fluctuation of the temperature control. After the first few minutes of the reaction, there was not so much heat released and the temperature fluctuated around the set point. When the temperature fell below set point, the heated jacket was activated to heat the solution up. When the temperature went above the set point, the internal cooling coil was activated to cool it down. The temperature fluctuated greatly, when cold water was used as internal coolant, as cold water cooled down the system too much, bringing down the temperature 2-3 ℃. So, instead of cold water, hot water was used as internal coolant for the current system to reduce the temperature fluctuation.

(4) Coolant pipeline design

When hot water was used as coolant, the coolant pipeline designed should ensure that the water introduced into the internal cooling coil was still hot. There was around 60 degree's difference between the hot water and the room temperature. The plastic tubing used was quarter inch in outside diameter, with a relatively large specific surface area. The water in the tubing was not flowing all the time, as the internal cooling coil was not activated when the actual temperature was below the set point. So, the cooling water introduced into the cooling coil was almost near room temperature.

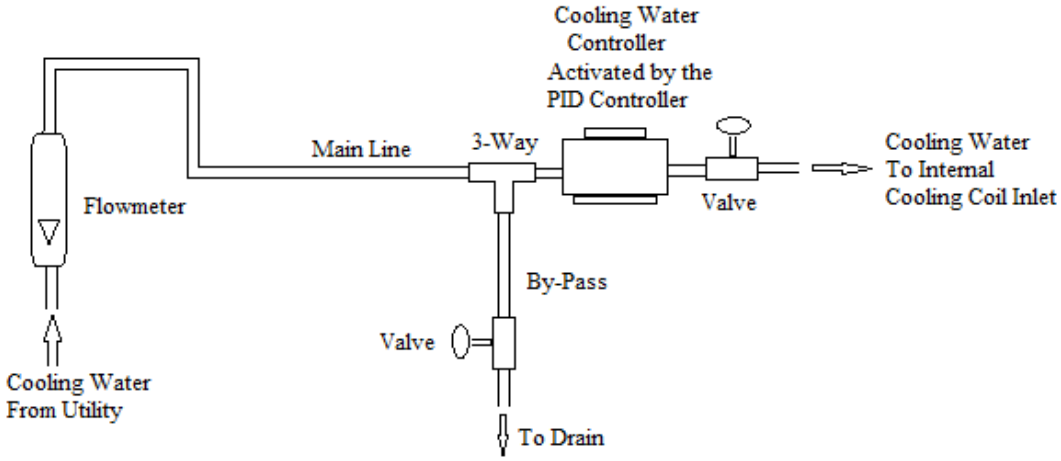

Figure 5-5 Design of Cooling Water Pipeline

In the improved pipeline design (Figure 5-5), the cooling water controller was installed very close to the inlet of internal cooling coil. By-pass tubing was designed just before the cooling water controller. When the cooling water controller was not activated, i.e. the actual temperature was below set point, all the cooling water went through the by-pass to keep the water in the main line hot and the typical reading of flowmeter was 0.5L/min. When the cooling water controller was activated, i.e. the actual temperature was over the set point, the cooling water went through both the internal cooling coil in the reactor and

the by-pass. At this time, the typical flow rate of cooling water was 1.5 L/min. In this way, cooling water was kept hot before introduced into internal cooling coil. Figure 5-6 shows the temperature-time curve after improvement.

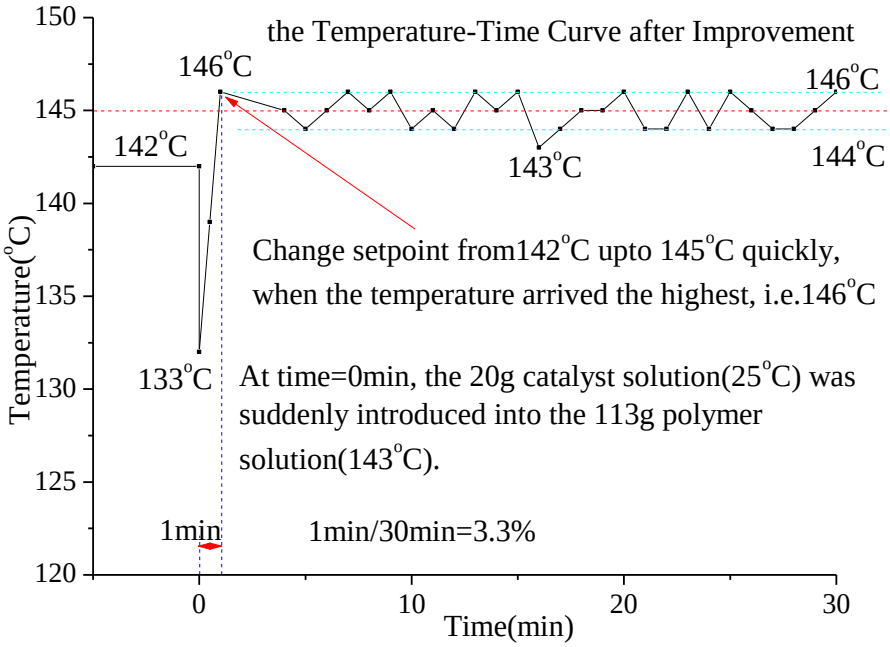

Figure 5-6 Temperature-Time Curve after Improvement

In Figure 5-6, the polymer solution was preheated to 142 ℃, into which the 25 ℃ catalyst solution was introduced at time=0min. The temperature dropped from 142 ℃ to 133 ℃ suddenly. Then, the temperature went up to 146 ℃ in about 1min and this was the highest it could go with the activated cooling water. At this time, the PID controller was re-set to be 145°C and the system went into the fluctuation stage. Later on, the temperature fluctuated around 145 ℃, with an error of about ±1 ℃. In this case, the 1min for temperature to become steady was very short, which was 3.3% of the total reaction time (30min). Table 5-2 shows the improvement of temperature control system.

Table 5-2 Changes of Temperature Control System

Iterms		Original		Improved	
		Heater	Coolant	Heater	Coolant
PID Parameters	P(℃) (proportional term/*gain*)	25	1	1	6
	I(reset/minute) (integral term/*reset*)	0.01	0	0.20	0
	D(minute) (Derivative term/*rate*)	0	0	3	0
	Cycle Time(seconds)	5.0	5.0	5.0	5.0
Pre-heat Temperature(℃)		145		142	
Coolant Temperature		≈12 ℃ (Cold Water)		≈80 ℃ (Hot Water)	
Cooling Water Pipeline		Controller Faraway from Coil inlet; No By-pass; No Flowmeter		Controller close to Coil inlet; By-pass Designed; Flowmeter installed.	
Coolant Rate(Liter/minute)		N/A		≈1	

5.4.2 Purging and Sampling

With improved temperature control, the reproducibility became better. When studying the effect of stirring speed on reaction rate, it was observed that liquid level had an apparent effect on the kinetics for these viscous solutions. Thus, liquid level should be kept constant to get better reproducibility.

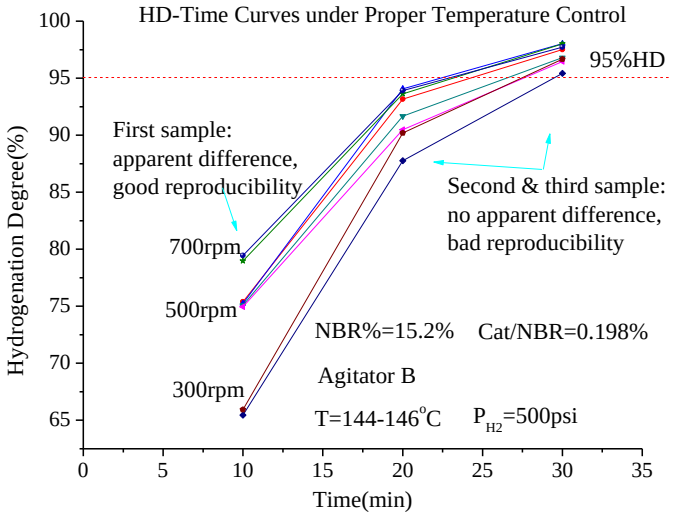

Figure 5-7 HD-Time Curves under Proper Temperature Control

In the experiments shown in Figure 5-7, a few millilitre of the solution was purged before each sample was taken in order to empty the residence in the dip tube. The 1st sample taken at 10min had good reproducibility. However, the reproducibility of 2nd and 3rd sample was not good. This might be caused by purging process before sampling. If the purge amount was not enough, the HD of the sample would be lower than the actual HD. If purged too much, the liquid level would be influenced as the total amount of liquid in the reactor was only about 140ml. It was difficult to control the purge at the same amount every time when sampling. According to experience, if more than 5 samples were taken, the liquid level would be so low that the turbine could not reach the liquid. In this case, the reaction was fast at the beginning, but it became very slow after the 5th sample was taken. It was suggested to take only one sample in each run to keep liquid level constant.

5.4.3 Reproducibility

Figure 5-8(a) is the HD-time curve for 15% system, with old temperature control and varied liquid level. Figure 5-8(b) is the HD-time curve for 15% system, with proper temperature control and constant liquid level.

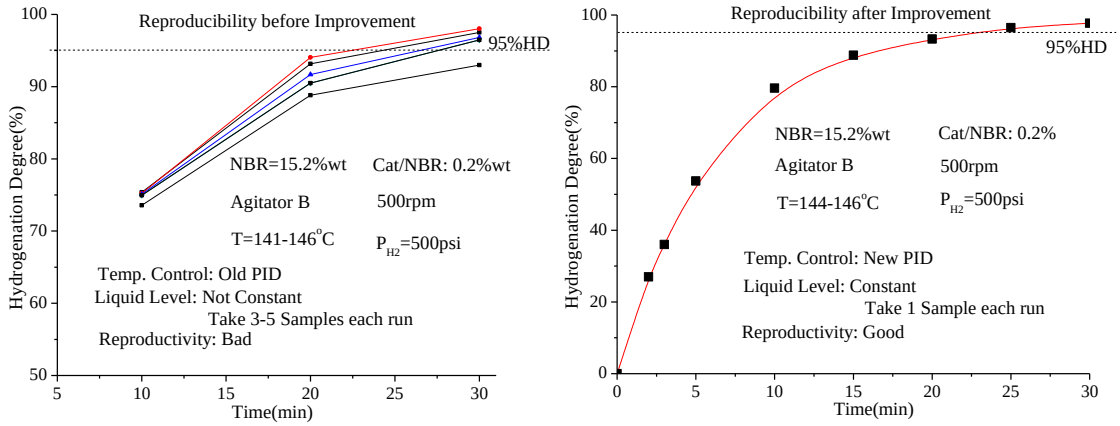

(a) (b)

Figure 5-8 Reproducibility before vs. after Improvement

5.5 Results and Discussion

Hydrogenation experiments were carried out in a Parr reactor. Agitator shapes, stirring speeds, hydrogen pressures, polymer concentrations and catalyst concentrations were varied to investigate the kinetic behavior.

5.5.1 Agitators

Hydrogenation of high-concentration NBR solution was carried out in batch reactor to study the mass transfer process. Three different agitators (Figure 5-2) were used to study the mass transfer problem of the system. Figure 5-9 is a summary of the experimental results for 15% system and Figure 5-10 is the summary for 7% system.

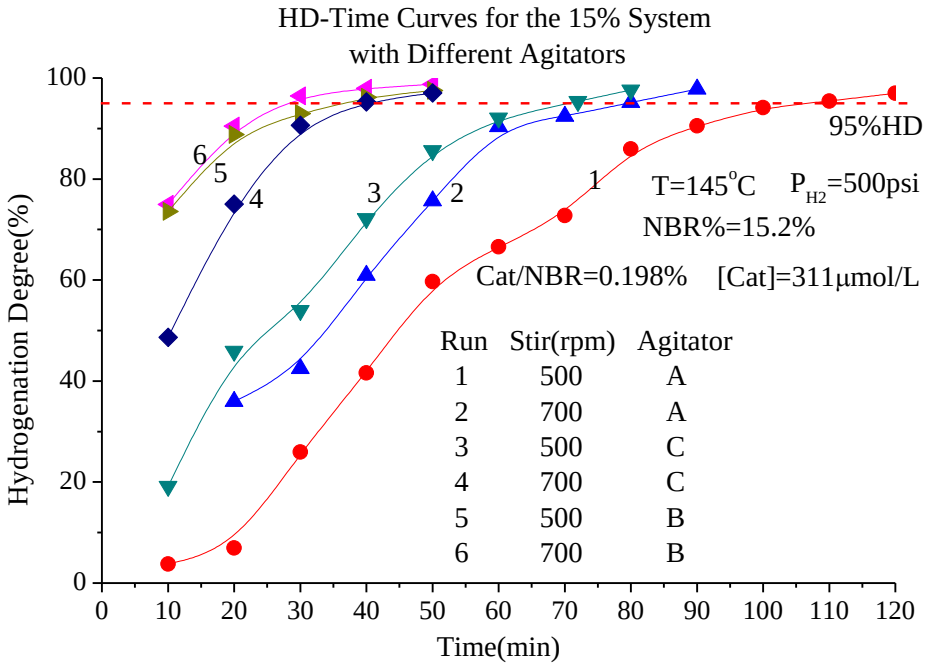

Figure 5-9 Experiment Results for 15% System with Different Agitators

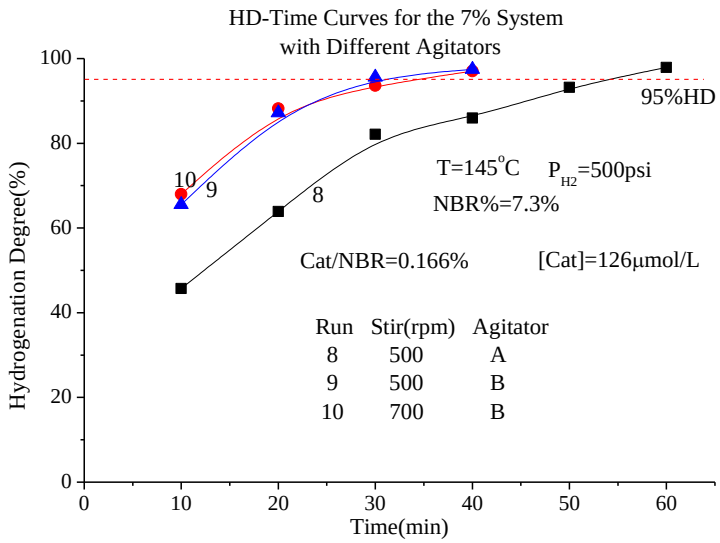

Figure 5-10 Experiment Results for 7% System with Different Agitators

It can be concluded that mass transfer processes affect the reaction rate greatly, especially in the 15% system. Agitator B provides better mixing than Agitator C, while Agitator C provides better mixing than Agitator A.

5.5.2 Stirring Speed

Stirring speed of mechanical mixing was studied for the 15% NBR solution, using turbine-anchor combined agitator. The experiment results were shown in Figure 5-11.

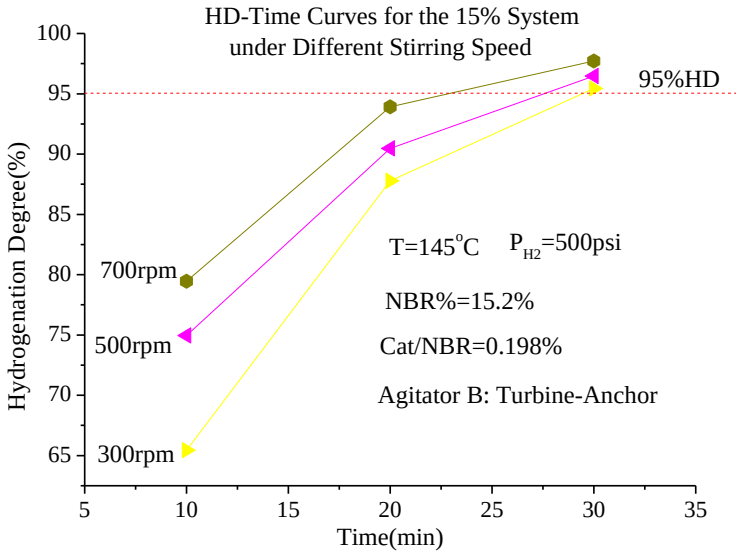

Figure 5-11 HD-Time Curves for 15% System under Different Stirring Speed

It is shown in Figure 5-11 that reaction rate increases as stirring speed increases. The reaction rate in the viscous system is mass transfer controlled instead of chemical controlled. Higher stirring speed means better mass transfer, resulting in higher hydrogenation rates.

5.5.3 Hydrogen Pressure

The effect of hydrogen pressure on reaction rate was studied for the 15% NBR solution. The experimental results were shown in Figure 5-12.

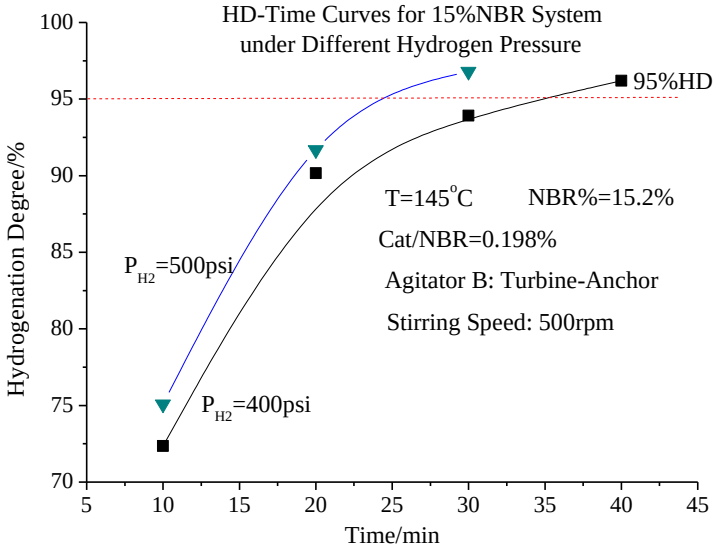

Figure 5-12 HD-Time Curves for 15% System under Different Hydrogen Pressure

As shown in Figure 5-12, reaction rate decreases when lower hydrogen pressure was applied. Lower hydrogen pressure means lower partial pressure in the gas phase for hydrogen. Assuming hydrogen obeys Raoult's law in the system, less hydrogen concentration was provided in the liquid phase and this resulted in lower reaction rate according to the hydrogenation kinetics.

5.5.4 Polymer Concentration

The effect of polymer concentrations on the reaction rate was studied with experimental results shown in Figure 5-13.

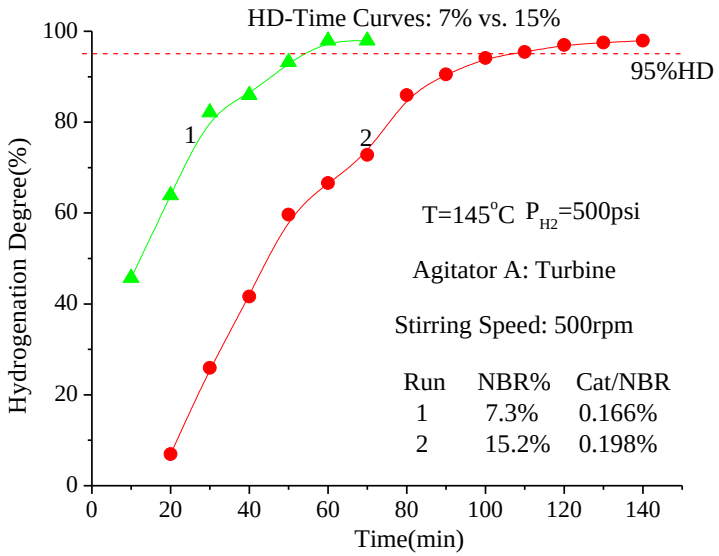

Figure 5-13 HD-Time Curves: 7% vs. 15%

As shown in Figure 3, with a lower catalyst concentration, the reaction rate of 7% NBR solution is still faster than that in 15% NBR solution. However, according to rate law, as the concentration of reactant increases, the reaction rate increases. So, this phenomenon should be caused by the great difficulty in mass transfer for the 15% solution, when using the turbine agitator.

5.5.5 Catalyst Concentration

The effect of catalyst concentration on reaction rate was studied, using turbine-anchor agitator at 500rpm. Reactions were carried under 145℃ and 500psi. The experimental results were shown in Figure 5-14.

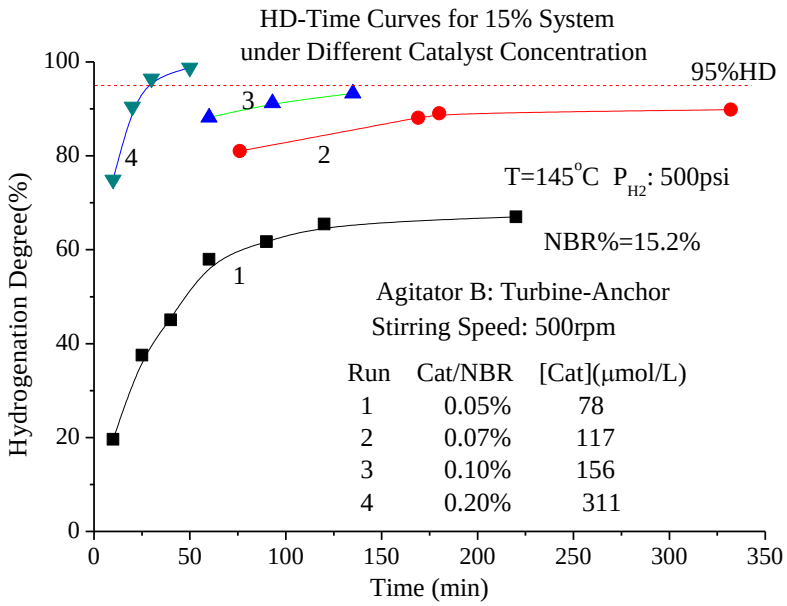

Figure 5-14 HD-Time Curves for 15% System under Different Catalyst Concentration

As can be seen in Figure 5-14, catalyst concentration affects the reaction rate greatly. Higher catalyst concentration will result in fast reaction. However, it was observed that when the catalyst concentration was reduced under a certain value the reaction conversion was affected. This phenomenon will be studied in detail in Chapter 6.

5.5.6 The Apparent Rate Constant k'

The hydrogenation could be regarded as a first-order reaction (Equation 2-1) and the apparent rate constant k' could be expressed by Equation 2-2. For the 15% NBR system with 0.2%wt catalyst shown in Figure 5-15(a), the theoretical value of k' is $k'_{theory} = 3.29 \times 10^{-3} s^{-1}$. The detail calculation process can be found in Chapter 6. On the other hand, the integrated form of the kinetic equation (Equation 2-1) is given by:

$$\ln \frac{[C = C]}{[C = C]_0} = -k't \tag{5-1}$$

Also, the hydrogenation degree is given by Equation 3-1. Then, Equation 5-2 was obtained from Equation 3-1 and Equation 5-1.

$$\ln(1-HD) = -k't \tag{5-2}$$

By plotting $\ln(1-HD)$ against t, the experimental value of k' was calculated to be $k'_{experiment} = 2.13\times10^{-3}\,s^{-1}$, as shown in Figure 5-15(b).

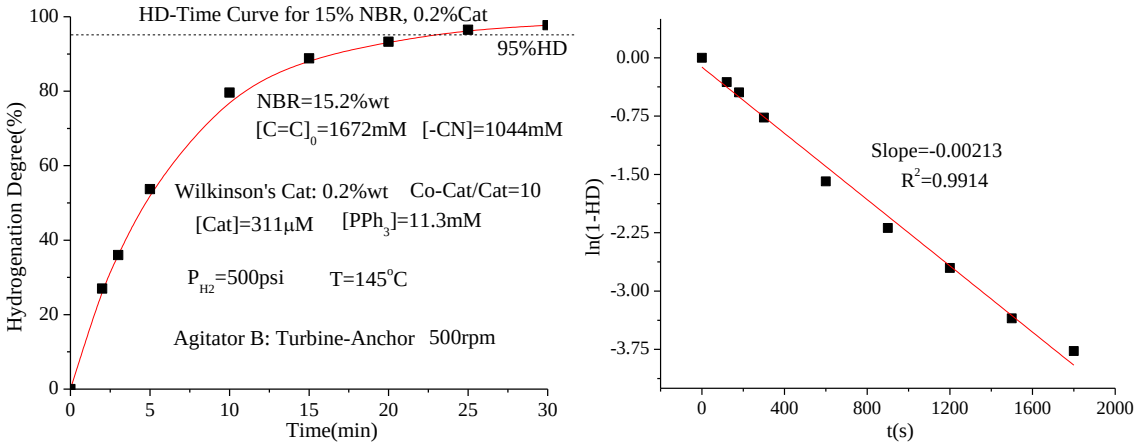

(a) (b)

Figure 5-15 HD-Time Curve for 15% System with 0.2%wt Catalyst

The experimental value is smaller than the theoretical value for the system shown in Figure 5-15(a), although the anchor-turbine agitator was used to provide relatively sufficient mechanical mixing. The ratio of experimental and theoretical values is:

$$\frac{k'_{experiment}}{k'_{theory}} = 0.647$$

This means that the rate is almost halved and time needed to reach 95%HD (HNBR) doubled. When in other cases, i.e. insufficient mixing, lower catalyst concentration and lower hydrogen pressure, the experimental value is even smaller. Thus the mass transfer process affects the hydrogenation rate greatly, when high concentration polymer solution was used for reaction.

5.6 Summary

NBR was hydrogenated in high concentration solutions in the presence of Wilkinson's catalyst. Experimental equipment was modified for this very exothermic process. It was observed that the kinetic behavior was affected by mass transfer processes. Mechanical mixing for the viscous system was studied with different agitators and compared. Parameters which will affect the hydrogenation rate were investigated. The apparent rate constant in the pseudo-first-order reaction was calculated, both theoretically and experimentally.

Chapter 6 Kinetic Behavior at Low Catalyst Concentration

For a catalytic reaction, when catalyst concentration was reduced the reaction rate would be expected to decrease. However, the conversion of the reaction should not be affected. That is to say, provided enough time, the reaction carried out at low catalyst concentration should reach the same conversion as in the case of high catalyst concentration. In the catalytic hydrogenation of NBR by Wilkinson's catalyst, an interesting phenomenon was observed when reducing the catalyst concentration. Hydrogenation degree could not reach 95%, if catalyst concentration is lower than a certain value, i.e. the hydrogenation reaction stopped at a certain time.

6.1 Kinetic Behavior Reported in Literature

6.1.1 Kinetics of NBR Hydrogenation with Wilkinson's Catalyst

The reaction kinetics for hydrogenation of NBR in MCB with Wilkinson's catalyst has been well established [6][28] (Chapter 2). However, in the previous work [28], NBR solutions used were at low concentration and the catalyst applied was in relatively high concentration. That is to say, the catalyst, used for the catalytic reaction, was in large amount, based on the polymer mass in the solution. In the current research, polymer in solution was in high concentration, thus the amount of catalyst was relatively low. In this case, kinetic behavior might deviate from the normal manner.

6.1.2 Derivation of the Kinetic Equation

The derivation process of the kinetic equation reported in the work of Parent et al. [6] will be presented here for a better understanding of the reaction. The catalytic mechanism was shown in Figure 6-1 and the detail deduction process was shown below.

First of all, hydrogenation of the Wilkinson's catalyst octet generates species A.

$$RhCl(PPh_3)_3 + H_2 \overset{K}{\rightleftharpoons} RhClH_2(PPh_3)_3$$

Then, species A generates species B, which enters two circles. Circle 1: the catalytic circle, where C=C bonds will be hydrogenated; Circle 2: the nitrile circle, where rhodium will be trapped. (Figure 6-1)

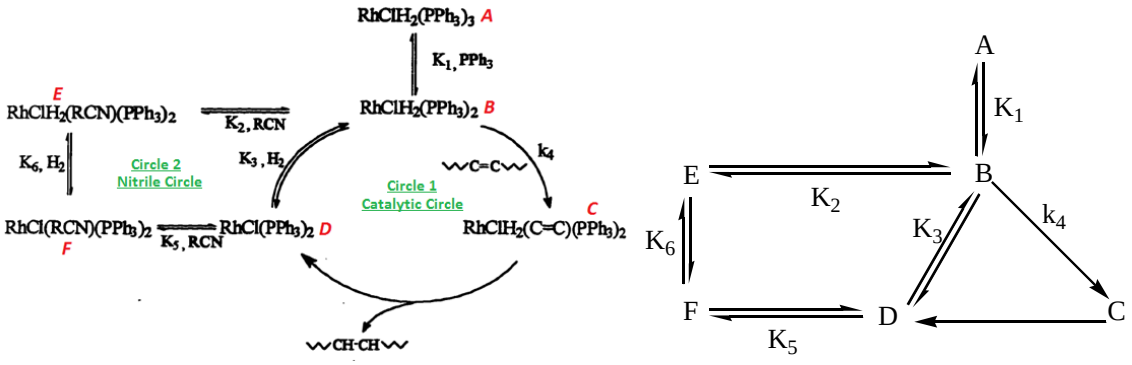

Figure 6-1 Reaction Mechanism (Modified from the Work of Parent et al.[6])

Pseudo first-order reaction:

$$Rate_{Overall} = -\frac{d[C=C]}{dt} = k'[C=C]$$

Rate determining step:

$$Rate_{Overall} = Rate_{RDS} = k_4[B][C=C]$$

Thus,

$$-\frac{d[C=C]}{dt} = k'[C=C] = k_4[B][C=C],\ k' = k_4[B]$$

Assuming that at a certain moment all the reversible steps are at an equilibrium state, the following equations were obtained.

$$K_1 = \frac{[B][PPh_3]}{[A]},\ K_2 = \frac{[E]}{[B][C \equiv N]},\ K_3 = \frac{[B]}{[D][H_2]},\ K_5 = \frac{[F]}{[D][C \equiv N]}$$

Also, the total concentration of rhodium is given by

$$[Rh]_T = [A]+[B]+[D]+[E]+[F]$$

So, equation sets were obtained, comprising 5 independent equations and 5 unknown values *[A]*, *[B]*, *[D]*, *[E]* and *[F]*.

$$Equations\begin{cases} K_1 = \dfrac{[B][PPh_3]}{[A]}, K_2 = \dfrac{[E]}{[B][C\equiv N]}, K_3 = \dfrac{[B]}{[D][H_2]}, K_5 = \dfrac{[F]}{[D][C\equiv N]} \\ [Rh]_T = [A]+[B]+[D]+[E]+[F] \end{cases}$$

After solving the equation set, the analytic solution of $[B]$ was obtained.

$$[B] = \frac{K_1K_3[Rh]_T[H_2]}{K_1 + K_1K_3[H_2] + K_3[H_2][PPh_3] + K_1K_5[C\equiv N] + K_1K_2K_3[H_2][C\equiv N]}$$

So,

$$k' = k_4[B] = \frac{k_4K_1K_3[Rh]_T[H_2]}{K_1 + K_1K_3[H_2] + K_3[H_2][PPh_3] + K_1K_5[C\equiv N] + K_1K_2K_3[H_2][C\equiv N]}$$

6.2 Experimental

Compared with the catalytic hydrogenation experiments in Chapter 5, the catalyst concentration used here was relatively low, around 0.05%-0.15%wt based on polymer mass. All the reaction conditions and operation procedure were the same as described in Chapter 5.

6.3 Results and Discussion

When the catalyst concentration is reduced, the hydrogenation reaction rate becomes slower and it takes more time to complete the reaction. In other words, 100% conversion should be reached, if enough time is provided. A very typical catalyst concentration used in the kinetic study is 0.2%wt based on the mass of polymer. However,

it was observed that the hydrogenation reaction stopped at a certain conversion if the catalyst concentration was lower than a certain value. Figure 6-2 shows the kinetic curve for such a reaction, in which polymer concentration was 15%wt, and catalyst concentration was 0.05%wt based on polymer. The hydrogenation reaction almost stopped after 200min, and the finally conversion was 67%.

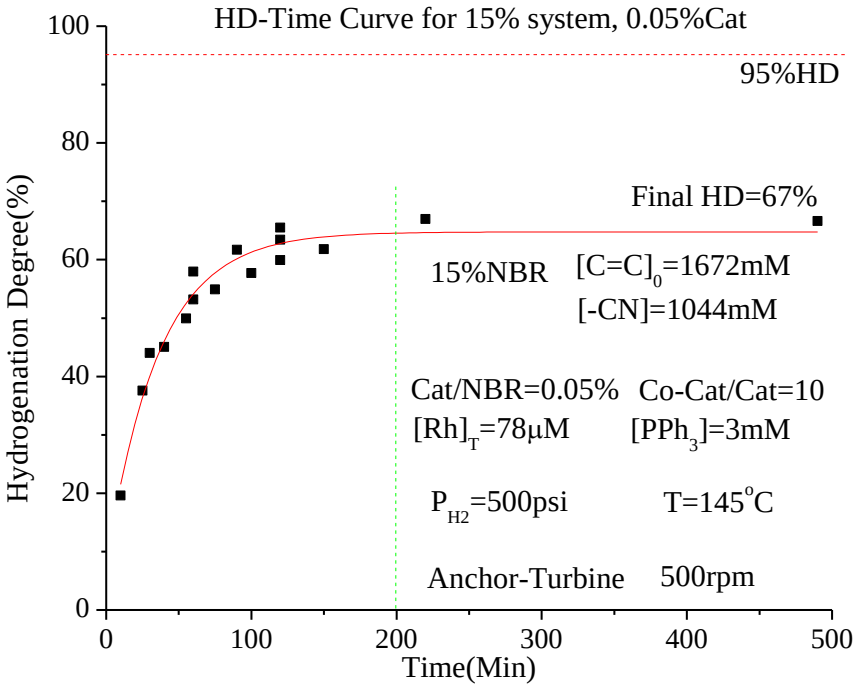

Figure 6-2 Kinetic Behavior under Low Catalyst Concentration

A series of hydrogenation experiments were designed to study these phenomena, trying to explain the reason, as shown below.

6.3.1 Catalyst Concentration

The effect of catalyst concentrations on final hydrogenation degree in various NBR solutions was studied. The experimental results were shown in Table 6-1.

Table 6-1 Effect of Catalyst Concentration on Final HD

	Polymer			Catalyst		Co-Catalyst		
Run	NBR Con.	[C=C] mol/L	[C≡N] mol/L	Cat./NBR (mass ratio)	Cat.Con. n(cat)/V(Ttl) μmol/L	TPP/Cat (mass ratio)	TPP. Con. μmol/L	Final HD
1	15.2%	1.67	1.04	0.05%	78	10	2746	67%
2	15.2%	1.67	1.04	0.074%	117	10	4119	89%
3	15.2%	1.67	1.04	0.1%	156	10	5492	94%
4	15.2%	1.67	1.04	0.15%	234	10	8239	>95%
5	10%	1.11	0.69	0.074%	77	10	2716	86%
6	7.3%	0.80	0.50	0.17%	126	10	4426	>95%

Notes: 1 all the other parameters: 500psi, anchor-turbine agitator, 500rpm, 145^{o}C.
2. all the reactions were provided with enough reaction time.

It was concluded from Table 6-1 that for all the 15% solution, 10% solution and 7% solution, more than 0.1% catalyst should be provided to get a final HD over 95%.

6.3.2 Degassing

The effect of the degassing step during operation on the final hydrogenation degree was studied, with the experimental results shown in Table 6-2.

Table 6-2 Effect of Degassing on Final HD

Run	NBR Con.	Cat./NBR (mass ratio)	TPP/Cat (mass ratio)	Degassing	Final HD
2	15.2%	0.074%	10	Hy, 1h	89%
2A	15.2%	0.074%	10	Hy, 2h	88%
2B	15.2%	0.074%	10	Ni, 1h	79%

Notes: 1 all the other parameters: 500psi, anchor-turbine agitator, 500rpm, 145^{o}C.
2. all the reactions were provided with enough reaction time.

As can be seen in Table 6-2 that longer degassing time made no difference. If degassing with Nitrogen, the HD was even lower. In this case, around 100 psi out of 500 psi of total pressure was nitrogen, so the reaction was slower with a lower hydrogen partial pressure. If the catalyst was totally deactivated at a certain time, the reaction with a lower rate could not go to a higher conversion.

6.3.3 Co-Catalyst Concentration

The effect of the co-catalyst (TPP) concentration on final hydrogenation degree was studied, with the experimental results shown in Table 6-3.

Table 6-3 Effect of Co-Catalyst Concentration on Final HD

	Polymer			Catalyst		Co-Catalyst		
Run	NBR Con.	[C=C] mol/L	[C≡N] mol/L	Cat./NBR (mass ratio)	Cat.Con. n(cat)/V(Ttl) μmol/L	TPP/Cat (mass ratio)	TPP. Con. μmol/L	Final HD
2	15.2%	1.67	1.04	0.074%	117	10	4119	89%
2C	15.2%	1.67	1.04	0.074%	117	20	8239	93%
2D	15.2%	1.67	1.04	0.074%	117	40	16477	95%
2E	15.2%	1.67	1.04	0.074%	117	60	24716	94%

Notes: 1 all the other parameters: 500psi, anchor-turbine agitator, 500rpm, 145^{o}C.
2. all the reactions were provided with enough reaction time.

As shown in Table 6-3 that if TPP concentration was increased the final HD would become higher. However, the catalyst was still deactivated. The reaction still stopped right at 95%HD and it would not go further. On the other hand, if the TPP/Cat ratio was increased from 10 to 20, the final HD was increased a lot. If the TPP/Cat ratio was increased from 20 to 60, the final HD was not obviously changed.

6.3.4 Hydrogenation of SBR

Hydrogenation of SBR was carried out in a batch reactor, with Wilkinson's catalyst/TPP and MCB. The operation procedure, as well as the temperature & pressure, were exactly the same with NBR hydrogenation experiments. The results were shown in Table 6-4, comparing with NBR hydrogenation.

Table 6-4 Hydrogenation of SBR, Comparing with NBR Hydrogenation

	Polymer			Catalyst		
Run	Type	Rubber Con.(Wt%)	[C=C] mol/L	Cat./Rubber (mass ratio)	Cat.Con. n(cat)/V(Ttl) μmol/L	Final HD
9	SBR	6.0%	0.80	0.12%	78	94%
10	SBR	6.0%	0.80	0.07%	46	77%
6	NBR	7.3%	0.80	0.17%	126	>95%
11	SBR	8.3%	1.11	0.07%	62	79%
5	NBR	10%	1.11	0.07%	77	86%

Notes: 1 all the other parameters: 500psi, anchor-turbine agitator, 500rpm, 145^{o}C.
2. all the reactions were provided with enough reaction time.

For SBR system, if the catalyst concentration was lower than 0.1%wt. (based on polymer), the hydrogenation degree could not reach 95%. This result was similar with the NBR system.

6.4 Calculation of Reaction Species

The concentration of every species in the reaction system was calculated, based on the method reported in J. Parent's PhD thesis [28], to analysis this phenomena. The mechanism of NBR hydrogenation by Wilkinson's catalyst was shown in Figure 6-1.

One of the 15% hydrogenation reactions was taken as a sample calculation, with the following parameters:

$[C=C]_0 = 1.672 mol/L$, $[C \equiv N]_0 = 1.044 mol/L$ $[RhCl(PPh_3)_3]_0 = 3.114\times10^{-4} mol/L$,
$[PPh_3]_0 = 3.114\times10^{-4}\times3 + 1.099\times10^{-2} = 1.130\times10^{-2} mol/L$
$P = 500 psi + 1 atm = 3549 kPa$, $T = 418.15 K$

It is assumed that 1) during the integral time all the reversible steps are at equilibrium state; and 2) hydrogen is saturated in the liquid phase.

Step 1: Calculation of hydrogen concentration

In polymer solution, it was assumed that

$$P_{MCB} = x_1 P^*_{MCB} \approx P^*_{MCB}$$

where P^*_{MCB} is the saturation vapor pressure of MCB at the temperature of T

$$\ln P^*_{MCB} = 54.144 - \frac{6244.4}{T} - 4.5343 \ln T + 4.7030 \times 10^{-18} T^6 \text{ [54]}$$

So,

$$P_{MCB} = 1.425 \times 10^5 \text{ Pa},\ P_{H_2} = P - P_{MCB} = 3.407 \times 10^6 \text{ Pa},$$

The molar fraction of MCB and hydrogen in the gas phase were obtained

$$y_1 = \frac{P_{MCB}}{P} = 0.04012,\ y_2 = \frac{P_{H_2}}{P} = 0.9598$$

Also, the van der Waals co-volumes are

$$b_1 = 0.1454 L/mol,\ b_2 = 0.02651 L/mol \text{ [55]}$$

Thus, the compressibility factor Z could be calculated.

$$b = y_1 b_1 + y_2 b_2 = 0.03127 L/mol,\ B = \frac{bP}{RT} = 0.03192 \text{ [56]}$$

$$Z^3 - (1-B)Z^2 - (3B^2 + 2B)Z + (B^2 + B^3) = 0 \text{ [56]},\ Z = 1.03192$$

Then, fugacity of hydrogen was obtained.

$$\ln \frac{f_2}{y_2 P} = \frac{b_2}{b}(Z-1) - \ln(Z-B) \text{ [56]},\ f_2 = 3.5 \times 10^6 Pa$$

Also, the liquid molar volume of hydrogen is

$$v_{m,2} = \frac{2.02 g/mol}{67.8 kg/m^3} = 2.979 \times 10^{-5} m^3/mol$$

And, Henry's constant was given by

$$\ln K_2 = 19.061 + \frac{0.483}{T} - 1.915 \ln T,\ K_2 = 1814.42 bar = 1.8144 \times 10^8$$

So, the mole fraction of hydrogen in the liquid was obtained.

$$\ln\frac{f_2}{x_2}=\ln K_2+\frac{v_{m,2}}{RT}P_{H_2}$$

$$x_2=0.01873$$

The density of the solution could be calculated by

$$\rho=(0.0005371\times \mathrm{wt}_3\text{-}0.001149)\times(T-273.15)+1.131\text{-}0.1195\times \mathrm{wt}_3=0.9581 g/ml \quad [9]$$

Thus, the concentration and molar fraction of species in the liquid phase were

$$\frac{n_1}{V}=\frac{0.9581 g/cm^3\times 84.8\%}{112.56 g/mol}=7.2181 mol/L,\ \frac{n_3}{V}=\frac{0.9581 g/cm^3\times 15.2\%}{10^5\, g/mol}\ll\frac{n_1}{V},$$

$$x_2=\frac{n_2}{n_1+n_2+n_3}\approx\frac{n_2}{n_1+n_2},\ n_2=\frac{x_2}{1-x_2}n_1,$$

Finally, the concentration of hydrogen in the liquid phase was calculated.

$$[H_2]=\frac{x_2}{1-x_2}\times\frac{n_1}{V}=0.13778 mol/L$$

<u>Step 2: the Equation Set</u>

The equation set was given by

$$-\frac{d[C=C]}{dt}=k'[C=C],[C=C]_0=1672 mM,\ t=0-1800 s$$

$$k'=\frac{k_4K_1K_3[Rh]_T[H_2]}{K_1+K_1K_3[H_2]+K_3[H_2][PPh_3]+K_1K_5[C\equiv N]+K_1K_2K_3[H_2][C\equiv N]}$$

$$[B]=\frac{k'}{k_4},\ [A]=\frac{[B][PPh_3]}{K_1},\ [E]=K_2[B][C\equiv N],[D]=\frac{[B]}{K_3[H_2]},\ [F]=K_5[D][C\equiv N],$$

$$[C\equiv N]=[C\equiv N]_0=1044 mM,\quad [Rh]_T=[RhCl(PPh_3)_3]_0=0.3114 mM$$

$$[PPh_3]=[PPh_3]_0=11.30 mM,\quad [H_2]=137.78 mM$$

$$K_1 = 1.44mM\ , K_2 = 3.98\times10^{-2}mM^{-1}, K_3 = 3.41\times10^{-3}mM^{-1}\ k_4 = 1.19(mM\cdot s)^{-1}$$

$$K_5 = 2.71\times10^{-2}mM^{-1},$$

$$HD = \frac{[C=C]_0 - [C=C]}{[C=C]_0}$$

These equations could be solved in polymath to get concentration of all the species in the reaction solution. For Polymath Code, see Appendix IV. Table 6-5 is summary of the calculation results.

Table 6-5 Summary of the Calculation Results

Run	wt_{NBR}%	$[Rh]_T$ %*wt*	$[Rh]_T$ μM	$[PPh_3]$ *mM*	k' ms^{-1}	$1-\frac{[E]+[F]}{[Rh]_T}$	HD_{Final}
1	15.2%	0.05%	78	2.98	0.8666	4.90%	67%
2	15.2%	0.074%	117	4.47	1.287	5.80%	89%
2C	15.2%	0.074%	117	8.59	1.254	8.20%	93%
2D	15.2%	0.074%	117	16.83	1.192	12.70%	95%
3	15.2%	0.1%	156	5.96	1.699	6.70%	94%
4	15.2%	0.15%	234	8.94	2.502	8.40%	>95%
5	10%	0.074%	77	2.95	1.307	7.20%	86%
6	7.3%	0.17%	126	4.80	2.838	11.90%	>95%
7	3.74%	>2%	80	4.00	2.574	18.10%	>95%
8	0.70%	>2%	80	4.00	7.756	54.20%	>95%

It was shown in Table 6-5 that lots of rhodium was trapped in circle 2 (Figure 6-3) by the nitrile group, especially when polymer concentration was high. The percentage of rhodium trapped could be deduced, and the analytical solution is as follows.

$$\frac{[E]+[F]}{[Rh]_T} = \frac{K_1[C\equiv N]\left(K_2K_3[H_2]+K_5\right)}{K_1 + K_1K_3[H_2] + K_3[H_2][PPh_3] + K_1K_5[C\equiv N] + K_1K_2K_3[H_2][C\equiv N]}$$

This value almost goes to 95% in some cases, which means only 5% of the rhodium is available for the catalytic circle.

6.5 Conclusion

Conclusions are listed below for the kinetic behavior of hydrogenation reaction at low catalyst concentration.

1. A large portion of Rhodium is trapped in the nitrile circle, especially when polymer concentration is high.

2. The hydrogenation degree cannot reach 95%, neither for NBR nor SBR, if the catalyst concentration is lower than 0.1%wt, based on polymer mass. This phenomenon is observed both in 6% solution, the polymer concentration of which is not so high, and in 15% solution, the polymer concentration of which is really high.

3. Possible reasons for this phenomenon: 1) the catalyst is killed slowly by impurities; 2) rhodium might exit the catalytic circle slowly, and could not re-enter into the circle.

Chapter 7 Conclusions and Recommendations for Future Research

7.1 Conclusions

7.1.1 Hydrogenation of NBR in High Concentration Solutions

Hydrogenation of NBR in high concentration MCB solution was carried out. Reaction rate was observed to be affected by the mass transfer process due to the high viscosity of the solution. Different agitators were used to provide better mixing, so that mass and heat transfer could be improved. The reactor was modified to accommodate the viscous system. Parameters that affect the reaction rate were investigated. Experimental and theoretical values of the apparent rate constant in the pseudo-first-order reaction were compared.

7.1.2 Kinetic Behavior at Low Catalyst Concentration

Also, the kinetic behavior of NBR hydrogenation under low catalyst concentration was investigated. It was observed that if less than 0.01%wt catalyst was used, based on the mass of polymer, the hydrogenation degree of polymer could not reach 95%. Hydrogenation of SBR was also carried out for comparison and similar phenomenon was observed.

7.1.3 Rheological Studies

NBR metls, NBR-MCB solutions, as well as NBR-MEK solutions were tested in the rheometer for the rheological properties. The NBR melt presented viscoelastic property, while the NBR solution mainly showed viscous property. Viscosity of NBR-MCB solution was emphasized in the rheological studies. Parameters that might affect the viscosity of the solution were studied in detail. It was observed that those

concentrated NBR solutions with high hydrogenation degree presented non-Newtonian behavior, while solutions with low concentration or low hydrogenation degree could still be regarded as Newtonian fluids. However, at very low shear rate, the NBR-MCB solution deviated from Newtonian behavior. Viscosities measured in experiments were compared with the values reported in the literature.

7.2 Recommendations for Future Research

7.2.1 Hydrogenation Experiments

Hydrogen Concentration in the Liquid Phase

The actual concentration of molecular hydrogen in the liquid phase during hydrogenation reaction is an essential parameter for the reaction kinetics. In the calculation carried out in Chapter 6, the actual hydrogen concentration is assumed to be the same as the saturated concentration; while the calculation method for saturated concentration of hydrogen is based on solubility experiments for MCB-hydrogen system or NBR/MCB solution-hydrogen system. However, in the solubility experiments carried out by Parent, among the NBR/MCB solutions used the highest concentration is around 8%wt. Thus, the calculation method may be not suitable for 15%wt NBR/MCB solutions.

Also, the assumption that hydrogen is saturated in the liquid phase may be not suitable, as the reaction is greatly affected by the gas-liquid phase mass transfer. The rate of hydrogen molecule dissolving into liquid phase may be not fast enough compared with the rate of hydrogen consumption by the reaction.

So, it is suggested to design experiments to get the actual hydrogen concentration in the liquid phase.

Modification of the Batch Reactor

Although anchor-turbine agitator was used, there were still mass transfer problems, probably because this agitator cannot bring enough small bubbles into the liquid bulk. That is to say, the anchor-turbine agitator can provide good mixing for the liquid bulk improving liquid-liquid mass transfer; while this agitator could not create enough gas-liquid interfacial area to improve gas-liquid mass transfer.

One suggestion is to try new agitators which can provide better axial mixing. Another suggestion is make the gas bulk "flow".

After the reactor is pressurized to 500psi, the gas flow rate into the reactor almost equals to the rate of hydrogen consumption by the reaction. This rate is very slow and the gas bulk almost "frozen". The only drive force to bubble the gas into liquid bulk from the gas bulk is the vortex produced by the agitator. This driving force is not enough and bubbles produced by vortex are usually too large, i.e. very low specific surface areas. Thus, there are not enough gas-liquid interfacial areas.

To make the gas bulk "flow", one design is to make an outlet for gas bulk at the upper of the reactor, while the gas supplement pipe should reach the lower of the reactor, bubbling from the reactor bottom. A solvent trap should be installed on the gas outlet pipe to separate MCB vapor from hydrogen vented; otherwise the concentration of solution will keep increasing. Devices such as reflux condenser may be modified to serve as the solvent trap. Moreover, gas-inducing agitators could be used to improve the gas-liquid mass transfer.

7.2.2 Rheological Studies

Rheological Studies for NBR Melts

For the rheological studies of NBR melts, nitrogen protection in the heating chamber is suggested to prevent oxidation of the sample, especially for high temperatures.

Also, the parallel-plates sensor is preferred for the rheological study of polymer metls in rotational rheometers, other than the cone-plate sensor.

For more information, especially the elastic properties, capillary rheometers or torque rheometers may be more suitable than the rotational rheometer.

Rheological Studies for NBR/MCB Solutions

Parameters that Might Affect Viscosities

There are many factors which will affect the viscosity of NBR/chlorobenzene system.

Except parameters mentioned in Chapter 4, other parameters that might affect the viscosity include cross linking and mechanical mixing. During experiments, it is observed that samples with same polymer concentration, hydrogenation degree and catalyst concentration may still have different viscosity at same temperature and pressure. This may be caused by the mixing or crosslinking during sample preparation in different reactors. Samples may not be “uniform”, which means that some parts have low hydrogenation degree while other parts have high hydrogenation degree, if the mechanical mixing is not good in reactors. Also, invisible micro-gel formed by slight crosslinking will affect the viscosity.

So, it is suggested to design experiments to study these parameters.

Errors in Viscosity Measurement

Normally, the errors in viscosity measurement are not large, within 5%. However, in some case, such as high polymer concentration, low catalyst amount applied and long reaction time, the measurement errors become larger, sometimes even 20%. If the sample is kept in the cylinder sensor at 145^{o}C for several hours, sometimes measurement results of viscosity cannot be explained, e.g. viscosity may decreases from1000cP to 100cP after 6 hours for the 15% polymer-70%HD sample.

Thus, more detail research is suggested to figure this problem out.

Different Cylinder Sensors

Currently, there is only one cylinder sensor (D400/300 with PZ38b) in our lab. This sensor could not provide accurate measure for low viscosity samples, such as solutions with viscosity lower than 50cP. Also, for high viscosity samples, this sensor is not suitable for measurement under the dynamic mode. Thus, different cylinder sensors with various sizes are needed to extend the measurement range.

Notation

A	pre-exponential factor, $Pa \cdot s$
E_a	activity energy, kJ / mol
f_2	fugacity of hydrogen, Pa
f	frequency, Hz
FTIR	Fourier transform infrared spectroscopy
GPC	gel permeation chromatography
G^*	complex modulus
G'	storage modulus, the elastic component, Pa
$G"$	loss modulus, the viscous component, Pa
$\|G^*\|$	the value of complex modulus, Pa
HD	hydrogenation degree
HNBR	hydrogenated nitrile butadiene rubber
k	parameter in power law, $Pa \cdot s^n$
k', k_4	rate constant of chemical reaction
K_2	Henry's constant, bar , Pa
K_1, K_2, K_3, K_4, K_5, K_6	equilibrium constant of chemical reaction
MCB	mono-chlorobenzene
MEK	methyl ethyl ketone
n	parameter in power law; mole number
NBR	nitrile butadiene rubber; nitrile rubber
P	pressure, Pa , psi
R	gas constant
SBR	styrene butadiene rubber
t	time, s , min
T	temperature, °C , K
TPP, PPh_3	triphenylphosphine
V	volume, m^3 , L

$v_{m,2}$	liquid molar volume of hydrogen, m^3 / mol
y_1, y_2	mole fraction in gas phase
x_1	mole fraction in liquid phase

Greek Symbols

γ	strain, %
$\dot{\gamma}$	shear rate, s^{-1}
δ	phase lag between stress and strain, °; rad
η	viscosity, $Pa \cdot s$, cP
η^*	complex viscosity
η'	the in-phase elastic component, $Pa \cdot s$, cP
η"	the out-of-phase viscous component, $Pa \cdot s$, cP
$\|\eta^*\|$	the value of complex viscosity, $Pa \cdot s$, cP
ρ	density, g / ml, kg / m^3
τ	shear stress, Pa
ω	frequency, rad / s

Appendix I the Rheometer System

1. Structure of Cylinder Sensor (D400/300)*

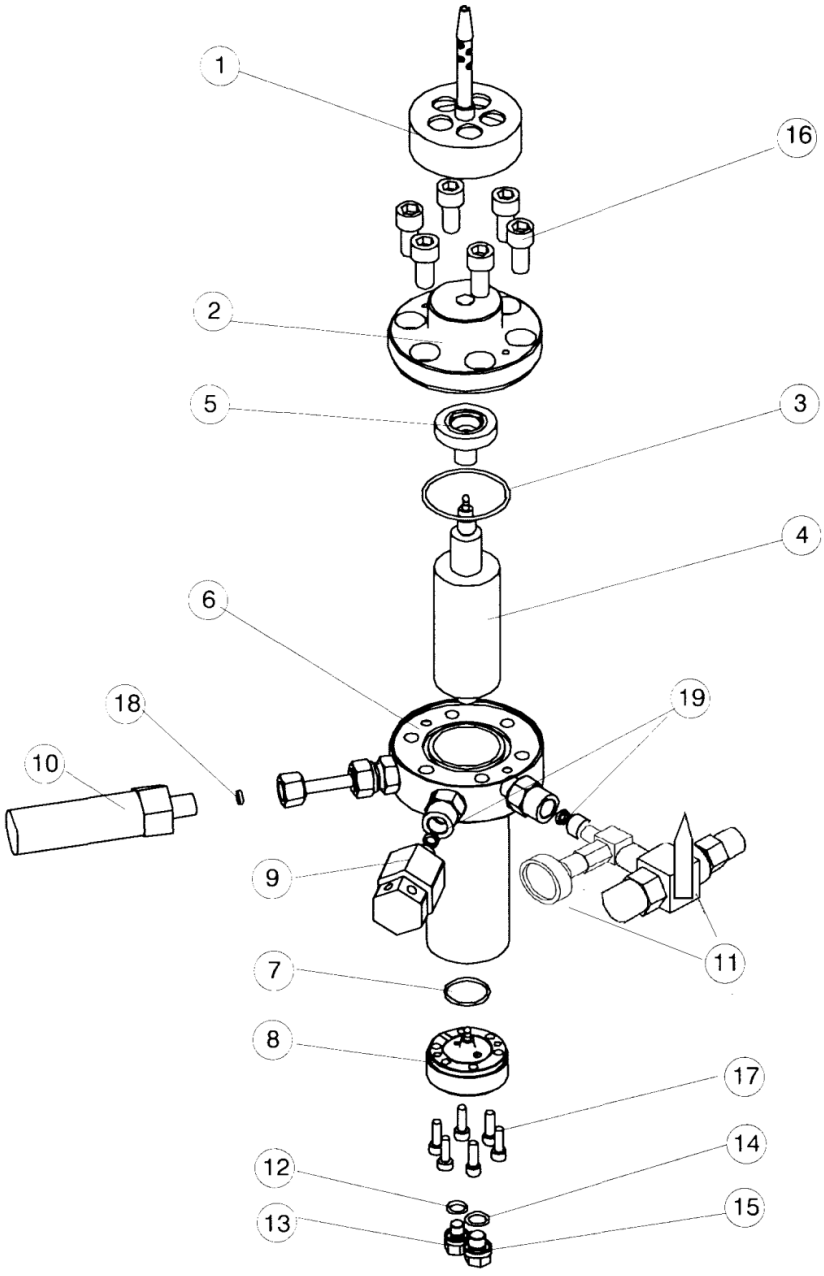

Functional Elements of the Sensor*

1 Outer magnet, attachable to the HAAKE rheometer (order no. 006-0293)

2 Cover flange (lid) with sapphire bearing (order no. 006-0292)

3 Kalrez gasket 45.89 x 2.62 (order no. 003-6983)

4 Rotor with sapphire bearing and centering pin (order no. see chapter 5.2)

5 Inner magnet (order no. 006-0296)

6 Measuring cup (order no. 006-0221)

7 Kalrez gasket 23.52 x 1.78 (order no. 006-0291)

8 Base with centering pin (order no. 006-0290)

9 Rupture disk unit (order no. 006-0952 Rupture disk 006-0307)

10 Pressure sensor 400 bar (with digital Pressure Meter) (order no. 222-125 Spare part)

11 Three way Valve, 1/4" ; Needle valve,1/4" (ordered from Swagelok)

12 Gasket 9.25 x 1.78 (order no. 006-0431)

13 Closing screw (connection for temperature sensor, thread M8 x 1) (order no. 006-0577)

14 Gasket 10.8 x 1.78 (order no. 006-0433)

15 Closing screw (connection for filling tube, thread G 1/8") (order no. 006-0300)

16 Cylinder head screw M10x20 DIN 912 St property class 12.9 (order no. 085-2259) clamping torque: 118 Nm

17 Cylinder head screw M5x16 DIN 912 St property class 12.9 (order no. 085-2258) clamping torque: 14 Nm

18 Gasket 5.5 x 8.5 x 2 Cu DIN 7603 (order no. 001-0809)

19 Gasket 6.5 x 9.5 x 1 Cu DIN 7603 (order no. 085-2263)

*Note: modified from original files in the manual of HAAKE rheometer

2. Pictures of the System:

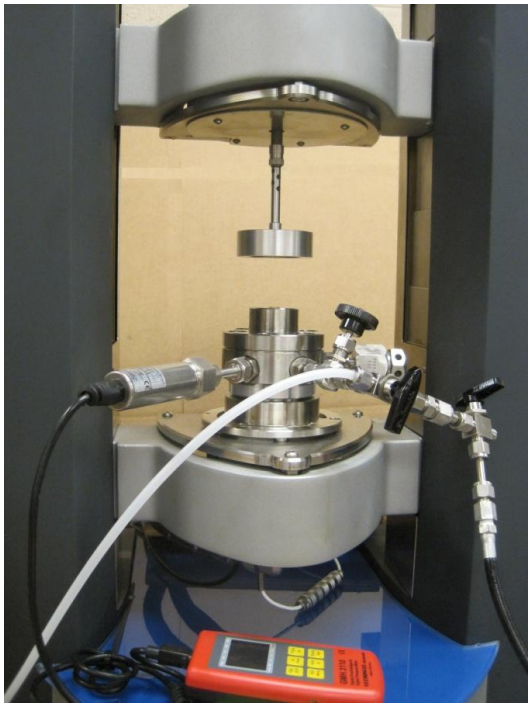

Rheometer with D400/300 Sensor

DC30-B5 Circulator

Appendix II Viscosities of NBR-MCB Solutions

Summary for viscosities of NBR-MCB solutions

[Poly]	HD	T&P①	η or $\lvert\eta^*\rvert$/cP	$\dot{\gamma}$ or ω ②
7%	0%	Rm	81	$\dot{\gamma}:10^1-10^2\,s^{-1}$
7%	0%	25 ℃, 0psi	157③, 301④	$\dot{\gamma}:10^1-10^2\,s^{-1}$
7%	35%	Rm	210	$\dot{\gamma}:10^1-10^2\,s^{-1}$
7%	66%	Rm	440	$\dot{\gamma}:10^1-10^2\,s^{-1}$
7%	96%	Rm	520	$\dot{\gamma}:10^1-10^2\,s^{-1}$
7%	0%	Rxn	17	$\dot{\gamma}:10^1-10^2\,s^{-1}$
7%	0%	145 ℃, 0psi	28③, 41④	$\dot{\gamma}:10^1-10^2\,s^{-1}$
7%	35%	Rxn	35	$\dot{\gamma}:10^1-10^2\,s^{-1}$
7%	66%	Rxn	50	$\dot{\gamma}:10^1-10^2\,s^{-1}$
7%	96%	Rxn	60	$\dot{\gamma}:10^1-10^2\,s^{-1}$
15%	0%	Rm	2,000cP,	$\dot{\gamma}:10^1-10^2\,s^{-1}$
15%	0%	25 ℃, 0psi	9093③, 3667④	$\dot{\gamma}:10^1-10^2\,s^{-1}$
15%	60%	Rm	6,600	$\dot{\gamma}:10^1-10^2\,s^{-1}$
15%	85%	Rm	$\eta=22.7\dot{\gamma}^{0.903-1}$	$\dot{\gamma}:10^1-10^2\,s^{-1}$
15%	96%	Rm	$\eta=26\dot{\gamma}^{0.9033-1}$	$\dot{\gamma}:10^1\,s^{-1}$

Summary for viscosities of NBR-MCB solutions-continued

[Poly]	HD	T&P①	η or $\lvert\eta^*\rvert$/cP	$\dot{\gamma}$ or ω ②
15%	0%	Rxn	160	$\dot{\gamma}: 10^1 - 10^2 s^{-1}$
15%	0%	145 ℃, 0psi	548③, 330④	$\dot{\gamma}: 10^1 - 10^2 s^{-1}$
15%	53%	Rxn	450	$\dot{\gamma}: 10^1 - 10^2 s^{-1}$
15%	79%	Rxn	$\eta = 0.9653\dot{\gamma}^{0.9496-1}$	$\dot{\gamma}: 10^1 - 10^2 s^{-1}$
15%	96%	Rxn	$\eta = 1.2275\dot{\gamma}^{0.9384-1}$	$\dot{\gamma}: 10^1 - 10^2 s^{-1}$
15%	98%	Rxn	$\eta = 1.2952\dot{\gamma}^{0.93313-1}$	$\dot{\gamma}: 10^1 - 10^2 s^{-1}$
15%	0%	Rxn	$\lvert\eta^*\rvert = 16.74\omega^{0.06251-1}$	$\omega: 0.1 - 2.0 rad/s$
15%	96%	Rxn	$\lvert\eta^*\rvert = 25.51\omega^{0.17902-1}$	$\omega: 0.1 - 1.5 rad/s$

①Note: Rm--25 ℃, 0psi; Rxn--145 ℃, 500psi.

②Note: the dynamic mode could extend the measurement range where the static mode is not suitable, according to the Cox-Merz rule $|\eta^*| = \eta$ when $\omega = \dot{\gamma}$, $(\omega = 2\pi f)$; $\eta = k\dot{\gamma}^{n-1}$ for the static mode, while $|\eta^*| = k\omega^{n-1}$ for the dynamic mode.

③Note: calculated from the correlate developed in the work of Lei et al. [8].

④Note: calculated from the correlate developed by method 3 in the work of Pan and Rempel [9].

Appendix III the Batch Reactor

1. Reactor Internals*

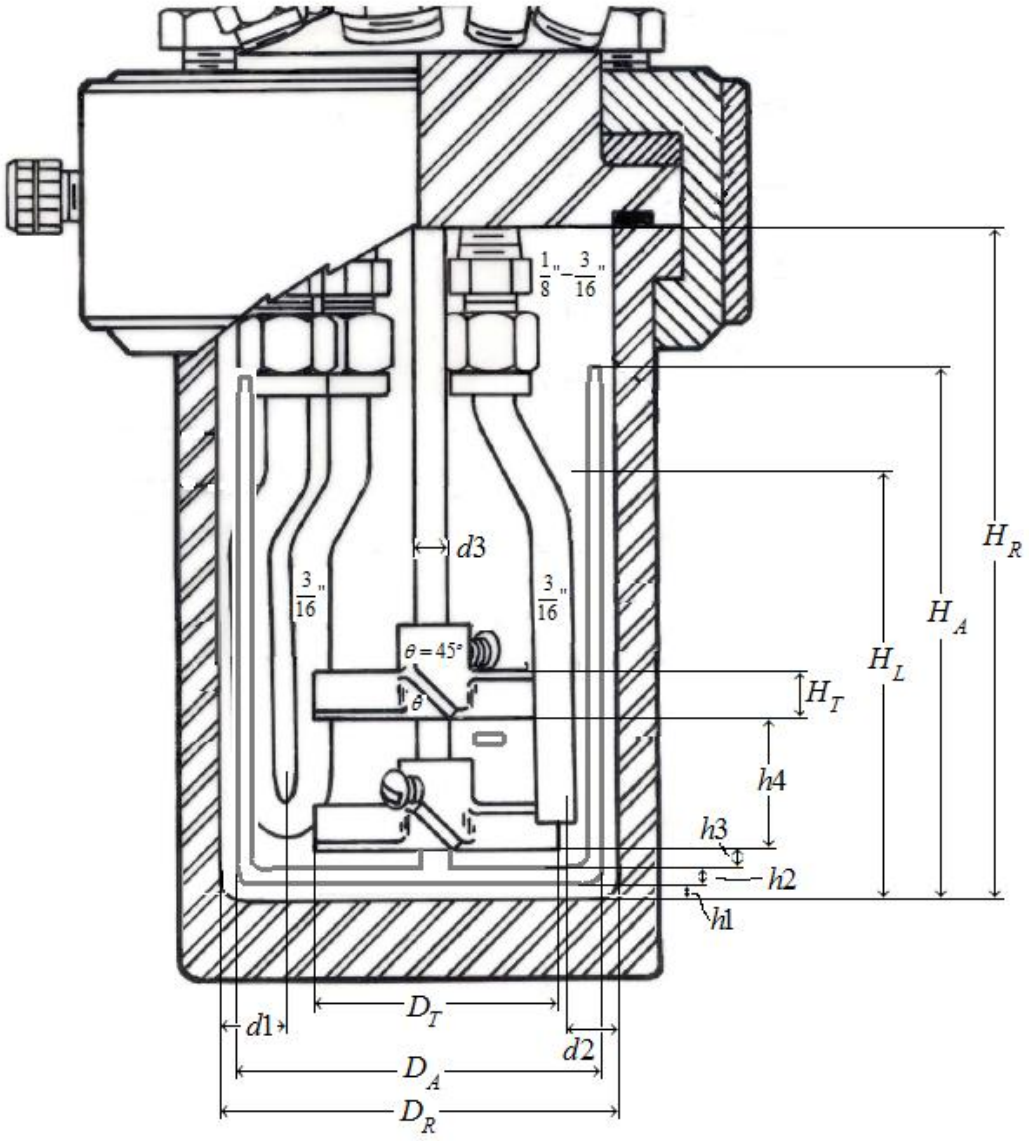

*Note: modified from the original picture in the manual of Parr reactor

Parameters	Dimensions/mm	Description
D_R	63	Internal Diameter of Reactor
D_T	35	Diameter of Turbine
D_A	61	External Diameter of Anchor
d_1	6	Clearance of Cooling Coil to Reactor Wall
d_2	6	Clearance of Dip Tube to Reactor Wall
d_3	4.7	Width of Stirrer Shaft
H_R	100	Internal Height of Reactor
H_T	7	Height of Turbine
H_A	81	Height of Anchor + h_1
H_L	45-50	Liquid Level
h_1	4	Clearance of Anchor to Reactor Bottom
h_2	3	Thickness of Anchor Arm
h_3	11	Distance between Turbine and Anchor
h_4	22	Distance between Turbine and Turbine

Note: when anchor was not used, i.e. when agitator A or agitator C was used, the clearance of the (lower) turbine to the reactor bottom was 11mm.

2. Reactor Head*

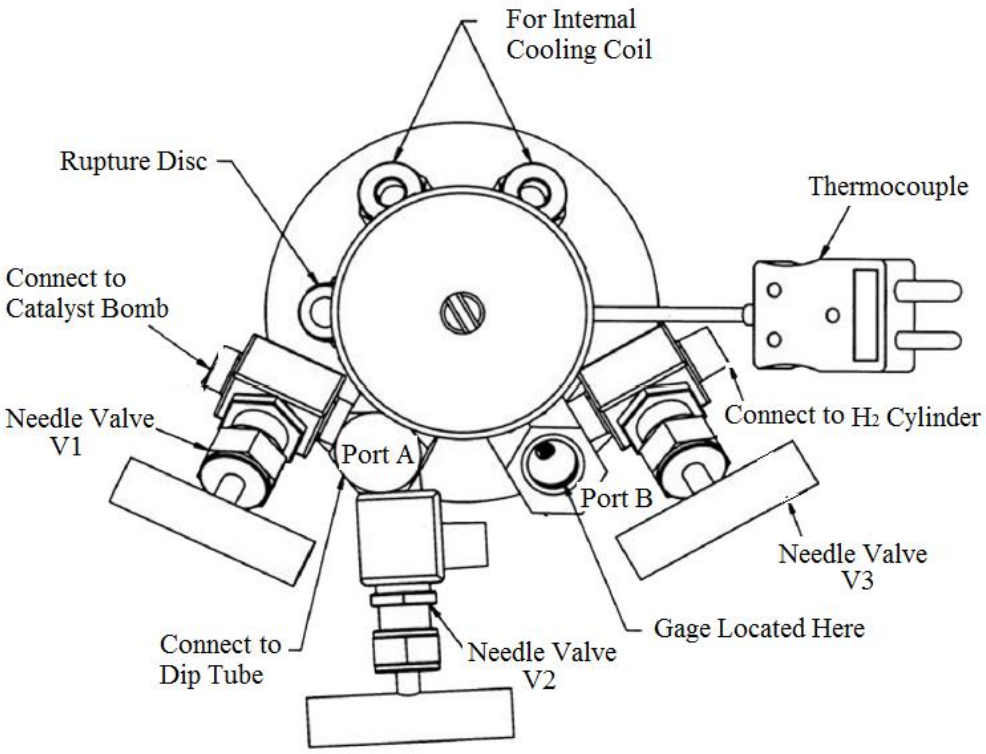

Port A Connection: Dip tube, Needle valve V1 and Needle valve V2.

Catalyst solution loading: V1-dip tube-vessel

Purging & Sampling: vessel-dip tube-V2

Port B Connection: Pressure Gage and Needle valve V3.

Gas pathway during degassing: vessel-V3

Gas pathway during hydrogenation reaction: V3-vessel

*Note: modified from the original picture in the manual of Parr reactor

3. Picture of the Reactor

Appendix IV Polymath Code

Polymath Code:

d(cc)/d(t)=-k*cc
cc(0)=1672
t(0)=0
t(f)=1800
HD=(1672-cc)/1672

k=(k4*K1*K3*Rh*H2)/(K1+K1*K3*H2+K3*H2*PPh3+K1*K5*CN+K1*K2*K3*H2*CN)

B=k/k4
A=B*PPh3/K1
E=K2*B*CN
D=B/(K3*H2)
F=K5*D*CN

CN=1044
Rh=0.3114
PPh3=11.30
H2=137.78

K1=1.44
K2=3.98E-2
K3=3.41E-3
k4=1.19
K5=2.71E-2

References

[1]. Pan, Q., Li, G., Rempel, G. L. and Ng, F., Analysis of Diffusion and Reaction of NBR Hydrogenation in super critical CO2, *51st Canadian Chemical Engineering Conference*, Halifax, Canada (**2001**)

[2]. Wei, Z., Direct Catalytic Hydrogenation of Unsaturated Diene-Based Polymers in Latex Form, PhD thesis, University of Waterloo (**2006**)

[3]. Rempel, G. L., Pan, Q., and Wu, J., Homogeneous Catalytic Hydrogenation of Polymers, in "*Handbook of Homogeneous Hydrogenation*", edited by Johannes G. de Vries and Cornelis J., V2, page 547-583, Elsevier, Wiley-VCH (**2007**)

[4]. Madhuranthakam, C.R.,Pan,Q., Rempel,G.L., Continuous Process for Production of Hydrogenated Nitrile Butadiene Rubber using a Kenics Static Mixer Reactor, *AIChE J*, 55(11), 2934- 2944 (**2009**)

[5]. Zhang, L., Pan, Q., Rempel, G. L., Hydrogenation of nitrile butadiene rubber in a multistage agitated contactor: Experiments and numerical simulation, *Chem. Eng. Sci.*, 65(6), 2027-2036 (**2010**)

[6]. Parent, J.S., McManus, N.T., and Rempel, G.L., $RhCl(PPh_3)_3$ and $RhH(PPh_3)_4$ Catalyzed Hydrogenation of Acrylonitrile-Butadiene Copolymers, *Industrial and Engineering Chemistry Research*, 35, 4417-4423 (**1996**)

[7]. Pan, Q., and Rempel, G.L., Numerical Investigation of Semi-Batch Processes for Hydrogenation of Diene-Based Polymers, *Industrial & Engineering Chemistry Research*, 39, 277-284 (**2000**)

[8]. Lei, H., Lu, Y., Pan, Q., and Rempel, G.L., Rheological behaviour of Nitrile Butadiene Rubber-Chlorobenzene Solutions, *China Synthetic Rubber Industry*,3(25), 164-166 (**2002**)

[9]. Pan, Q. and Rempel, G.L., Investigation of Fundamental Data for Nitrile Butadiene Rubber in Monochlorobenzene and o-Dichlorobenzene, *Journal of Polymer Engineering and Science*. 44, (1) 88-95 (**2004**)

[10]. Kubo, Y. and Khotaki, T., US Patent 4,510,393 (**1985**)

[11]. Kubo, Y. and Ohura, K., US Patent 4954576 (**1990**)

[12]. Rempel, G. L. and Azizian, H., US Patent 4,464,515 (**1984**)

[13]. Mohammadi, N.A., and Rempel, G.L., Catalytic Hydrogenation of Unsaturated Nitrile Polymers, *Macromolecules*, 20, 2362-2368 (**1987**)

[14]. Hoxmeier, R. J. and Slaugh, L. H. US Patent 4,876,314 (**1989**)

[15]. Hoxmeier, R. J. US Patent 4,892,928 (**1990**)

[16]. Rempel, G. L., Mohammadi, N.A. and Farwaha, R., US Patent 4,812,528 (**1989**)

[17]. Rempel, G. L. and McManus, N. T., US Patent 5,075,388 (**1991**)

[18]. Rempel, G. L., McManus N. T., and Parent, J. S., US Patent 5,561,197 (**1996**)

[19]. Hsu, K., Wu, G., Xu, R., Yue, D., Zhou, S., US Patent 6,084,033 (**2000**)

[20]. Rempel, G. L., Guo, X. US Patent 5,208,296 (**1993**)

[21]. Rempel, G. L., Pan, Q., Wu, J. US Patent 7,385,010 (B2) (**2008**)

[22]. Pan, Q., Rempel, G. L., Wei, Z. US Patent 7,803,883 (B2) (**2010**)

[23]. Rempel, G. L., Pan, Q., Wu, J. US Patent 7,345,115 (B2) (**2008**)

[24]. Rempel, G. L., Pan, Q., Wu, J. US Patent 7,897,695 (B2) (**2011**)

[25]. Mohammadi, N.A., and Rempel, G.L., Control, Data Acquisition and Analysis of Catalytic Gas-Liquid Mini Slurry Reactors using a Personal Computer, *Computers and Chemical Engineering*, 11, 27-35 (**1987**)

[26]. Halpern, J. and Wong, C. S., Hydrogenation of Tris(triphenylphosphine) chlororhodium(I). *J. Chem. Soc., Commun.* 629-630 (**1973**)

[27]. Bhattacharjee, S., Bhowmick, A. K., Avasthi, B. N., High-pressure hydrogenation of nitrile rubber: thermodynamics and kinetics, *Industrial and Engineering Chemistry Research*, 30 1086-1092 (**1991**)

[28]. Parent, J. S., Catalytic Hydrogenation of Butadiene Copolymers, PhD thesis, University of Waterloo (**1996**)

[29]. Kehl, S., Catalytic Hydrogenation of Nitrile Butadiene Rubber in a Packed Reactor., MASc Thesis, University of Waterloo (**1998**)

[30]. Pan, Q., Kehl, S., and Rempel, G.L., Liquid holdup in an upflow cocurrent packed bed reactor involving butadiene rubber and hydrogen, *Ind. Eng. Chem. Res.*, , 41(15), 3505-3511(**2002**)

[31]. Pan, Q., Rempel, G.L., and Ng, F.T.T., Numerical Investigation of Continuous Processes for Catalytic Hydrogenation of Nitrile Butadiene Rubber, *Polym. Eng. Sci.*, 42(5), 899-910 (**2002**)

[32]. Madhuranthakam, C. M. R., Design, Modeling and Analysis of a Continuous Process for Hydrogenation of Diene Based Polymers Using a Static Mixer Reactor., PhD thesis, University of Waterloo (**2007**)

[33]. Madhuranthakam, C.R., Pan,Q.,Rempel,G.L., Residence Time Distribution and Liquid Holdup in Kenics KMX Statis Mixer with Hydrogenated Nitrile Butadiene Rubber Solution and Hydrogen Gas System, *Chem. Eng. Sci.*, 64 (14), 3320-3328 (**2009**)

[34]. Madhuranthakam, C. M., Pan, Q., Rempel, G. L., Hydrodynamics in Sulzer SMX Static Mixer with Air/Water System, *Ind. Eng. Chem., Res.*, 48,719-726 (**2009**)

[35]. Zhang, L., Development of a Novel Continuous Process for Hydrogenation of NBR., PhD thesis, University of Waterloo (**2007**)

[36]. Zhang, L., Pan, Q., Rempel, G. L., Phase Holdup and Backmixing in a Multistage Agitated Contactor, *Industrial Chem. & Eng. Res.*, 44(14), 5304-5311 (**2005**)

[37]. Zhang, L., Pan, Q., Rempel, G. L., Liquid phase mixing and gas holdup in a multistage-agitated contactor with co-current upflow of air/viscous fluids, *Chem. Eng. Sci.*, 61(18), 6189-6198 (**2006**)

[38]. Zhang, L., Pan, Q., Rempel, G. L., Residence time distribution in a multistage agitated contactor with Newtonian fluids: CFD prediction and experimental validation, *Ind. Eng. Chem., Res.*46(11), 3538-3546 (**2007**)

[39]. Hemrajani, R. and Tatterson, G., Mechanically Stirred Vessels, in "*Handbook of Industrial Mixing: Science and Practice*", edited by Paul, E., Atiemo-Obeng, V. and Kresta, S. page 345-390 (**2004**)

[40]. Shah, Y. T., Design Parameters for Mechanically Agitated Reactors, *Advances in Chemical Engineering*, 17, 1-206 (**1991**)

[41]. Zlokarnik, M. and Judat, H., Stirring, in "*Ullmann's Encyclopedia of Industrial Chemistry*" 5th Ed. Vol. B2 (**1988**)

[42]. Gu, P., Sun, J., Qian, W. and Pan, Q., Agitating Characteristics of Combined Agitators, *China Synthetic Rubber Industry*, 17(3), 142-145 (**1994**)

[43]. Gu, P., Sun, J., Qian, W. and Pan, Q., Macromixing Characteristics of Combined Agitators, *China Synthetic Rubber Industry*, 17(6), 384-351 (**1994**)

[44]. Todd, D., Mixing of Highly Viscous Fluids, Polymer, and Pastes, in "*Handbook of Industrial Mixing: Science and Practice*", edited by Paul, E., Atiemo-Obeng, V. and Kresta, S. page 987-1025 (**2004**)

[45]. Zhou, C. Rheology of Polymer: Experiments and Application. Shanghhai: Shanghai Jiaotong University Press, **2003**

[46]. Carreau, P. J., De Kee, D. and Chhabra, R. P., Rheology of Polymeric Systems: Principles and Application, New York: Hanser Publishers, **1997**

[47]. Shaw, M. T. and MacKnight, W. J., Introduction to Polymer Viscoelasticity, 3rd Ed., New Jersey: John Wiley & Sons, **2005**

[48]. Brydson, J. A., Flow Properties of Polymer Melts 2nd Ed., London: George Godwin, **1981**

[49]. Rohn, C. L., Analytical Polymer Rheology, Munich: Hanser Publishers, **1995**

[50]. Anandhan, S., De, P. P., De, S. K., Bhowmick, A. K. and Swayajith, S., Thermorheological properties of thermoplastic elastomeric blends of NBR/SAN containing waste nitrile rubber vulcanizate powder, *Kautschuk Gummi Kunststoffe*, 57, 599-606 (**2004**)

[51]. Anandhan, S., De, P. P., De, S. K., Swayajith, S. and Bhowmick, A. K. Thermorheological Studies of Novel Thermoplastic Elastomeric Blends of NBR and SCP based on ABS, *Plastics, Rubber and Composites*, 32, 377-384 (**2003**)

[52]. Nayak, N. C., Bhattacharya, A. K. and Tripathy, D. K., Acrylonitrile Butadiene Rubber and High Styrene Resin, *Kautschuk Gummi Kunststoffe*, 54, 550-553 (**2001**)

[53]. Kumar, C. R., Nair, S. V., George, K. E., Oommen, Z. and Thomas, S., Blends of Nylon/Acrylonitrile Butadiene Rubber: Effects of Blend Ratio, Dynamic Vulcanization and Reactive Compatibilization on Rheology and Extrudate Morphology, *Polymer Engineering and Science*, 43(9) 1555-1565 (**2003**)

[54]. Poling, Bruce E. et al. Perry's Chemical Engineers' Handbook, 8th Ed, Section 2: Physical and Chemical Data **2008**

[55]. Lange's Handbook of Chemistry, 15th Ed, Section 5.9, **1999**

[56]. Peng, D. and Robinson, D., A New Two-Constant Equation of State, *Ind. Eng. Chem., Fundam.*, 15, 59-64 (**1976**)